doc. Ing. Ivo Petráš, PhD.
Ústav riadenia a informatizácie výrobných procesov
FBERG TU v Košiciach

Súbor vybraných publikácií

Zoznam vybraných publikácií:

1. **Petráš, I. [100%]:** Tuning and implementation methods for fractional-order controllers, *Fractional Calculus and Applied Analysis*, vol. 15, no. 2, 2012, pp. 282-303.
2. **Petráš, I. [33%]**, Sierociuk, D. [33%], Podlubny, I. [33%]: Identification of parameters of a half-order system, *IEEE Transactions on Signal Processing*, vol. 60, no. 10, 2012, pp. 23-28.
3. **Petráš, I. [100%]**: Fractional-order nonlinear systems: modeling, analysis and simulation, HEP, Springer-Verlag, 2011, p.218. ISBN 978-3-642-18100-9.
4. **Petráš, I. [100%]**: Modeling and numerical analysis of fractional-order Bloch equations, *Computers & Mathematics with Applications*, vol. 61, no. 2, 2011, pp. 341-356.
5. Caponetto, R. [33%], Dongola, G. [17%], Fortuna, L. [17%], and **Petráš, I. [33%]:** Fractional Order Systems: Modelling and Control Applications, World Scientific Publishing, Singapore, 2010, p.178. ISBN 978-981-4304-19-1.
6. **Petráš, I. [100%]**: Fractional-order memristor-based Chua's circuit, *IEEE Transactions on Circuits and Systems II-Express Briefs*, vol. 57, no. 12, 2010, pp. 975-979.
7. **Petráš, I. [100%]**: Fractional-order feedback control of a DC motor, *Journal of Electrical Engineering*. vol. 60, no. 3, 2009, pp. 117-128.
8. Vinagre, B. M. [34%], Chen, Y.Q. [33%], **Petráš, I. [33%]**: Two Direct Tustin Discretization Methods for Fractional-Order Differentiator/Integrator, *Journal of The Franklin Institute*, vol. 340, no. 5, 2003, pp. 349 – 362.
9. Podlubny, I. [20%], **Petráš, I. [20%]**, Vinagre, B.M. [20%], O'Leary, P. [20%], Dorčák, Ľ. [20%]: Analogue Realization of Fractional-Order Controllers, *Nonlinear Dynamics*, vol. 29, no. 1-4, 2002, pp. 281-296.

Dátum: 11.9.2012

....	....	....
doc. Ing. Ivo Petráš, PhD.	prof. Ing. Gabriel Weiss, PhD. dekan FBERG TUKE	prof. Ing. Miroslav Fikar, DrSc. riaditeľ ÚIAM FCHPT STU

VERSITA

Fractional Calculus & Applied Analysis
An International Journal for Theory and Applications
VOLUME 15, NUMBER 2 (2012) (Print) ISSN 1311-0454
(Electronic) ISSN 1314-2224

SURVEY PAPER

TUNING AND IMPLEMENTATION METHODS FOR FRACTIONAL-ORDER CONTROLLERS

Ivo Petráš

Abstract

This survey paper presents methods of tuning and implementation of Fractional-Order Controllers (FOC). In the article are presented tuning, auto-tuning and self-tuning methods for the FOC. As the FOC are considered fractional PID controllers, the Commande Robuste d'Ordre Non Entier (CRONE) controller and fractional-order lead-lag compensators. As implementation techniques are described the IIR and FIR filters forms of approximation methods, which can be easily implemented in microprocessor devices such as for example the Programmable Logic Controller (PLC), etc. The possibility for analogue implementation of such kind of controllers is also mentioned. An example of practical implementation of the FOC together with all problems and restrictions are described as well.

MSC 2010: Primary 26A33, Secondary 93C05

Key Words and Phrases: fractional calculus, fractional-order controller, tuning, implementation

1. Introduction

It is well-known that fractional calculus is more than 300 years old topic. There is a number of applications in various areas, that were already published, for instance [6, 13, 17, 20, 23, 31]. One important area of application is control theory. During the last 20 years a huge effort has been made to describe various possibilities of how to implement the fractional calculus techniques in control theory. We can mention for example:

pp. 282–303 , DOI: 10.2478/s13540-012-0021-4

Springer

new type of fractional-order controllers, new fractional-order model for the plant (process), etc. In this article we will focus on fractional-order controllers because of a wide area of applications. As already noted in [8, 9], fractional-order control, namely fractional PID controllers, could be ubiquitous in industry. The main motivation is that in process control more than 95% of the control loops are of PI/PID type [1]. For example a typical mill in Canada has more than 2000 control loops, where 97% loops are based on PI control. However, only 20% of control loops work well. The reason is bad tuning, actuator and sensor problems and so on. This is the reason, why we focus on fractional-order controllers, tuning techniques, implementation techniques, their restrictions and limitations, while the fractional-order controllers are based on microprocessors and also on the control performance assessment technology for industrial applications.

This article is organized as follows: The essential definitions of fractional calculus are described in the next section. Then the typical fractional order controllers and their tuning, implementation technique are described. The article is concluded with an example of practical implementation of the FOC to control a temperature of electrical heater.

2. Fractional calculus fundamentals

Fractional calculus is a generalization of integration and differentiation to non-integer order fundamental operator ${}_aD_t^\alpha$, where a and t are the bounds of the operation.

Definition **2.1**. The continuous fractional integro-differential operator is defined as

$$ {}_aD_t^\alpha = \begin{cases} \frac{d^\alpha}{dt^\alpha} & : \ \alpha > 0, \\ 1 & : \ \alpha = 0, \\ \int_a^t (d\tau)^{-\alpha} & : \ \alpha < 0. \end{cases} $$

Several alternative definitions of the fractional derivative exist, see e.g. [31]. We will consider just two of them, Caputo's definition and the Grünwald-Letnikov definition.

Definition **2.2**. Caputo's definition [7] of fractional derivative can be written as (see e.g. [31]):

$$ {}_aD_t^\alpha f(t) = \frac{1}{\Gamma(n-\alpha)} \int_a^t \frac{f^{(n)}(\tau)}{(t-\tau)^{\alpha-n+1}} d\tau, \tag{2.1} $$

for $(n-1 < \alpha < n)$. It holds an important property: the initial conditions for fractional-order differential equations with Caputo's derivative are in the same form as for integer-order differential equations.

Definition **2.3**. If we consider $k = \frac{t-a}{h}$, where a is a real constant, which expresses a limit value, we can write the Grünwald-Letnikov (GL) definition as (see [31]):

$$ {}_aD_t^\alpha f(t) = \lim_{h\to 0} \frac{1}{h^\alpha} \sum_{j=0}^{[\frac{t-a}{h}]} (-1)^j \binom{\alpha}{j} f(t-jh), \tag{2.2}$$

where $[x]$ means the integer part of x, a and t are the bounds of operation for ${}_aD_t^\alpha f(t)$. This form of definition is very helpful for obtaining a numerical solution of fractional differential equations.

For zero initial conditions and lower limit $a = 0$, the Laplace transform of fractional derivatives (Grünwald-Letnikov and Caputo), reduces to [31]:

$$\mathscr{L}\{{}_0D_t^\alpha f(t)\} = s^\alpha F(s). \tag{2.3}$$

The fractional differentiation/integration are linear operations:

$$ {}_0D_t^\alpha (af(t) + bg(t)) = a\,{}_0D_t^\alpha f(t) + b\,{}_0D_t^\alpha g(t). \tag{2.4}$$

Some other important properties of the fractional derivatives and integrals can be found in several works (e.g.: [17, 20, 22, 23, 31], etc.).

3. Fractional-order controllers

The fractional-order controller (FOC) $PI^\lambda D^\delta$ (also known as $PI^\lambda D^\mu$ controller) was proposed in [30] as a generalization of the PID controller with integrator of real order λ and differentiator of real order δ. The transfer function of such controller in the Laplace domain has this form:

$$C(s) = \frac{U(s)}{E(s)} = K_p + T_i\, s^{-\lambda} + T_d\, s^\delta, \qquad (\lambda, \delta > 0), \tag{3.1}$$

where K_p is the proportional constant, T_i is the integration constant and T_d is the differentiation constant.

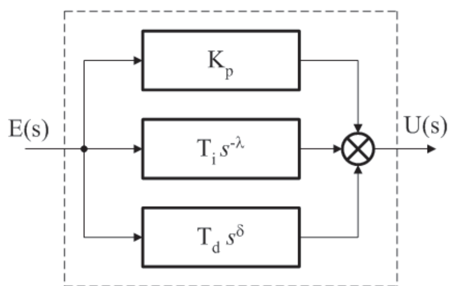

Figure 1. General structure of a fractional $PI^\lambda D^\delta$ controller.

As we can see in Fig. 1, the internal structure of the fractional-order controller consists of the parallel connection, the proportional, integration, and derivative part. The transfer function (3.1) corresponds in time domain to the fractional differential equation of the form:

$$u(t) = K_p\, e(t) + T_i\, {}_0D_t^{-\lambda} e(t) + T_d\, {}_0D_t^{\delta} e(t), \tag{3.2}$$

or discrete transfer function given in the following expression:

$$C(z) = \frac{U(z)}{E(z)} = K_p + \frac{T_i}{(\omega(z^{-1}))^{\lambda}} + T_d(\omega(z^{-1}))^{\delta}, \tag{3.3}$$

where $\omega(z^{-1})$ denotes the discrete operator, expressed as a function of the complex variable z or the shift operator z^{-1}.

Taking $\lambda = 1$ and $\delta = 1$, we obtain a classical PID controller. If $\lambda = 0$ and $T_i = 0$, we obtain a PD^{δ} controller, etc. All these types of controllers are particular cases of the fractional-order controller, which is more flexible and gives an opportunity to better adjust the dynamical properties of the fractional-order control system.

It can also be mentioned that there are many other modifications of the fractional $PI^{\lambda}D^{\delta}$ controller [15, 20, 19, 39] and other considerations of the fractional-order controller. For example, we can mention several of them:

- *CRONE controller* (2nd generation), characterized by the band-limited lead effect [23, 32]:

  $$C(s) = C_0 \frac{(1 + s/\omega_b)^r}{(1 + s/\omega_h)^{r-1}}, \tag{3.4}$$

  where $0 < \omega_b < \omega_h$, $C_0 > 0$ and $r \in (1, 2)$. There are a number of real-life applications of three generations of the CRONE controller [23].

- *Fractional lead-lag compensator* [20], which is given by

  $$C(s) = k_c \left(\frac{s + 1/\lambda}{s + 1/x\lambda}\right)^r = k_c x^r \left(\frac{\lambda s + 1}{x\lambda s + 1}\right)^r, \tag{3.5}$$

  where $0 < x < 1$, $x \in \mathrm{R}$, $\lambda \in \mathrm{R}$, and $r \in \mathrm{R}$.

- *Non-integer integral* and its application to control as a reference function [5, 18]; Bode suggested an ideal shape of the loop transfer function in his work on design of feedback amplifiers in 1945. Ideal loop transfer function has the form:

  $$L(s) = \left(\frac{s}{\omega_{gc}}\right)^{\alpha}, \quad (\alpha < 0), \tag{3.6}$$

where ω_{gc} is desired crossover frequency and α is the slope of the ideal cut-off characteristic.

The phase margin is $\Phi_m = \pi(1 + \alpha/2)$ for all values of the gain. The amplitude margin A_m is infinity. The constant phase margin 60^o, 45^o, and 30^o correspond to the slopes $\alpha = -1.33$, -1.5, and -1.66. The Nyquist curve for ideal Bode transfer function is simply a straight line through the origin with $\arg(L(j\omega)) = \alpha\pi/2$.

- *TID compensator* [16], which has structure similar to a PID controller but the proportional component is replaced with a tilted component having a transfer function s to the power of $(-1/n)$. The resulting transfer function of the TID controller has the form:

$$C(s) = \frac{T}{s^{1/n}} + \frac{I}{s} + Ds, \tag{3.7}$$

where T, I and D are the controller constants and n is a non-zero real number, preferably between 2 and 3. The transfer function (3.7) more closely approximates an optimal transfer function and an overall response is achieved, which is closer to the theoretical optimal response determined by Bode [5].

4. Design of controller parameters

There are already a large number of controller parameters design methods. Most of them have been developed only recently. A good review of tuning methods for fractional PID controllers has been done in [34, 35]. They mentioned modified Ziegler and Nichols method and various analytical methods such as for example dominant poles, internal model control, etc. and the numerical methods, which are usually based on the numerical evaluation of an objective function (minimization). Some other methods can be found in [4, 6, 10, 33]. It can be expected that FOC (3.1) may enhance the systems control performance due to more tuning knobs introduced.

Here, we mention three basic strategies of the parameters tuning (classical, self and auto tuning).

4.1. Classical tuning methods

The tuning of $PI^\lambda D^\delta$ controller parameters is determined according to the given requirements. These requirements are, for example, the damping ratio, the steady-state error (e_{ss}), dynamical properties, etc. One of the methods being developed is the method of dominant roots [24], based on the given stability measure and the damping ratio of the closed control loop. Assuming that, the desired dominant roots are a pair of complex conjugate root as follows:

$$s_{1,2} = -\sigma \pm j\omega_d,$$

designed for the damping ratio ζ and natural frequency ω_n. The damping constant (stability measure) is $\sigma = \zeta\omega_n$ and the damped natural frequency of oscillation $\omega_d = \omega_n\sqrt{1-\zeta^2}$. The design of parameters: K_p, T_i, λ, T_d and δ can be computed numerically from characteristic equation. More specifically, for simple plant model $P(s)$, this can be done by solving

$$\min_{K_p,T_i,\lambda,T_d,\delta} ||C(s)P(s)+1||_{s=-\sigma\pm j\omega_d}.$$

Another possible way to obtain the controller parameters is using the tuning formula, based on gain A_m and phase Φ_m margins specifications for crossover frequency ω_{cg}. Gain and phase margins have always served as important measures of robustness. The equations that define the phase margin and the gain crossover frequency are expressed as [20, 37]:

$$\begin{aligned} |C(j\omega_{cg})P(\omega_{cg})|_{\mathrm{dB}} &= 0\,\mathrm{dB} \\ \arg(C(j\omega_{cg})P(\omega_{cg})) &= -\pi + \Phi_m \end{aligned} \tag{4.1}$$

The above equations are also often used for so-called auto-tuning techniques.

Last but not least we should mention the optimization algorithm based on the integral absolute error (IAE) minimization [30]:

$$\mathrm{IAE} = \int_0^t |e(t)|dt = \int_0^t |r(t)-y(t)|dt,$$

where $r(t)$ is the desired value of closed control loop and $y(t)$ is the real value of the closed control loop. This method does not ensure the desired stability measure of the closed control loop. Ths measure of stability has to be checked out additionally by some known method as for example frequency method [9].

Other minimization algorithms can be based on other type of cost functions or on the H_∞ norm minimisation [25].

4.2. Self-tuning methods

It is well-known that Model Reference Adaptive Control (MRAC) has become a standard part in textbooks on adaptive control (e.g.: [1, 2]). The fractional-order calculus can be introduced into MRAC scheme in two ways. One is the use of fractional derivatives for the adjustment rules and the other one is the use of fractional-order reference models. The new adjustment rule and modification of MRAC problem by introducing fractional-order system as the reference model has been studied in [37].

4.3. Auto-tuning methods

The relay auto-tuning process is widely used in industrial applications, see [1]. Some considerations have to be taken into account concerning the auto-tuning method for this fractional-order structure, [39]:

(1) The simplicity of the auto-tuning method is an important goal to achieve, since it is the aim to implement it for industrial applications by using, for instance, a PLC or a PC with a data acquisition board. That is, the tuning rules for the parameters of the fractional-order controller must be given by simple equations and computable within a sample time appropriate for the control hardware and for the plant.

(2) It would be convenient to apply the relay test to obtain experimentally the information of the plant, due to the reliability of this method.

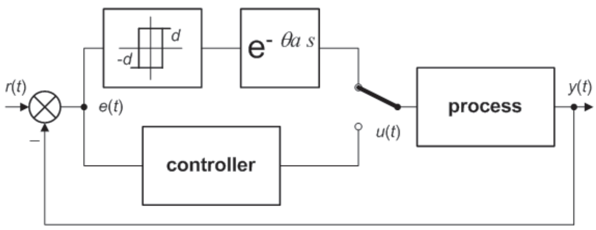

FIGURE 2. Relay auto-tuning scheme with delay.

A standard relay test, which is shown in Fig. 2, can be also used for the fractional-order controllers auto-tuning [19]. For this scheme are given the following relations:

$$\begin{aligned} \arg(P(j\omega_c)) &= -\pi + \omega_c\theta_a, \\ |P(j\omega_c)| &= \frac{\pi a}{4d} = \frac{1}{N(a)}, \end{aligned} \tag{4.2}$$

where $P(j\omega_c)$ is the transfer function of the process at the frequency ω_c, which is the frequency of the output signal $y(t)$ corresponding to the delay θ_a, d is the relay output, a is the amplitude of the output signal, and $N(a)$ is the equivalent relay gain. The condition for oscillation is

$$N(a)P(j\omega) = -1$$

and this condition can be easily checked graphically by plotting $1/N(a)$ on the Nyquist plot.

The problem would be how to select the right value of θ_a, which corresponds to a specific frequency ω_c. An iterative method can be used to solve this problem. This technique was already developed and decribed for the fractional-order controller of PI^{λ}, PD^{μ}, and $PI^{\lambda}D^{\mu}$ types [19]. Such method allows a flexible and direct selection of the parameters of the controller through the knowledge of the magnitude and phase of the plant at the frequency of interest, obtained with the relay test.

5. Implementation techniques

Implementation techniques for the FOC have been described in several works. Some proposals we can be found in the work [38]. An analogue implementation was proposed in the book [26] and a digital implementation was suggested in the book [6]. We will focus only on the digital implementation techniques. Having tuned the controllers, to implement them we have to take into account other considerations, such as memory size and computational load required by the algorithm, knowing that, in any case, the fractional orders must be approximated by integer ones.

5.1. Fractional derivative/integral approximation

In general, if a function $f(t)$ is approximated by a grid function, $f(kh)$, where h is the grid size, the approximation for its fractional derivative of order r can be expressed as [6, 20]:

$$y_h(kh) = h^{\mp r} \left(\omega\left(z^{-1}\right)\right)^{\pm r} f_h\left(kh\right), \tag{5.1}$$

where z^{-1} is the backward shift operator and $\omega\left(z^{-1}\right)$ is a generating function. This generating function and its expansion determine both the form of the approximation and the coefficients. In this way, the discretization of continuous fractional-order differentiator/integrator $s^{\pm r}$ $(r \in \mathrm{R})$ can be expressed as $s^{\pm r} \approx (\omega(z^{-1}))^{\pm r}$.

As a generating function $\omega(z^{-1})$ the following formula can be used in general [3]:

$$\omega(z^{-1}) = \left(\frac{1}{\beta T}\frac{1-z^{-1}}{\gamma + (1-\gamma)z^{-1}}\right), \tag{5.2}$$

where β and γ are denoted the gain and phase tuning parameters, respectively, and T is the sampling period. For example, when $\beta = 1$ and $\gamma = \{0, 1/2, 7/8, 1, 3/2\}$, the generating function (5.2) becomes the forward Euler, the Tustin, the Al-Alaoui, the backward Euler, the implicit Adams rules, respectively. In this sense, the generating formula can be tuned more precisely.

The expansion of the generating functions can be done by Power Series Expansion (PSE) or Continued Fraction Expansion (CFE). It is very important to note that PSE scheme leads to approximations in the form of polynomials of degree p, that is, the discretized fractional-order derivative is in the form of FIR filters, which have only zeros. The CFE scheme leads to approximations in the form of rational function and the discretized fractional-order derivative is in the form of IIR filters.

Then, the resulting transfer function, approximating the fractional-order operators via PSE method, can be obtained by applying the relationship

$$D^{\pm r}(z) = \frac{Y(z)}{F(z)} \approx \text{ PSE}\left\{(\omega(z^{-1})^{\pm r}\right\}_p \simeq P_p(z^{-1}), \tag{5.3}$$

where $Y(z)$ is the Z transform of the output sequence $y(kT)$, $F(z)$ is the Z transform of the input sequence $f(kT)$, and PSE$\{u\}$ denotes the expression, which results from the power series expansion of the function u, $D^{\pm r}(z)$ denotes the discrete equivalent of the fractional-order operator, considered as processes, and $P_p(z^{-1})$ is the polynomial with degree p of variable z^{-1}.

The resulting discrete transfer function, approximating fractional-order operators via CFE method, can be expressed as:

$$\begin{aligned} D^{\pm r}(z^{-1}) &= \frac{Y(z)}{F(z)} \approx \text{CFE}\left\{(\omega(z^{-1}))^{\pm r}\right\}_{p,q} \\ &\simeq \frac{P_p(z^{-1})}{Q_q(z^{-1})} = \frac{p_0 + p_1 z^{-1} + \cdots + p_m z^{-m}}{q_0 + q_1 z^{-1} + \cdots + q_n z^{-n}}, \end{aligned}$$

where CFE$\{u\}$ denotes the continued fraction expansion of u; p and q are the orders of the approximation and P and Q are polynomials of degrees p and q. Normally, we can set $p = q = n$.

Both above described approximation techniques are usable for the FOC implementation in MATLAB, [29].

5.2. Control algorithm

Generally, the control algorithm can be based on the canonical form of IIR filter, which can be expressed as follows:

$$F(z^{-1}) = \frac{Y(z^{-1})}{U(z^{-1})} = \frac{b_0 + b_1 z^{-1} + b_2 z^{-2} + \cdots + b_M z^{-M}}{a_0 + a_1 z^{-1} + a_2 z^{-2} + \cdots + a_N z^{-N}}, \tag{5.4}$$

where $a_0 = 1$ for compatibility with the definitions used in MATLAB. Normally, we choose polynomials degrees (approximation order) $M = N$.

The FOC in the form of FIR or IIR filter can be directly implemented to any microprocessor based devices as for instance the PLC, PIC or IPC. A direct form of such implementation using canonical form with input $e(k)$ and output $u(k)$ range mapping to the interval 0 - UFOC [V] divided into two sections: initialization code and loop code. The pseudo-code for the position algorithm implementation of the discretized FOC controller has the following form [6, 9, 28]:

```
(* initialization code *)
scale := 32752; % input and output
order := 5; % order of approximation
U_FOC := 10; % input and output voltage
%  range: 5[V], 10[V], ...
a[0] := 1;   a[1] := ...; a[2] := ...;
a[3] := ...; a[4] := ...; a[5] := ...;
b[0] := ...; b[1] := ...; b[2] := ...;
b[3] := ...; b[4] := ...; b[5] := ...;
loop i := 0 to order do
s[i] := 0;
endloop

(* loop code *)
in := (REAL(input)/scale) * U_FOC;
feedback := 0;
feedforward := 0; loop i:=1 to order do
feedback := feedback - a[i] * s[i];
feedforward := feedforward + b[i] * s[i];
endloop
s[0] := in + a[0] * feedback;
out := b[0] * s[1] + feedforward;
loop i := order downto 1 do
s[i] := s[i-1];
endloop
output := INT(out*scale)/U_FOC;
```

The disadvantage with this solution is that the complete controller is calculated using floating point arithmetic.

There are many softwares for programming the above pseudocode. For example: Microchip MPLAB, HiTech C Compiler, PICBasic Pro, Structured Text, Automation Basic, Ladder Diagram, etc. These software kits provide us with simple communication between PC and the microprocessor, and control algorithm programming and loading to the memory of the microprocessor.

5.3. Controller inputs/outputs

The fractional-order controller input/output signals are normally analog signals. In the case of current outputs on module it is 0-20 mA or 4-20 mA. In the case of voltage outputs on module it is 0-10 V, ± 5 V or 0-5 V. It is important to note that AD/DA converter resolution (12-bits, 14-bits, ...) influences the precision. In some cases the actuator accepts only two values, on (logical 1) or off (logical 0). In such case, the cycle time τ_c is specified (fixed), and controller gives a pulse of width [1]:

$$\tau_p(t) = \frac{u(t) - u_{min}}{u_{max} - u_{min}} \tau_c \,.$$

The above approach is known as a pulse width modulation (PWM). Fig. 3 illustrates the principles of the PWM ($\tau_p(t) = f(u(t))$).

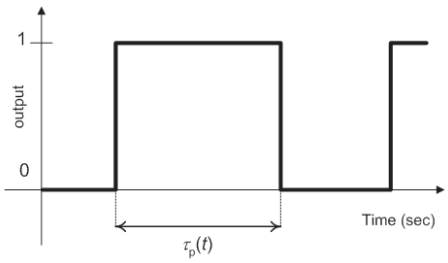

FIGURE 3. Pulse width modulation principle.

The output voltage range of TTL signal for many industrial devices is 24 V (log 1). The voltage range for analog signal is usually expressed in the form 0 - 10 V or as a number between 0 and 32767.

5.4. Devices for implementation of discrete FOC

There are many possibilities how to implenent a discrete FOC. Having a discrete transfer function in form of IIR or FIR filter we can use a general control algorithm described in previous subsection. Such algorithm can be implemented in any known processor devices as for example: IPC, PIC, AVR, PC with IO card or PLC [14, 21, 28]. Nowadays, the PLC plays a very important role in automation. It is necessary to have prepared the FOC algorithm for such devices and the form of function block e.g. FOC. Another possibility for implementing the controllers is the use of specific microelectronic devices, such as FPGA, FPAA and switched capacitors.

In addition, we will consider the PLC as the best solution for the FOC industrial implementation. The main advantages are: modular system with large memory and CPU speed, well developed SW environment, operating system (runtime) with solved service for interruption, AD/DA conversion, timing, etc. All tasks are located in n cyclic classes as it is depicted in Fig. 4. Each class has some priority and sampling time (period). We have to take into account that distribution of tasks to the cyclic classes is a very important role. Usually the cyclic class #1 has highest priority and so on. If the task in cyclic class #1 is not finished, task in cyclic class #2 does not start, etc. It is necessary to consider the time for AD (input reading) and DA (output writing) conversions and the time for task calculation itself. For instance if we have task FOC depicted in Fig. 4, the duration of task $\tau_{calc}(t) << T$, where T is the sampling period of certain class. This is the main reason why we need a good approximation of the fractional-order derivative/integral with an appropriate number of coefficients type (INT, REAL, ...), that will not occupy the memory of the PLC/IPC and will not consume the processor time.

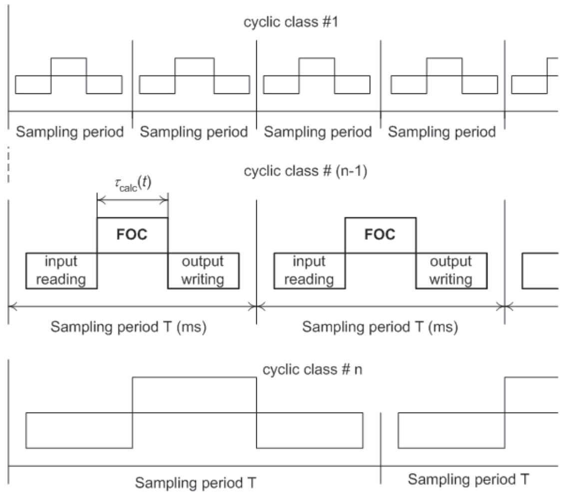

Figure 4. Cyclic classes in PLC runtime.

For sampling period T selection we can use common recommendations used for the integer-order system, which are described in standard control books (e.g. [11]).

6. Limitations on control system design

Typical sources for fundamental limitations in control systems design are, see [1]:

- *Process dynamics:* is very often the limiting factor, namely time delays, poles and zeros in the right half plane, gain of the system, etc.
- *Nonlinearities*: there are many reasons, why the nonlinearities should be considered. Let us show only few of them: nonlinear characteristic of the actuator, nonlinearity in the controlled plant, noise in measured signals, actuator saturation, and so on.

- *Disturbances*: disturbances and noise in measurement often limit the accuracy. The disturbances with combination of nonlinearity can limit for example the controller gain.
- *Process uncertainties*: process models are only approximation of reality. The process dynamic may change during the operation and therefore model parameters have some uncertainties, which can be compensated by changing the controller parameters.

7. Modifications of fractional-order control

Several modifications of the fractional-order control can be used. Among the most used ones are the following:

- *Filtering the desired value $r(t)$*: filtering the desired value $r(t)$ by first or second order filter is a very frequently used trick. Instead of step change of the desired value, which could be a problem especially for derivative part in controller, the control algorithm executes slow change of the desired value and changes of the control signal are not that extreme. For most applications, a first-order filter is satisfactory. We recommend the first-order prefilter in the form:

  $$H_p(z) = \frac{k_f}{1 - k_f z^{-1}},$$

  where k_f is the prefilter constant.
- *Using a controlled value in proportional and derivative parts of controller:* above-mentioned problem related to step changes of control signal due to step changes of desired value $r(t)$ can also be solved via replacing the control error $e(t) = r(t) - y(t)$ by controlled value $y(t)$. This modification can help a lot, especially, when desired value has changed rapidly and therefore the actuator becomes saturated (nonlinearity of actuator).
- *Filtering the derivative action:* due to noisy signal on measured controlled value, the differentiation of noise can involve inappropriate changes of control signal. Derivative action is more sensitive to higher-frequency terms in the inputs. Because of this the derivative part in the controller can be filtered by first- and second-order high frequency filter. For the first-order filter in derivative part and with a genuine integral action, we can write the transfer function of the fractional-order controller in the form:

  $$C(s) = \frac{U(s)}{E(s)} = K_p + T_i \frac{s^{1-\lambda}}{s} + \frac{T_d\, s^{\delta}}{T_f s + 1}, \quad (\lambda, \delta > 0), \tag{7.1}$$

where $T_f = N/T_d$ is the filter constant. For $N = 0$, we obtain the usual FOC described by relation (3.1).

- *Limitation of integral action:* this limitation is also known as wind-up of the controller. It is due to the fact that actuator has also limitations and for instance if the actuator is at the end position and the control error is not zero, integral part of the controller rapidly grows and the controller calculates unreal value of the control signal and therefore the actuator stays at the end position until the sign of control error is changed. This problem is known as wind-up or integral saturation and it can be solved via limitation of integral part in the controller. Another possibility of how to avoid wind-up is to introduce limiters of the desired values so that the controller output will never reach the actuator bounds.

Obviously there are many other modifications of the control algorithms, which help us to implement the fractional-order controller in practice. For instance, we can mention initial conditions for a non-impact controller connection to control loop, analog and digital filtering of measured values, etc.

8. Control performance assessment index

There are many sources of poor control performance in industrial processes. It has been estimated that almost 60% control systems have performance problem due to some reason, such as for example inadequate controller tuning, missing feed-forward compensation, inappropriate control structure, and so on. The natural question is: "How healthy is the control system?" The problem statement is depicted in Fig. 5.

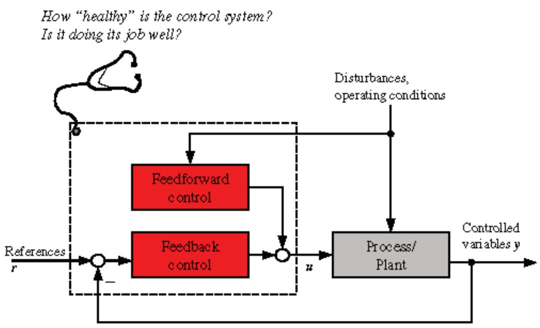

FIGURE 5. Control performance assessment problem formulation [12].

As mentioned in the book [1], the design, tuning and implementation of control strategies and controllers are only the first phase in the solution of a control problem. The second phase includes operation, supervision, and maintenance. After some time in operation, the control system performances may deteriorate because of variations in the process and the operation. Therefore it is important to supervise the control loop and detect these faults. One of the most widely used supervisory functions is based on the Harris index, where the idea is based on calculating the variance of the process output and then comparing it with the minimum variance obtainable. The Harris index is defined as

$$I_H = 1 - \frac{\sigma_{MV}^2}{\sigma_y^2},$$

where σ_{MV}^2 is the minimum variance of the process output, and σ_y^2 is the actual process output variance. The Harris index I_H can have value between zero and one. Such monitoring of the performances provides information about the loop performance compared to the ideal performance. The Harris index has been extended to multi-input multi-output systems as well.

If the control performance assessment shows that control system does not work properly, it is necessary to do a redesign of the control system and again calculate the performance indexes and compare them to alarm limits. The test procedure has been suggested in [12] and can be adopted also for the fractional-order control system.

9. Example: Application of FOC to temperature control

9.1. Control system description

The mathematical model of the object used as the system to be controlled has the form [27]:

$$G(s) = \frac{1}{39.69s^{1.26} + 0.598} \tag{9.1}$$

for which the parameters were obtained by an identification method based on the measured step response of the system depicted in Fig. 6.

The controller design was done in [27], according to the method (poles placement) described in [24], for desired stability measure $\sigma = 2.0$. The obtained fractional-order PD^δ controller designed for the fractional-order model (9.1) has continuous transfer function:

$$C(s) = 64.47 + 48.99s^{0.5}. \tag{9.2}$$

Let us consider the single input - single output feedback control system shown in Fig. 7, where $r(t)$ is the required value, $e(t)$ is control error, $u(t)$ is control value and $y(t)$ is actual controlled value. We have used prefilter as well as control signal limiters.

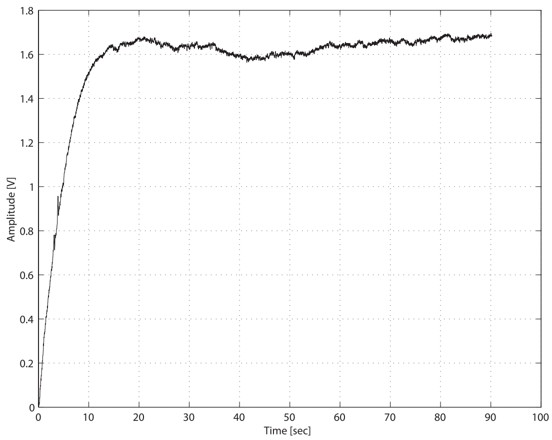

FIGURE 6. Unit-step response of controlled object.

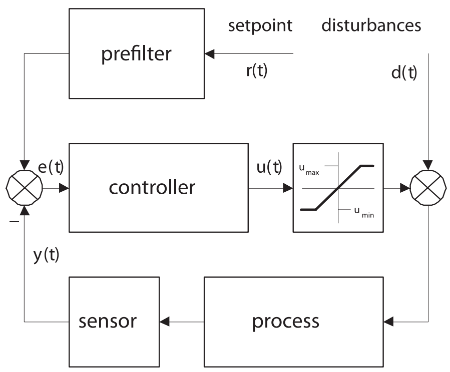

FIGURE 7. Experimental set-up HW loop.

Since the advantages of using a fractional controller in this particular case were shown in [27], in this section we compare two possible realizations of the fractional-order PD^{δ} controllers.

The first controller is the FOC implemented in the form of FIR filter and the second one is in the form of IIR filter.

For implementing the controllers a position algorithm with reference digital prefiltering has been used. This algorithm consists of several steps (calculating the control error, calculating the control value, etc.).

9.2. Experimental setup and results

The system to be controlled is a heater (electrical radiator). The temperature is measured by a radiating pyrometer, filtered by an analogue active filter, and driven to host PC with IO card PCL 812. The control signal from analogue output on the PCL card is connected to the actuator (thyristor changer) where 0-5V signal is changed to 20-220V. The reference value follows the law:

$$r[^oC] = \frac{330}{5} r[V] + 20 \,. \tag{9.3}$$

In the experiments the following parameters have been used:

- $T = 1$ sec, ($\simeq 1\%$ of the system rise time);
- $L = 100$ (order of the FIR filter);
- $k_f = 0.5$; (prefilter parameter);
- $p = q = 4$ (order of the IIR filter).

With these parameters, the implemented controllers are [36]:

$$\begin{aligned} C_R(z) &= 64.47 + 48.99 \frac{\sum_{k=0}^{100} (-1)^k \binom{0.5}{k} z^{100-k}}{z^{100}}, \\ C_T(z) &= 64.47 + 48.99 \times \\ &\times \frac{0.316z^4 - 1.038z^3 + 1.248z^2 - 0.645z + 0.119}{0.256z^4 - 0.639z^3 + 0.488z^2 - 0.078z - 0.027}. \end{aligned} \tag{9.4}$$

The transfer function of the digital prefilter is:

$$H_p(z) = \frac{0.5}{1 - 0.5z^{-1}}.$$

This prefiltering improved control loop performances e.g. less overshoot, etc. Usually, it is suitable to use the first-order system as a prefilter with time constant which corresponds to the time constant of controlled systems.

The simulation results are obtained by applying the controllers $C_R(z)$ and $C_T(z)$ to the process transfer function. Presented results consider the ideal case, that is, no actuator saturation and unity feedback. Simulated step responses of the controlled system with controllers $C_R(z)$ and $C_T(z)$ are shown in Fig. 8. In this figure it can be observed that the performances for both controllers are identical.

The measured step responses of the controlled system with controllers $C_R(z)$ and $C_T(z)$ are shown in Fig. 9. As in the case of simulations, the almost identical performances obtained with both controllers can be observed.

The advantage of using the second method for implementation is clear: while the controller $C_R(z)$ is a FIR filter of order 100, the controller $C_T(z)$ is

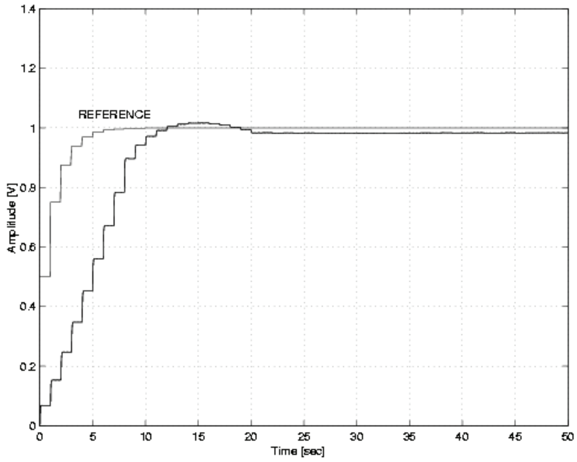

FIGURE 8. Simulated responses to unit-step input.

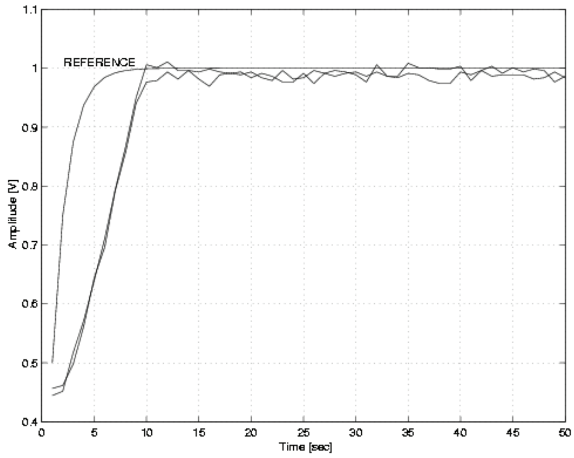

FIGURE 9. Measured responses to unit-step input.

an IIR filter of order 4. From the obtained results it can be concluded that for implementing the digital fractional controller it is highly interesting to use the generating function (Tustin rule) and continued fraction expansion, because it reduces, without performance degradation, the digital system requirements. This means that the implementation of $C_T(z)$ has reduced requirements on memory and computation time. Such form of the FOC implementation is also applicable in most industry applications.

10. Conclusions

In this paper we described a survey of tuning and implementation techniques for the fractional-order controllers. We demonstrated the mentioned methods on illustrative example, where a limitation due to nonlinearity as well as a modification (prefilter) have been considered.

Acknowledgements

This work is partially supported by grants VEGA: 1/0729/12, 1/0497/11, 1/0746/11, and grant APVV-0040-07.

This work was presented in part at The Fifth Symposium on Fractional Derivatives and Their Applications (FDTA'11) as a part of the joint conferences ASME (MESA & IDETC/CIEC), held in Washington, DC, USA, August 29-31, 2011.

References

[1] K. J. Astrom, T. Hagglund, *Advanced PID Control.* ISA (2006).
[2] K. J. Astrom, B. Wittenmark, *Adaptive Control: Second Edition.* Dover Publications (2008).
[3] R. S. Barbosa, J. A. T. Machado, M. F. Silva, Time domain design of fractional differintegrators using least-squares. *Signal Processing* **86** (2006), 2567–2581.
[4] R. S. Barbosa, M. F. Silva, J. A. T. Machado, Tuning and Application of Integer and Fractional Order PID Controllers. In: *Intelligent Engineering Systems and Computational Cybernetics*, Springer (2009).
[5] H. W. Bode, *Network Analysis and Feedback Amplifier Design.* Tung Hwa Book Company (1949).
[6] R. Caponetto, G. Dongola, L. Fortuna, I. Petráš, *Fractional Order Systems: Modeling and Control Applications.* World Scientific, Singapore (2010); http://www.worldscibooks.com/chaos/7709.html
[7] M. Caputo, Linear model of dissipation whose Q is almost frequency Independent - II. *Geophysical J. Royal Astronomic Society* **13** (1967), 529–539; Reprinted in: *Fract. Calc. Appl. Anal.* **11**, No 1 (2008), 3–14.
[8] Y. Q. Chen, Ubiquitous fractional order controls ?. In: *Proc. of the Second IFAC Symposium on Fractional Derivatives and Applications FDA'06*, July 19 - 21 (2006), Porto, Portugal (plenary talk paper).
[9] Y. Q. Chen, I. Petráš, D. Xue, Fractional order control - A Tutorial. In: *Proc. of the American Control Conference*, Hyatt Regency Riverfront, St. Louis, MO, USA June 10-12 (2009).
[10] Y. Q. Chen, Tuning method for fractional-order controllers, *United States Patent, US2006/0265085 A1*, USA (2006).

[11] R. C. Dorf, R. H. Bishop, *Modern Control Systems.* Addison-Wesley, New York (1990).

[12] M. Jelali, An overview of control performance assessment technology and industrial applications. *Contr. Eng. Pract.* **14** (2006), 441–466.

[13] Z. Jiao, Y. Q. Chen, Stability analysis of fractional-order systems with double noncommensurate orders for matrix case. *Fract. Calc. Appl. Anal.* **14**, No 3 (2011), 436-453; DOI: 10.2478/s13540-011-0027-3; at http://www.springerlink.com/content/1311-0454/14/3/

[14] P. Lanusse, J. Sabatier, PLC implementation of a CRONE controller. *Fract. Calc. Appl. Anal.* **14**, No 4 (2011), 505–522; DOI: 10.2478/s13540-011-0031-7; at http://www.springerlink.com/content/1311-0454/14/4/

[15] Y. Luo, Y. Q. Chen, Fractional-order [Proportional Derivative] Controller for Robust Motion Control: Tuning Procedure and Validation. In: *Prof. of the American Control Conference*, Hyatt Regency Riverfront, St. Louis, MO, USA, June 10-12 (2009).

[16] B. J. Lurie, Three-Parameter Tunable Tilt-Integral-Derivative (TID) Controller. *United States Patent, 5 371 670*, USA (1994).

[17] R. L. Magin, *Fractional Calculus in Bioengineering.* Begell House Publishers, Redding (2006); http://www.begellhouse.com/books/191e554a15da03bf.html

[18] S. Manabe, The Non-Integer Integral and its Application to Control Systems. *ETJ of Japan* **6**, No 3-4 (1961), 83–87.

[19] C. A. Monje, B. M. Vinagre, F. Feliu, Y. Q. Chen, Tuning and autotuning of fractional order controllers for industry applications. *Control Engineering Practice* **16** (2008), 798–812.

[20] C. A. Monje, Y. Q. Chen, B. M. Vinagre, D. Xue, V. Feliu, *Fractional Order Systems and Control - Fundamentals and Applications.* Advanced Industrial Control Series, Springer-Verlag, London (2010); http://www.springer.com/engineering/control/book/978-1-84996-334-3

[21] C. A. Monje, B. M. Vinagre, G. E. Santamara, I. Tejado, Auto-tuning of fractional order $PI^{\lambda}D^{\mu}$ controllers using a PLC. In: *Proc. of the 14th IEEE ETFA Conference*, Palma de Mallorca, Spain (2009).

[22] K. B. Oldham, J. Spanier, *The Fractional Calculus.* Academic Press, New York (1974).

[23] A. Oustaloup, *La Derivation Non Entiere: Theorie, Synthese et Applications.* Hermes, Paris (1995).

[24] I. Petráš, The fractional-order controllers: Methods for their synthesis and application. *J. Electr. Eng.* **50**, No 9-10 (1999), 284–288.

[25] I. Petráš, M. Hypiusova, Design of fractional-order controllers via H_∞ norm minimisation. In: *Selected Topics in Modelling and Control* **3** (2002), 50–54.
[26] I. Petráš, I. Podlubny, P. O'Leary, Ľ. Dorčák, B. M. Vinagre, *Analogue Realization of Fractional Order Controllers*. FBERG, Technical University of Košice (2002).
[27] I. Petráš, B. M. Vinagre, Practical application of digital fractional-order controller to temperature control. *Acta Montanistica Slovaca* **7**, No 2 (2002), 131–137.
[28] I. Petráš, Ľ. Dorčák, I. Podlubny, J. Terpák, P. O'Leary, Implementation of fractional-order controllers on PLC B&R 2005. In: *Proceedings of the ICCC2005*, Miskolc, Hungary, May 24-27 (2005), 141–144.
[29] I. Petráš, Discrete Fractional-Order PID Controller, Matlab Central File Exchange, MathWorks, Inc. (2011); http://www.mathworks.com/matlabcentral/fileexchange/33761
[30] I. Podlubny, Fractional-order systems and $PI^\lambda D^\mu$-controllers. *IEEE Transactions on Automatic Control* **44**, No 1 (1999), 208–214.
[31] I. Podlubny, *Fractional Differential Equations*. Academic Press, San Diego (1999).
[32] H. F. Raynaud, A. Zergainoh, State-space representation for fractional order controllers. *Automatica* **36** (2000), 1017–1021.
[33] G. E. Santamaria, I. Tejado, B. M. Vinagre, C. A. Monje, Fully automated tuning and implementation of fractional PID controllers. In: *Proc. of the ASME*, San Diego, CA, USA, Aug. 30 - Sept. 2 (2009).
[34] D. Valerio, J. Sa da Costa, Tuning-rules for fractional PID controllers. In: *Proc. of the 2nd IFAC Workshop on Fractional Differentiation and its Applications FDA'06*, Porto, Portugal, July 19 - 21 (2006).
[35] D. Valerio, J. Sa da Costa, A review of tuning methods for fractional PIDs. In: *Proc. of the 4th IFAC Workshop Fractional Differentiation and its Applications FDA'10*, Badajoz, Spain, October 18-20 (2010).
[36] B. M. Vinagre, I. Petráš, P. Merchan, Ľ. Dorčák, Two digital realizations of fractional controllers: Application to temperature control of a solid. In: *Proc. of the European Control Conference*, Porto, Portugal, September 4-7 (2001), 1764–1767.
[37] B. M. Vinagre, I. Petráš, I. Podlubny, Y. Q. Chen, Using Fractional order adjustment rules and fractional order reference models in model-reference adaptive control. *Nonlinear Dynamics* **29** (2002), 269–279.
[38] B. M. Vinagre, Y. Q. Chen, I. Petráš, Two direct Tustin discretization methods for fractional-order differentiator/integrator. *Journal of Franklin Institute* **340** (2003), 349–362.

[39] B. M. Vinagre, C. A. Monje, A. J. Calderon, J. I. Suarez, Fractional PID controllers for industry application. A brief introduction. *Journal of Vibration and Control* **13**, No 9-10 (2007), 1419–1429.

Institute of Control and Informatization of Production Processes
Faculty of BERG, Technical University of Košice
B. Němcovej 3, 04200 Košice, SLOVAK Republic
e-mail: ivo.petras@tuke.sk
Received: December 21, 2011

Please cite to this paper as published in:
Fract. Calc. Appl. Anal., Vol. **15**, No 2 (2012), pp. 282–303;
DOI: 10.2478/s13540-012-0021-4

Recall that $P_j \in \mathbb{R}^{p\times p}$ and $W_j \in \mathbb{R}^{L\times L}$ for $j = 1,\cdots,L$. By [1, Properties (44,45)], (25) equals to

$$\sum_{j=1}^{L}\mathbb{E}\left\{\left\{I_L\otimes\left[\left(\overrightarrow{\boldsymbol{I}}_{pn_f}^{T}\otimes I_\ell\right)\cdot\left(I_{pn_f}\otimes\boldsymbol{\Theta}_f\right)\right]\right\}\cdot\left(W_j\otimes P_j\otimes I_{n_f}\right)\right.$$
$$\left.\cdot\left\{I_L\otimes\left[\left(I_{pn_f}\otimes\boldsymbol{\Theta}_f^T\right)\cdot\left(\overrightarrow{\boldsymbol{I}}_{pn_f}\otimes I_\ell\right)\right]\right\}\right\}$$
$$=\sum_{j=1}^{L}\mathbb{E}\left\{\left\{W_j\otimes\left[\left(\overrightarrow{\boldsymbol{I}}_{pn_f}^{T}\otimes I_\ell\right)\cdot\left(I_{pn_f}\otimes\boldsymbol{\Theta}_f\right)\cdot\left(P_j\otimes I_{n_f}\right)\right]\right\}\right.$$
$$\left.\cdot\left\{I_L\otimes\left[\left(I_{pn_f}\otimes\boldsymbol{\Theta}_f^T\right)\cdot\left(\overrightarrow{\boldsymbol{I}}_{pn_f}\otimes I_\ell\right)\right]\right\}\right\}.$$

Note that $P_j\otimes I_{n_f}\in\mathbb{R}^{pn_f\times pn_f}$, and equals to $(P_j\otimes I_{n_f})\otimes 1$; and $\boldsymbol{\Theta}_f\in\mathbb{R}^{\ell pn_f\times 1}$. Therefore,

$$\left(I_{pn_f}\otimes\boldsymbol{\Theta}_f\right)\cdot\left(P_j\otimes I_{n_f}\right)=\left(I_{pn_f}\otimes\boldsymbol{\Theta}_f\right)$$
$$\cdot\left[\left(P_j\otimes I_{n_f}\right)\otimes 1\right]=\left(P_j\otimes I_{n_f}\right)\otimes\boldsymbol{\Theta}_f.$$

Now by [1, Property (45)], (25) further reduces to

$$\sum_{j=1}^{L}\mathbb{E}\left\{\left\{W_j\otimes\left[\left(\overrightarrow{\boldsymbol{I}}_{pn_f}^{T}\otimes I_\ell\right)\cdot\left(\left(P_j\otimes I_{n_f}\right)\otimes\boldsymbol{\Theta}_f\right)\right]\right\}\right.$$
$$\left.\cdot\left\{I_L\otimes\left[\left(I_{pn_f}\otimes\boldsymbol{\Theta}_f^T\right)\cdot\left(\overrightarrow{\boldsymbol{I}}_{pn_f}\otimes I_\ell\right)\right]\right\}\right\}$$
$$=\sum_{j=1}^{L}\mathbb{E}\left\{\left(W_j\cdot I_L\right)\otimes\left[\left(\overrightarrow{\boldsymbol{I}}_{pn_f}^{T}\otimes I_\ell\right)\cdot\left(\left(P_j\otimes I_{n_f}\right)\otimes\boldsymbol{\Theta}_f\right)\right.\right.$$
$$\left.\left.\cdot\left(I_{pn_f}\otimes\boldsymbol{\Theta}_f^T\right)\cdot\left(\overrightarrow{\boldsymbol{I}}_{pn_f}\otimes I_\ell\right)\right]\right\}$$
$$=\sum_{j=1}^{L}W_j\otimes\left\{\left(\overrightarrow{\boldsymbol{I}}_{pn_f}^{T}\otimes I_\ell\right)\cdot\left[\left(P_j\otimes I_{n_f}\right)\otimes\mathbb{E}\left(\boldsymbol{\Theta}_f\cdot\boldsymbol{\Theta}_f^T\right)\right]\right.$$
$$\left.\cdot\left(\overrightarrow{\boldsymbol{I}}_{pn_f}\otimes I_\ell\right)\right\}$$
$$=\sum_{j=1}^{L}W_j\otimes\left\{\left(\overrightarrow{\boldsymbol{I}}_{pn_f}^{T}\otimes I_\ell\right)\cdot\left[\left(P_j\otimes I_{n_f}\right)\otimes\left(\Omega\otimes\Sigma_e\right)\right]\right.$$
$$\left.\cdot\left(\overrightarrow{\boldsymbol{I}}_{pn_f}\otimes I_\ell\right)\right\}$$
$$=\sum_{j=1}^{L}W_j\otimes\left[\overrightarrow{\boldsymbol{I}}_{pn_f}^{T}\cdot\left(P_j\otimes I_{n_f}\otimes\Omega\right)\cdot\overrightarrow{\boldsymbol{I}}_{pn_f}\right]\otimes\Sigma_e.$$

Now, by Lemma 4,

$$\overrightarrow{\boldsymbol{I}}_{pn_f}^{T}\cdot\left(P_j\otimes I_{n_f}\otimes\Omega\right)\cdot\overrightarrow{\boldsymbol{I}}_{pn_f}=tr\left(\Omega\cdot\left(P_j^T\otimes I_{n_f}\right)\right)$$
$$=tr\left(\left(P_j\otimes I_{n_f}\right)\cdot\Omega\right).$$

The second equality is due to $tr(M^T) = tr(M)$. Thus, (25) finally boils down to

$$\sum_{j=1}^{L}tr\left(\left(P_j\otimes I_{n_f}\right)\cdot\Omega\right)\cdot\left(W_j\otimes\Sigma_e\right). \quad (26)$$

On the other hand,

$$\mathbb{E}\left\{\left\{I_L\otimes\left[\left(\overrightarrow{\boldsymbol{I}}_{pn_f}^{T}\otimes I_\ell\right)\cdot\left(I_{pn_f}\otimes\boldsymbol{\Theta}_f\right)\right]\right\}\right.$$
$$\cdot\left[\left(\sum_{j=1}^{L}W_j^T\otimes P_j^T\right)\otimes I_{n_f}\right]$$
$$\left.\cdot\left\{I_L\otimes\left[\left(I_{pn_f}\otimes\boldsymbol{\Theta}_f^T\right)\cdot\left(\overrightarrow{\boldsymbol{I}}_{pn_f}^{T}\otimes I_\ell\right)\right]\right\}\right\}.$$

is the transpose of the matrix in (25), and hence equals to

$$\sum_{j=1}^{L}tr\left(\left(P_j\otimes I_{n_f}\right)\cdot\Omega\right)\cdot\left(W_j^T\otimes\Sigma_e\right). \quad (27)$$

Similarly,

$$\mathbb{E}\left\{\left\{I_L\otimes\left[\left(\overrightarrow{\boldsymbol{I}}_{pn_f}^{T}\otimes I_\ell\right)\cdot\left(I_{pn_f}\otimes\boldsymbol{\Theta}_f\right)\right]\right\}\cdot\left(-I_{pn_fL}\right)\right.$$
$$\left.\cdot\left\{I_L\otimes\left[\left(I_{pn_f}\otimes\boldsymbol{\Theta}_f^T\right)\cdot\left(\overrightarrow{\boldsymbol{I}}_{pn_f}^{T}\otimes I_\ell\right)\right]\right\}\right\}$$
$$=-tr(\Omega)\cdot\left(I_L\otimes\Sigma_e\right). \quad (28)$$

Now, substituting (26)–(28) into (24), (20) follows.

References

[1] J. Dong, M. Verhaegen, and F. Gustafsson, "Robust fault detection with statistical uncertainty in identified parameters," *IEEE Trans. Signal Process.*, vol. 60, no. 10, pp. 5064–5076, Oct. 2012.

[2] J. Gertler and D. Singer, "A new structural framework for parity equation based failure detection and isolation," *Automatica*, vol. 26, pp. 381–388, 1990.

[3] S. Qin and W. Li, "Detection and identification of faulty sensors in dynamic processes," *AIChE J.*, vol. 47, pp. 1581–1593, 2001.

[4] A. Chiuso, "On the relation between CCA and predictor-based subspace identification," *IEEE Trans. Autom. Control*, vol. 52, no. 10, pp. 1795–1812, 2007.

[5] Y. Wang, S. Ding, H. Ye, and G. Wang, "A new fault detection scheme for networked control systems subject to uncertain time-varying delay," *IEEE Trans. Signal Process.*, vol. 56, no. 10, pp. 5258–5268, 2008.

Identification of Parameters of a Half-Order System

Ivo Petráš, Dominik Sierociuk, and Igor Podlubny

***Abstract*—This correspondence presents the half-order system behavior and its parameter identification. The identification is based on fitting the measured data using the Mittag-Leffler function. The data were collected for a discharge of a half-order system. The values of parameters obtained by a new identification method are in good agreement with the calculated interval for theoretical values, which takes into account the manufacturing tolerances of the used electrical elements.**

***Index Terms*—Domino ladder, fractance, fractional calculus, fractional integrator, half-order system, Mittag-Leffler function.**

I. Fractional Calculus Introduction

Non integer order calculus (a. k. a fractional calculus) is more then 300 years old. However, only during recent decades has it become a powerful and widely used tool for better modeling, control of processes, and signal processing in many fields of science and engineering [1]–[9]. The term "fractional calculus" has some historical background

Manuscript received November 29, 2011; revised January 28, 2012 and June 12, 2012; accepted June 13, 2012. Date of publication June 25, 2012; date of current version September 11, 2012. The associate editor coordinating the review of this manuscript and approving it for publication was Dr. TaHsin Li. This work was partially supported by the Polish Ministry of Science and Higher Education Grant 4125/B/T02/2009/36 and the European Union in the framework of European Social Fund through the Warsaw University of Technology Development Programme (by Center for Advanced Studies WUT). This work was also supported in parts by the Slovak Grant Agency for Science under Grants 1/0497/11, 1/0746/11, 1/0729/12, and also by Grants SK-FR-0037-09, SK-PL-0052-09, SK-UA-0042-09, and SK-AT-0024-10.

I. Petráš and I. Podlubny are with Institute of Control and Informatization of Production Processes, BERG Faculty, Technical University of Košice, 042 00 Košice, Slovakia (e-mail: ivo.petras@tuke.sk; igor.podlubny@tuke.sk).

D. Sierociuk is with the Institute of Control and Industrial Electronics, Warsaw University of Technology, 00-661 Warsaw, Poland (e-mail: dsieroci@isep.pw.edu.pl).

Digital Object Identifier 10.1109/TSP.2012.2205920

and is used for denoting the theory of integration and differentiation of arbitrary real (not necessarily integer) order.

The standard notation for denoting the left-sided fractional-order differentiation of a function $f(t)$ defined in the interval $[a,b]$ is ${}_aD_t^\alpha f(t)$, with $\alpha \in R$. Sometimes a simplified notation $f^{(\alpha)}(t)$ or $d^\alpha f(t)/dt^\alpha$ is used. In some applications also right-sided fractional derivatives ${}_tD_b^\alpha f(t)$ are used, but in the present article we will use only left-sided fractional derivatives. Even from the notation one can see that evaluation of the left-sided fractional-order operators require the values of the function $f(t)$ in the interval $[a,t]$. When α becomes an integer number, this interval shrinks to the vicinity of the point t, and we obtain the classical integer-order derivatives as particular cases. There are several definitions of the fractional derivatives and integrals, but in this work we use only the Caputo definition of fractional differentiation, which can be written as [1]:

$$ {}_a^CD_t^\alpha f(t) = \frac{1}{\Gamma(n-\alpha)} \int_a^t \frac{f^{(n)}(\tau)}{(t-\tau)^{\alpha-n+1}} d\tau, \quad (n-1 \le \alpha < n), \tag{1} $$

where $\Gamma(z)$ is Euler's gamma function.

The Caputo definition (1) is extremely useful in the time domain studies, because the initial conditions for the fractional-order differential equations with the Caputo derivatives can be given in the same form as for the integer-order differential equations. This is an advantage in applied problems, which require the use of initial conditions containing starting values of the function and its integer-order derivatives $f(a), f^{'}(a), f^{''}(a), \ldots, f^{(n-1)}(a)$. Other definitions of fractional differentiation do not have such a convenient property.

The formula for the Laplace transform of the Caputo fractional derivative (1) has the form [1]:

$$ \int_0^\infty e^{-st}\, {}_0^CD_t^\alpha f(t) dt = s^\alpha F(s) - \sum_{k=0}^{n-1} s^{\alpha-k-1} f^{(k)}(0), \quad (n-1 \le \alpha < n). \tag{2} $$

If the process $f(t)$ is considered from the state of absolute rest, so $f(t)$ and its integer-order derivatives up to $(n-1)$-th order are equal to zero at the starting time $t=0$, then the Laplace transform of the α-th derivative of $f(t)$ is simply $s^\alpha F(s)$.

II. Fractional Devices

A. Fractances

A circuit that exhibits fractional-order behavior is called a fractance [1]. The fractance devices have the following characteristics [10]. First, the phase angle is constant independent of the frequency within a wide frequency band. Second, it is possible to construct a filter having a moderate frequency characteristics which can not be realized by using the conventional devices.

Generally speaking, there are three basic types of fractances. The most popular are a domino ladder circuit network [11] and a constant phase element [12]. Another type is a tree structure of electrical elements [10], and finally, we can consider a transmission line circuit (or symmetrical domino ladder [13]). The review of most of the previous efforts can be found in [14].

Design of fractances having given order α can be done easily using any of the rational approximations or a truncated continued fraction expansion (CFE), which also gives a rational approximation [15], [16]. Truncated CFE does not require any further transformation; a rational approximation based on any other methods must be first transformed to the form of a continued fraction; then the values of the electrical elements, which are necessary for building a fractance, are determined from the obtained finite continued fraction. If all coefficients of the obtained finite continued fraction are positive, then the fractance can be made of classical passive elements (resistors and capacitors). If some of the coefficients are negative, then the fractance can be made with the help of negative impedance converters [14], [15].

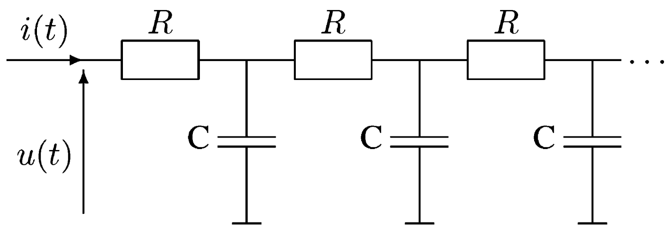

Fig. 1. Domino ladder scheme.

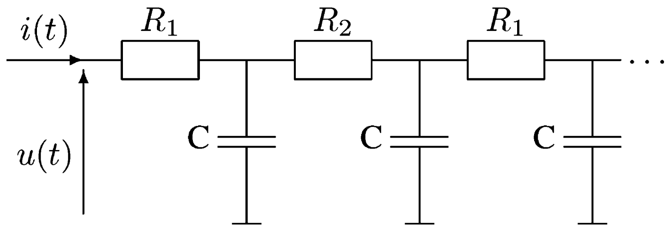

Fig. 2. Proposed analogue model of half-order integrator (capacitor).

B. Traditional Domino Ladder (Half-Order Integrator)

Several different algorithms for approximation the fractional order integrators are currently available (e.g., [11], [14], [17], [18]). Most of them are based on some form of approximation of irrational transfer functions in the complex domain. The commonly used approaches include the aforementioned CFE method and its modifications, or representation by a quotient of polynomials in s in a factorized form.

The main disadvantage of these algorithms is that the values of electrical elements (like resistors and capacitors) needed for the approximation are not the standard values of elements produced by manufacturers.

However, it is still possible to obtain highly accurate and practically usable implementations of a fractional-order integrator using only standard elements with the standard values available in the market. The idea of this practical approach to implementation of fractional-order systems is based on the domino ladder structure.

The domino ladder circuit shown in Fig. 1 has the following impedance [19]–[21]:

$$ Z(s) = R + \cfrac{1}{sC + \cfrac{1}{R + \cfrac{1}{sC + \cfrac{1}{R + \cfrac{1}{sC + \cfrac{1}{R + \cfrac{1}{sC + \cdots}}}}}}} = \sqrt{\frac{R}{C}} \frac{1}{s^{0.5}}. \tag{3} $$

In the ideal case of infinite realization, (3) gives a half-order integrator or capacitor; a truncated realization gives its approximation.

C. Domino Ladder With Alternating Resistors

For building an accurate analog approximation of the half-order integrator using easily accessible elements available in the market, the approach presented in Fig. 2 can be used.

Based on the observation made in article [22], we can formulate the following design algorithm:

a) Choose the values of R_1 and C in order to obtain the required low frequency limit.
b) Choose the value of R_2 in order to satisfy the condition $R_2 \approx 4R_1$. This condition allows one to select those values of resistors that are available as manufactured.

c) Choose the ladder length n (number of steps in the domino ladder) in order to obtain the desired frequency range of approximation.

Because the ladder shown in Fig. 2 is not a usual domino ladder circuit, for calculation of the impedance we cannot use the relationship (3), but we have to use a modified version in the form:

$$Z(s) = R_1 + \cfrac{1}{sC + \cfrac{1}{R_2 + \cfrac{1}{sC + \cfrac{1}{R_1 + \cfrac{1}{sC + \cfrac{1}{R_2 + \cfrac{1}{sC + \cdots}}}}}}} \tag{4}$$

and a n-truncated realization gives its approximation. In the ideal case of infinite realization, (4) gives a half-order integrator or a capacitor. If we consider a ladder that is long enough, we can write the following formula for the ladder impedance:

$$Z(s) \approx \frac{\sigma}{(Ts)^{0.5}} = \frac{1}{C^* s^{0.5}}, \tag{5}$$

where $T = C(R_1 + R_2)/2 = \sigma C$ is the time constant of the ladder and $\sigma = (R_1 + R_2)/2$ is the resistance per unit length of the ladder. As it has mentioned above, a domino ladder can be built to approximate a fractional order capacitor [23], with capacitance $C^* = T^{0.5}/\sigma = C/T^{0.5}$ as well. Physical unit of such capacitance is Farad/(second)$^{0.5}$, which is (second)$^{0.5}$/Ohm. The time constant T of the domino ladder can be expressed as $\mathrm{Farad} \times \mathrm{Ohm} = \mathrm{second}$. It is not consistent, so the time constant τ is used in order to maintain the physical unit consistency and desired unit of the impedance $Z(s)$ in Ohm.

Following the considerations in [24], we have to introduce the time scaling constant $\tau^{1-\alpha}$, where in our case $\alpha = 0.5$, to maintain a consistent set of units for the fractional-order system in Fig. 2. This gives the following modified domino ladder impedance in the general form:

$$\hat{Z}(s) = Z_{DL}(s) \approx \frac{\tau^{1-\alpha}\sigma}{(Ts)^{\alpha}} = \frac{\tau^{1-\alpha}}{C^* s^{\alpha}} = \frac{1}{\tau_{DL} s^{\alpha}}, \tag{6}$$

where $\tau_{DL} = C^*/\tau^{1-\alpha}$ and for $\alpha = 0.5$ we obtain the impedance in ohm of the half-order capacitor with a unit in farad. Scaling time constant τ has small value, i.e., $\tau = T_s$. Relation between the integer time scale and the fractional "transformed" time scale was clearly described in [25].

III. Experimental Results

A. Experimental Setup

The tested circuit has the following parameters of the circuit presented in Fig. 2: $R_1 = 2000\ \Omega, R_2 = 8200\ \Omega, C = 470$ nF, and numbers of steps in the ladders was taken $n = 130$. The sampling period was $T_s = 0.0001$ second. The manufacturing tolerance of the elements used for making such ladders is 1% for resistors and 20% for capacitors. For such values of the resistors and capacitors we obtain the following impedance of the domino ladder:

$$Z_{DL}(s) \approx \frac{1}{\tau_{DL} s^{0.5}}, \tag{7}$$

where the constant $\tau_{DL} = 9.5998 \times 10^{-4}$ is in Farad.

As we can observe in the Bode plots depicted in Fig. 3, the domino ladder with 130 steps approximates the half-order integral or capacitor over three decades, which is very good approximation. It is well known that ideal fractional integrator has phase $\phi(\omega) = -\alpha\pi/2$ and magnitude $M(\omega) = -20\alpha$ dB/dec. In our case for $\alpha = 0.5$ they are $\phi(\omega) = -45^\circ$ and $M(\omega) = -10$ dB/dec.

The electronic scheme presented in Fig. 4 uses two operational amplifiers. The first one is working in the half-order system configuration and the second one is working in the inverse unit-gain for compensating the signal inversion of the amplifier. The u_1 is an input and u_2 is an output of the half-order system.

For the experimental verification of the method introduced in this work, the circuit presented in Fig. 4 has been built. For measurements, the modified domino ladder circuit was connected to the amplifier electronic circuit of the operational amplifiers TL071 and to the dSPACE DS1103 DSP card connected to a computer with Matlab. We have chosen the TL071 specially because it has a circuit for compensating the DC offset. The actual laboratory setup is shown in Fig. 5.

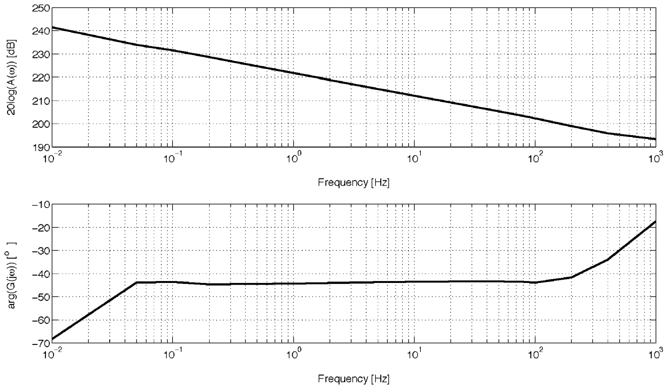

Fig. 3. Measured Bode plots of half-order integrator (capacitor) approximated by the domino ladder (4) of 130 steps with the values of electrical elements: $R_1 = 2000\ \Omega, R_2 = 8200\ \Omega$, and $C = 470$ nF.

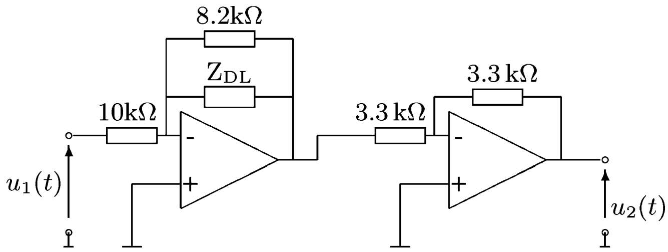

Fig. 4. Electronic circuit of measurement setup for half-order system.

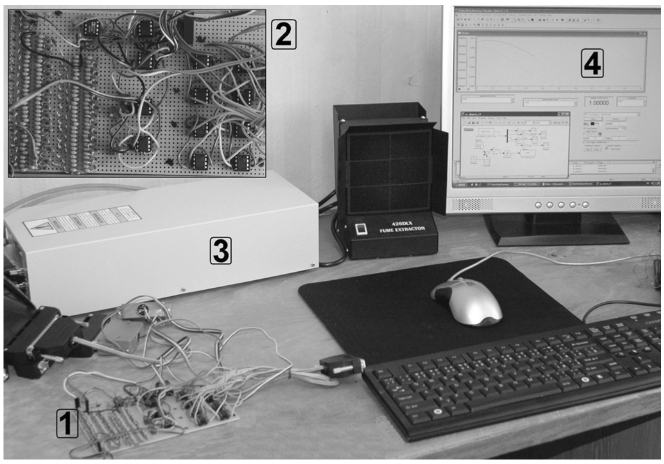

Fig. 5. Experimental setup used for measurements: 1—domino ladder, 2—detail of ladder, 3—dSPACE card, 4—computer with Matlab/Simulink SW.

B. Half-Order Model Derivation

The final impedance of the circuit presented in Fig. 4 is given as:

$$Z_f(s) = \frac{U_2(s)}{U_1(s)} = \frac{8200}{10000(8200\tau_{DL}s^{0.5}+1)} = \frac{0.82}{7.8719s^{0.5}+1}. \tag{8}$$

The time constant 7.8719 in the (8) of the circuit presented in Fig. 4 is in the unit of seconds, which is usual time constant of such circuit connection, also so called an inertial system.

The transfer function (8) corresponds with the fractional differential equation:

$$7.8719\,{}_0^C D_t^{0.5} u_2(t) + u_2(t) = 0.82 u_1(t). \tag{9}$$

Equation (9) can be rewritten to the form:

$${}_0^C D_t^{0.5} u_2(t) + 0.1270 u_2(t) = 0.1042 u_1(t), \tag{10}$$

where input voltage $u_1(t) = K$ and $u_2(0) = 0$ for charging the system, and $u_1(t) = 0$ and $u_2(0) = K$ for discharge of the system; where K is a constant voltage.

It is worth noting that constants in the fractional differential equation (10), which were obtained by calculation from electrical elements, are under some inaccuracy because of the mentioned electrical elements manufacturing tolerance (1% for resistors and 20% for capacitors). The estimated average error is approximately within $\pm 10\%$.

Based on the estimated tolerance, we can write the (10) in the following form with the interval parameters:

$${}_0^C D_t^{[0.45,0.55]} u_2(t) + [0.114, 0.139] u_2(t) = [0.093, 0.114] u_1(t), \tag{11}$$

that is, $\alpha \in [0.45, 0.55]$ and $a \in [0.114, 0.139]$. Alternatively, we can consider the domino ladder with $n = 130$ as a long enough and fix the order to $\alpha = 0.5$. In such case we get:

$${}_0^C D_t^{0.5} u_2(t) + [0.114, 0.139] u_2(t) = [0.093, 0.114] u_1(t). \tag{12}$$

In our case we use the (12) for the discharge, so $u_1(t) = 0$ and $u_2(0) = K$. Then the final form of the initial-value problem for the fractional differential equation describing the behavior of the considered half-order system is:

$$\begin{aligned} {}_0^C D_t^{0.5} u_2(t) + [0.114, 0.139] u_2(t) &= 0 \\ u_2(0) &= K \end{aligned} \tag{13}$$

C. Derivation of the Type of the Identification Problem

After the system is fully charged, the voltage $u_1(t)$ is switched off. After this, the discharge of the system is described by the equation for the voltage $u_2(t)$ in terms of the Caputo derivative:

$${}_0^C D_t^{\alpha} u_2(t) + a u_2(t) = 0 \tag{14}$$

The initial condition is the value of the voltage at the instance when the voltage $u_1(t)$ was switched off:

$$u_2(0) = K. \tag{15}$$

Since the Caputo derivative of a constant is zero, substitution

$$u_2(t) = y(t) + K \tag{16}$$

gives the problem

$${}_0^C D_t^{\alpha} y(t) + a y(t) = -aK, \quad y(0) = 0. \tag{17}$$

The Laplace transform gives:

$$Y(s)(s^{\alpha} + a) = -\frac{aK}{s} \tag{18}$$

and after rearrangement we have

$$Y(s) = -\frac{aKs^{-1}}{s^{\alpha}+a} \tag{19}$$

Using the inverse Laplace transform we obtain

$$y(t) = -aKt^{\alpha} E_{\alpha,\alpha+1}(-at^{\alpha}) \tag{20}$$

where $E_{\alpha,\beta}(z)$ is the Mittag-Leffler function defined as [1] (Matlab code with calculation algorithm is available in [26]):

$$E_{\alpha,\beta}(z) = \sum_{k=0}^{\infty} \frac{z^k}{\Gamma(\alpha k + \beta)}. \tag{21}$$

Returning to $u_2(t)$ and using the properties of the Mittag-Leffler function yields

$$u_2(t) = K\{1 - at^{\alpha} E_{\alpha,\alpha+1}(-at^{\alpha})\} = K E_{\alpha,1}(-at^{\alpha}). \tag{22}$$

D. Data Fitting Using the Mittag-Leffler Function

In order to obtain a model for the measured data, we have developed a new approach to data fitting, which is based on using the Mittag-Leffler function and which, in fact, allows obtaining models of non-integer order [27].

In the present article the measured data are fitted by the function of the same structure as (22), that is

$$y = y_0 E_{\alpha,1}(-at^{\alpha}), \tag{23}$$

The parameters to be identified are α, a, and y_0.

If the data are fitted by the function (23), then this means that they are modeled by the solution of the following initial-value problem for a two-term fractional-order differential equation containing the Caputo fractional derivative of order α:

$${}_0^C D_t^{\alpha} y(t) + a y(t) = 0, \quad y(0) = y_0. \tag{24}$$

E. Identification Results

The measurements were realized for the process of discharge of the inertial connection of a ladder depicted in Fig. 4. The data were collected for the time period of 1 sec. The measured data were fitted by the function

$$u_2(t) = K E_{\alpha,1}(-at^{\alpha}), \tag{25}$$

where the parameters α, K, a were subjects for identification.

For this purpose we created a Matlab routine "MLFFIT"; this routine is published at the Matlab Central File Exchange [28]. The results of the parameter identification are:

$$\alpha = 0.4820, \quad K = 1.2259, \quad a = 0.1364 \tag{26}$$

Since the infinite ladder should have the order equal to $\alpha = 0.5$, another attempt has been undertaken, where α was fixed as equal to 0.5, and only K and a were subjects for identification. In this case, we obtained:

$$\alpha = 0.5, \quad K = 1.2225, \quad a = 0.1341 \tag{27}$$

which is practically the same as the result of identification of all three parameters. This means that the ladder with $n = 130$ steps is long enough to be considered as an approximation of an infinite ladder.

Therefore, the process of discharge of a ladder in the studied circuit is described by the following initial value problem for a two-term fractional differential equation:

$$\begin{aligned} {}_0^C D_t^{0.5} u_2(t) + 0.1341 u_2(t) &= 0 \\ u_2(0) &= 1.2225 \end{aligned} \tag{28}$$

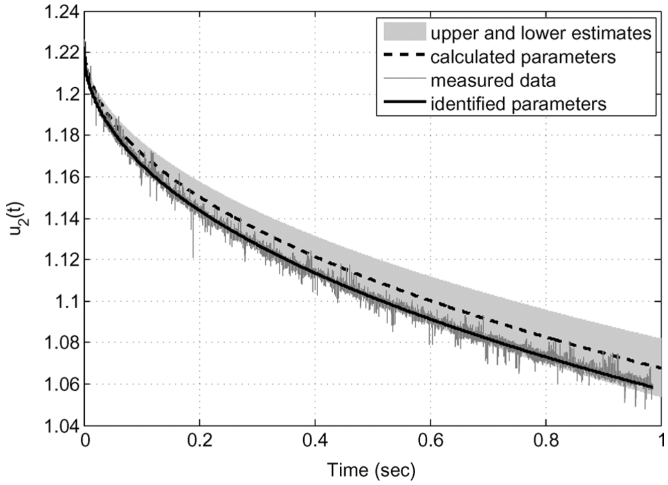

Fig. 6. Fitting half-order system discharge by the Mittag-Leffler function.

The measured data and the fitting curve are shown in Fig. 6. The parameters obtained by identification are very close to the calculated ones if we take into account the estimated errors due to the manufacturing tolerances of the electrical elements used in the studied circuit.

When using our MLFFIT routine for Matlab, it is worth remembering that the underlying Matlab function FMINSERCH used for minimization is based on simplex search method, which may sometimes lead to finding a local minimum instead of the global one; changing the initial guess is a standard approach in such situations.

IV. Discussion

As we can observe in Fig. 6, the measured data, mathematical model with the parameters obtained by identification and mathematical model with the parameters obtained by calculation fit very well. The identified model gives satisfactory results, the calculated mean square error is $\mathrm{MSE} = 2.94 \times 10^{-6}$. The response of the model with identified parameters is in the corridor of the possible responses for the model with calculated parameters expressed in the interval form because of the electrical elements tolerances. Even the measured data lie in this corridor, which confirm the correctness of our approach. It also confirms that estimation of the average error was correct.

The small difference between the calculated and the identified order α is due to the finite number of the domino ladder steps. In our case the number of steps was $n = 130$ and the order was identified as $\alpha = 0.4820$. Clearly, the theoretical value of the order, $\alpha = 0.5$, can be obtained only for the infinite ladder, which is physically unrealizable. In the considered case it has been demonstrated that the ladder with $n = 130$ is long enough to be considered as having order $\alpha = 0.5$ within some tolerance.

The presented half-order system can be used for additional experiments, such as measurement of responses to various inputs and also in control systems using fractional-order controllers [29], signal processing using new type of filters [30], new type of neural networks [31], and as well as for identification of the thermal processes [32].

V. Conclusion

In this work we have presented the experimental study of the half-order system behavior described by two-term fractional differential equation, and its parameters identification by a new Mittag-Leffler function fitting method. In order to have a good consistency of the parameter obtained by the identification and calculated parameters, a time scaling constant τ has been introduced, and also a different approach for calculation of the domino ladder constant. The obtained experimental results confirm the validity of our approach. Similar results were obtained in [33], where a fractional-order system described by three-term fractional differential equation was studied.

Besides the studied behavior of the considered half-order system, the variable-order behavior of domino ladder for long time intervals has been observed [27]. In the further work we will described a voltage distribution in a ladder circuit using the model based on fractional partial differential equations.

References

[1] I. Podlubny, *Fractional Differential Equations*. San Diego, CA: Academic, 1999.

[2] K. B. Oldham and J. Spanier, *The Fractional Calculus*. New York: Academic, 1974.

[3] R. L. Magin, *Fractional Calculus in Bioengineering*. Redding, CT: Begell House, 2006.

[4] C. A. Monje, Y. Q. Chen, B. M. Vinagre, D. Xue, and V. Feliu, *Fractional-order Systems and Controls*. London, U.K.: Springer, 2010.

[5] R. Caponetto, G. Dongola, L. Fortuna, and I. Petráš, *Fractional Order Systems: Modeling and Control Applications*. Singapore: World Scientific, 2010.

[6] A. Oustaloup, *La Derivation Non Entiere: Theorie, Synthese et Applications* (in French). Paris, France: Hermes, 1995.

[7] I. Petráš, *Fractional-Order Nonlinear Systems: Modeling, Analysis and Simulation*. London/Beijing: Springer/HEP, 2011.

[8] M. D. Ortigueira, "On the fractional linear scale invariant systems," *IEEE Trans. Signal Process.*, vol. 58, no. 12, pp. 6406–6410, 2010.

[9] S. Samadi, M. O. Ahmad, and M. N. S. Swamy, "Exact fractional-order differentiators for polynomial signals," *IEEE Signal Process. Lett.*, vol. 11, no. 6, pp. 529–532, 2004.

[10] M. Nakagawa and K. Sorimachi, "Basic characteristics of a fractance device," *IEICE Trans. Fundam.*, vol. E75-A, no. 12, pp. 1814–1818, 1992.

[11] S. D. Roy, "On the realization of a constant-argument immittance or fractional operator," *IEEE Trans. Circuit Theory*, vol. 14, no. 3, pp. 264–274, Sep. 1967.

[12] K. Biswas, S. Sen, and P. K. Dutta, "Realization of a constant phase element and its performance study in a differentiator circuits," *IEEE Trans. Circuits Syst. II, Exp. Brief*, vol. 53, no. 9, pp. 802–806, 2006.

[13] G. E. Carlson and C. A. Halijak, "Approximation of fractional capacitors $(1/s)^{1/n}$ by a regular Newton process," *IEEE Trans. Circuit Theory*, vol. 11, no. 2, pp. 210–213, 1964.

[14] I. Petráš, I. Podlubny, P. O'Leary, L. Dorčák, and B. M. Vinagre, "Analogue realization of fractional-order controllers," BERG Faculty, TU Košice, Slovakia, 2002.

[15] I. Podlubny, I. Petráš, B. Vinagre, P. O'Leary, and L. Dorčák, "Analogue realizations of fractional-order controllers," *Nonlinear Dynamics*, vol. 29, no. 1–4, pp. 281–296, 2002.

[16] S. Erfani, "Evaluation and realization of continued-fraction expansion revisited," *Comput. Electr. Eng.*, vol. 28, pp. 311–316, 2002.

[17] J. C. Wang, "Realizations of generalized Warburg impedance with RC ladder networks and transmission lines," *J. Electrochem. Soc.*, vol. 134, no. 8, pp. 1915–1920, Aug. 1987.

[18] A. S. Elwakil, "Fractional-order circuits and systems: An emerging interdisciplinary research area," *IEEE Circuits Syst. Mag.*, pp. 40–50, 4th Quart., 2010.

[19] S. Manabe, "The non-integer integral and its application to control systems," *ETJ Jpn.*, vol. 6, no. 3–4, pp. 83–87, 1961.

[20] K. B. Oldham, "Semiintegral electroanalysis: Analog implementation," *Analytic. Chem.*, vol. 45, no. 1, pp. 39–47, 1973.

[21] C. F. Lorenzo and T. T. Hartley, "Initialization, conceptualization, and application in the generalized fractional calculus," NASA, Lewis Research Center, Cleveland, OH, Rep. NASA/TP1998-208415, 1998.

[22] D. Sierociuk and A. Dzielinski, "New method of fractional order integrator analog modeling for orders $\alpha = 0.25$ and $\alpha = 0.5$," in *Proc. 16th Int. Conf. Methods Models Autom. Robot.*, Miedzyzdroje, Poland, Aug. 22–25, 2011.

[23] S. Westerlund and L. Ekstam, "Capacitor theory," *IEEE Trans. Dielectr. Electr. Insul.*, vol. 1, no. 5, pp. 826–839, 1994.

[24] R. Magin, X. Feng, and D. Baleanu, "Solving the fractional order bloch equation," *Concepts Magn. Reson.*, vol. 34A, pt. Part A, pp. 16–23, 2009.

[25] I. Podlubny, "Geometric and physical interpretation of fractional integration and fractional differentiation," *Fractional Calculus Appl. Anal.*, vol. 5, no. 4, pp. 367–386, 2002.
[26] I. Podlubny and M. Kacenak, "Mittag-Leffler Function," Matlab Central File Exchange, submission #8738 [Online]. Available: http://www.mathworks.com/matlabcentral/fileexchange/8738
[27] D. Sierociuk, I. Podlubny, and I. Petráš, "Experimental evidence of variable-order behavior of ladders and nested ladders," *IEEE Trans. Control Syst. Technol.*, 2012, DOI: 10.1109/TCST.2012.2185932, preprint.
[28] I. Podlubny, "Fitting Experimental Data Using the Mittag-Leffler Function," Matlab Central File Exchange, submission #32170 [Online]. Available: http://www.mathworks.com/matlabcentral/fileexchange/32170
[29] I. Podlubny, "Fractional-order systems and $\mathrm{PI}^{\lambda}\mathrm{D}^{\mu}$-controllers," *IEEE Trans. Autom. Control*, vol. 44, no. 1, pp. 208–213, 1999.
[30] R. Magin, M. D. Ortigueira, I. Podlubny, and J. Trujillo, "On the fractional signals and systems," *Signal Process.*, vol. 91, pp. 350–371, 2011.
[31] I. Petráš, "A note on the fractional-order cellular neural networks," in *Proc. IEEE Int. Joint Conf. Neural Netw. (IJCNN)*, Vancouver, BC, Canada, 2006, pp. 1021–1024.
[32] J. D. Gabano and T. Poinot, "Fractional modelling and identification of thermal systems," *Signal Process.*, vol. 91, pp. 531–541, 2011.
[33] Ľ. Dorčák, J. Terpák, I. Petráš, and F. Dorčáková, "Electronic realization of the fractional-order systems," *Acta Montan. Slovaca*, vol. 12, no. 3, pp. 231–237, 2007.

Enhancing the Resolution of the Spectrogram Based on a Simple Adaptation Procedure

Tsz K. Hon and Apostolos Georgakis

***Abstract*—This work is concerned with improving the quality of signal localization for the short-time Fourier transform by properly adjusting the size of its analysis window over time. The adaptation procedure involves the estimation of an area in the time-frequency plane which is more compact than the support of the fixed-window spectrogram. Then, at each time instant, the optimal window is selected such that the signal energy is maximized within the identified area. The proposed method achieves its objectives, and can compare favorably with alternative time-adaptive spectrograms as well as with advanced quadratic representations.**

***Index Terms*—Short-time Fourier transform, spectrogram, time-frequency analysis.**

I. Introduction

It is often useful to know the temporal distribution of the frequency content of a signal. A simple way to acquire this information is to perform the Fourier transform over short analysis intervals. The short-time Fourier transform (STFT) [1] remains to date the principal method for routine time-frequency (TF) analysis. Recent application examples of the STFT and its variants include signal denoising [2], [3], and instantaneous frequency estimation [4].

Manuscript received February 10, 2012; revised May 18, 2012 and June 20, 2012; accepted July 01, 2012. Date of publication July 13, 2012; date of current version September 11, 2012. The associate editor coordinating the review of this manuscript and approving it for publication was Prof. Yimin D. Zhang.

The authors are with the Division of Engineering, King's College London, London WC2R 2LS, U.K. (e-mail: tsz_kin.hon@kcl.ac.uk; apostolos.georgakis@kcl.ac.uk).

Digital Object Identifier 10.1109/TSP.2012.2208637

The STFT is simple, efficient, and robust. On the other hand, its performance is heavily dependent on the analysis window. In communities like speech and radar processing—for which the STFT has been a primary tool for decades—experience usually dictates the choice of this window. In general though, the selection is arbitrary, and this is why the STFT has been criticized as a heuristic method. What is worse, the application of a fixed window for the short-time analysis of the entire signal can be ineffective, since the signal may vary significantly over its lifespan.

Dealing with the window problem has been greatly facilitated by the fact that the STFT can be optimized locally. This has encouraged the development of methods for adapting the STFT to the local structure of the analyzed signal [5]–[9]. The associated methodologies can broadly be classified into two categories; those based on the conventional STFT definition, where the duration of the analysis window is usually the sole parameter optimized at each time instant, and those introducing modified versions of the STFT in which the window can be adjusted at every time-frequency location. Adapting the STFT both in time and frequency generally leads to computationally expensive algorithms. In addition, this degree of sophistication may be unnecessary in certain practical situations [7]. In such cases, the former class of methodologies is preferable because they combine good performance and efficient implementation.

In this work, we introduce a new method for the time adaptation of the STFT. In the following sections, we first briefly review the theoretical ideas underpinning our approach, and then provide a detailed account of the proposed scheme. Its performance is then illustrated by using test signals, and comparisons are made with other adaptive spectrograms as well as with renowned quadratic TF representations.

II. Theoretical Background

The following sections provide a brief overview of the main ideas pertaining to this work.

A. The Classical Short-Time Fourier Transform

The STFT of a signal $x(t)$ can be defined as [1]:

$$X(t,\omega;w_L) = \int w_L(t-\tau)x(\tau)e^{-j\omega\tau}\,d\tau, \quad (1)$$

where $w_L(t)$ is the short-time analysis window. This is typically a real and symmetric function centered at zero, tapering off to zero away from its centre such that its effective duration is L. Hence, at each time instant, (1) computes the Fourier transform of a short portion of the signal around t. Accordingly, the short-time energy-density spectrum $S(t,\omega;w_L)$ can be obtained as the squared magnitude of (1), i.e., $S_x(t,\omega;w_L) = |X(t,\omega;w_L)|^2$, and is commonly called the spectrogram. When a unit-energy window is used then the total energy of the spectrogram equals that of the signal.

There exists an elemental relationship between the spectrogram and the Wigner distribution (WD) $W_x(t,\omega) = \int x(t+\frac{\tau}{2})x^*(t-\frac{\tau}{2})e^{-j\omega\tau}d\tau$. Namely, the convolution of the WD of the signal with the WD of the STFT window renders the spectrogram, i.e.,

$$S_x(t,\omega;w_L) = \int\int W_x(t',\omega')W_{w_L}(t-t',\omega-\omega')\,dt'\,d\omega'. \quad (2)$$

The WD is widely recognized for its high TF concentration [10], [11]. On the other hand, it suffers from the presence of cross-term interference which limits its readability, and prevents it from being strictly positive. Although the process in (2) is known to eliminate interference and restore positivity, it also smears the signal in the TF plane. So, despite its relative advantages, the spectrogram yields inferior TF signal localization compared to the WD. This deterioration depends on

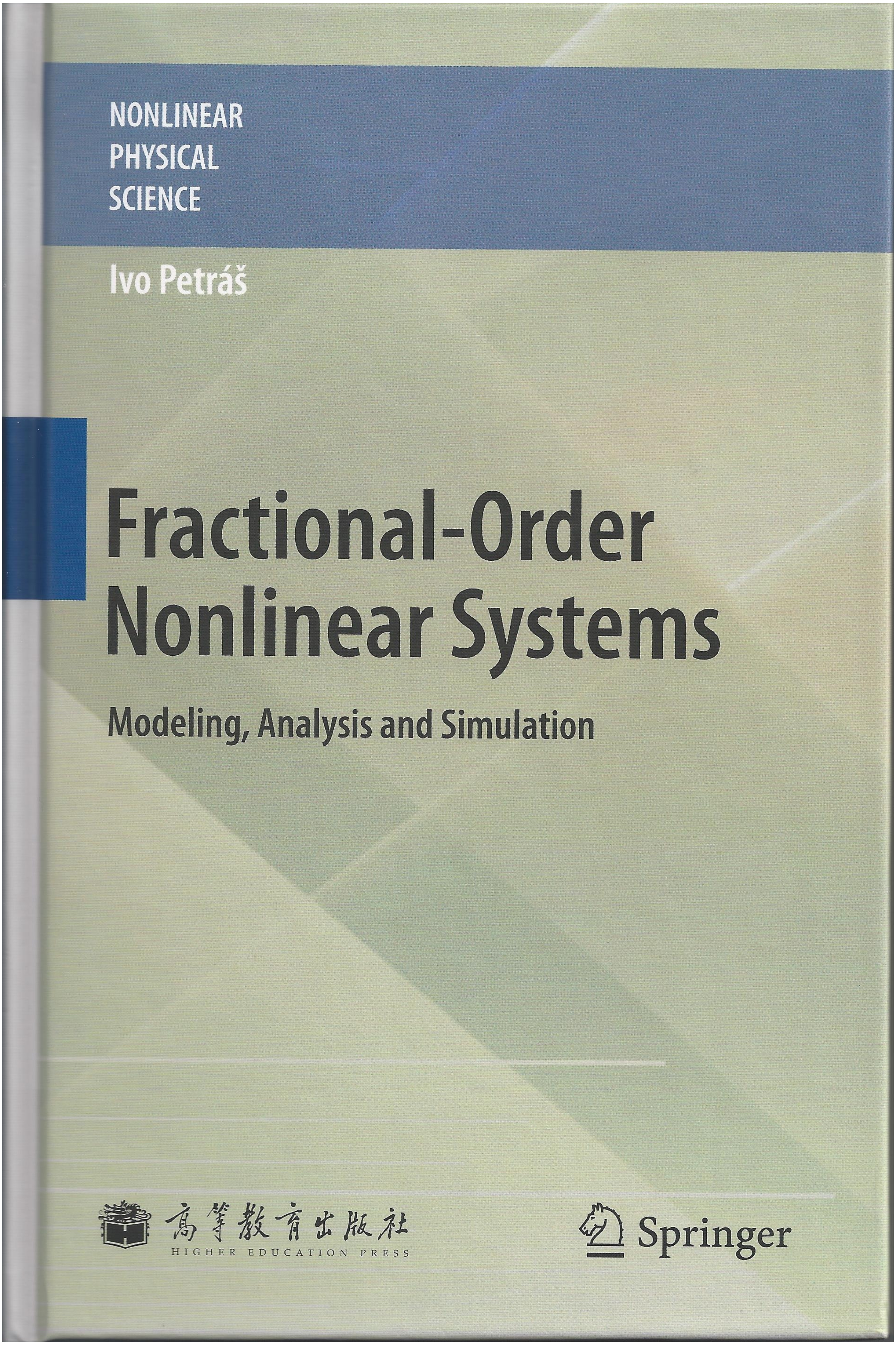
NONLINEAR
PHYSICAL
SCIENCE
Ivo Petráš
Fractional-Order
Nonlinear Systems
Modeling, Analysis and Simulation
高等教育出版社
HIGHER EDUCATION PRESS
Springer

NONLINEAR PHYSICAL SCIENCE

Nonlinear Physical Science focuses on recent advances of fundamental theories and principles, analytical and symbolic approaches, as well as computational techniques in nonlinear physical science and nonlinear mathematics with engineering applications.

Topics of interest in *Nonlinear Physical Science* include but are not limited to:

- New findings and discoveries in nonlinear physics and mathematics
- Nonlinearity, complexity and mathematical structures in nonlinear physics
- Nonlinear phenomena and observations in nature and engineering
- Computational methods and theories in complex systems
- Lie group analysis, new theories and principles in mathematical modeling
- Stability, bifurcation, chaos and fractals in physical science and engineering
- Nonlinear chemical and biological physics
- Discontinuity, synchronization and natural complexity in the physical sciences

Ivo Petráš

Fractional-Order Nonlinear Systems

Modeling, Analysis and Simulation

With 119 figures

高等教育出版社 HIGHER EDUCATION PRESS

Springer

Author
Ivo Petráš
Technical University of Košice, Faculty of BERG
Institute of Control and Information of Production Processes, B. Němcovej 3
042 00 Košice, Slovak Republic
Email: ivo.petras@tuke.sk

ISSN 1867-8440 e-ISSN 1867-8459
Nonlinear Physical Science

ISBN 978-7-04-031534-9
Higher Education Press, Beijing

ISBN 978-3-642-18100-9 e-ISBN 978-3-642-18101-6
Springer Heidelberg Dordrecht London New York

Library of Congress Control Number: 2011920976

Printed on acid-free paper

Springer is part of Springer Science+Business Media (www.springer.com)

NONLINEAR PHYSICAL SCIENCE

Nonlinear Physical Science focuses on the recent advances of fundamental theories and principles, analytical and symbolic approaches, as well as computational techniques in nonlinear physical science and nonlinear mathematics with engineering applications.

Series Editors: Albert C.J. Luo · Nail H. Ibragimov

Fractional-Order Nonlinear Systems
Modeling, Analysis and Simulation
Ivo Petráš

Fractional-Order Nonlinear Systems *Modeling, Analysis and Simulation* presents a study of fractional-order chaotic systems accompanied by Matlab programs for simulating their state space trajectories, which are shown in the illustrations in the book. Description of the chaotic systems is clearly presented and their analysis and numerical solution are done in an easy-to-follow manner. Simulink models for the selected fractional-order systems are also presented. Th e readers will understand the fundamentals of the fractional calculus, how real dynamical systems can be described using fractional derivatives and fractional diff erential equations, how such equations can be solved, and how to simulate and explore chaotic systems of fractional order.

The book addresses to mathematicians, physicists, engineers, and other scientists interested in chaos phenomena or in fractional-order systems. It can be used in courses on dynamical systems, control theory, and applied mathematics at graduate or postgraduate level.

Ivo Petráš is an Associate Professor of automatic control and the Director of the Institute of Control and Informatization of Production Processes, Faculty of BERG, Technical University of Košice, Slovak Republic. His main research interests include control systems, industrial automation, and applied mathematics.

PHYSICS

ISBN 978-7-04-031534-9
9 787040 315349
www.hep.com.cn

ISBN 978-3-642-18100-9
9 783642 181009
springer.com

Computers and Mathematics with Applications 61 (2011) 341–356

Contents lists available at ScienceDirect

Computers and Mathematics with Applications

journal homepage: www.elsevier.com/locate/camwa

Modeling and numerical analysis of fractional-order Bloch equations

Ivo Petráš *

Institute of Control and Informatization of Production Processes, Faculty of BERG, Technical University of Košice, B. Němcovej 3, 042 00 Košice, Slovak Republic

ARTICLE INFO

Article history:
Received 21 January 2010
Received in revised form 5 November 2010
Accepted 5 November 2010

Keywords:
Bloch equations
Fractional calculus
Fractional-order Bloch equations
Nuclear magnetic resonance

ABSTRACT

This paper deals with the Bloch equations which are a set of macroscopic equations that are used for modeling of nuclear magnetization as a function of time. These equations were introduced by Felix Bloch in 1946 and they are used for a description of the Nuclear Magnetic Resonance (NMR). This physical phenomenon is used in medicine, chemistry, physics, and engineering to study complex material. Fractional-order generalization of the Bloch equations was presented by Richard Magin et al. in 2008 as an opportunity to extend their use to describe a wider range of experimental situations involving heterogeneous, porous, or composite materials.

In this paper we describe numerical and simulation models (created for Matlab/Simulink) of the classical and the fractional-order Bloch equations. The behaviour and stability analysis of the Bloch equations are presented as well.

1. Introduction

Fractional calculus has been known for more then 300 years. These mathematical phenomena allow us to describe a real object more accurately than the classical "integer" order methods. The nature of real objects is "fractional" [1–3]. However, for many of them the fractionality is very low. A typical example of a fractional order system is the voltage–current relation of a semi-infinite lossy transmission line [4] or the diffusion of heat through a semi-infinite solid, where heat flow is equal to the half-derivative of the temperature [2].

At the present time there are many methods for approximation of fractional derivatives and integrals and fractional calculus can be easily used in wide areas of applications. Fractional order calculus plays an important role in physics [5,6], electrical engineering [7,8,3], control systems [9–11,1], robotics [12], signal processing [13,14], chemistry [15], chaos [16,17], bioengineering [18], etc.

In this paper, we offer an application of fractional calculus in NMR, which is modeled by Bloch equations. Basic definitions of fractional calculus, fractional order dynamic systems and numerical methods are presented first in Section 2. Then, stability conditions for the fractional order dynamical systems are introduced in Section 3. The integer-order and fractional-order Bloch equations are described and analyzed in Section 4. Additionally, several simulation examples are presented and commented in Section 5. Some concluding remarks are mentioned in Section 6. The code of the Matlab function is in Appendix.

2. Fractional calculus

2.1. Basic definitions and properties

Fractional calculus is a generalization of integration and differentiation to non-integer order fundamental operator ${}_aD_t^q$, where a and t are the bounds of the operation and $q \in \mathbb{R}$. The continuous integro-differential operator is defined as

* Tel.: +421 55 602 5194; fax: +421 55 602 5194.
E-mail address: ivo.petras@tuke.sk.

0898-1221/$ – see front matter © 2010 Elsevier Ltd. All rights reserved.
doi:10.1016/j.camwa.2010.11.009

$$
{}_aD_t^q = \begin{cases} \dfrac{\mathrm{d}^q}{\mathrm{d}t^q} & : q > 0, \\ 1 & : q = 0, \\ \displaystyle\int_a^t (\mathrm{d}\tau)^q & : q < 0. \end{cases}
$$

The most frequently used definitions for the general fractional differ-integral are: Grünwald–Letnikov (GL), Riemann–Liouville, Weyl, and Caputo's definition [15,2].

In this paper we will consider mainly the GL and Caputo's definitions. Both mentioned definitions are equivalent for a wide class of functions [2].

Definition 1. If we consider $n = \frac{t-a}{h}$, where a is a real constant, which expresses a limit value, we can write the GL definition as

$$
{}_aD_t^q f(t) = \lim_{h\to 0} \frac{1}{h^q} \sum_{j=0}^{[n]} (-1)^j \binom{q}{j} f(t - jh), \tag{1}
$$

where [.] means the integer part.

Definition 2. Caputo's definition of fractional derivatives can be written as

$$
{}_aD_t^q f(t) = \frac{1}{\Gamma(n-q)} \int_a^t \frac{f^{(n)}(\tau)}{(t-\tau)^{q-n+1}} \mathrm{d}\tau, \tag{2}
$$

for $(n - 1 < q < n)$.

The initial conditions for the fractional order differential equations with Caputo's derivatives are in the same form as for the integer-order differential equations.

Two general properties of the fractional-order derivative will be used. The first is a composition of a fractional with an integer-order derivative and the second is the property of linearity.

Property 1. *Similar to integer-order differentiation, fractional differentiation is a linear operation* [2]*:*

$$
{}_aD_t^q\left(\lambda f(t) + \mu g(t)\right) = \lambda\, {}_aD_t^q f(t) + \mu\, {}_aD_t^q g(t). \tag{3}
$$

Property 2. *The fractional-order derivative commutes with integer-order derivation* [2]*,*

$$
\frac{\mathrm{d}^n}{\mathrm{d}t^n}\left({}_aD_t^q f(t)\right) = {}_aD_t^q \left(\frac{\mathrm{d}^n f(t)}{\mathrm{d}t^n}\right) = {}_aD_t^{q+n} f(t), \tag{4}
$$

under the condition $t = a$ we have $f^{(k)}(a) = 0$, $(k = 0, 1, 2, \dots, n-1)$. The relationship (4) says the operators $\frac{\mathrm{d}^n}{\mathrm{d}t^n}$, $n \in \mathrm{N}$ and ${}_aD_t^q$, $q \in \mathrm{R}$ commute.

Some other properties and clear geometric and physical interpretations of the fractional integral and derivative are described in [19].

2.2. Fractional-order systems

The fractional-order linear time invariant (LTI) system can be represented by the following state–space model (e.g. [20,1,21])

$$
\begin{aligned} {}_0D_t^{\mathbf{q}} x(t) &= \mathbf{A}x(t) + \mathbf{B}u(t) \\ y(t) &= \mathbf{C}x(t), \end{aligned} \tag{5}
$$

where $x \in \mathrm{R}^n$, $u \in \mathrm{R}^r$ and $y \in \mathrm{R}^p$ are the state, input and output vectors of the system and $\mathbf{A} \in \mathrm{R}^{n\times n}$, $\mathbf{B} \in \mathrm{R}^{n\times r}$, $\mathbf{C} \in \mathrm{R}^{p\times n}$, and $\mathbf{q} = [q_1, q_2, \dots, q_n]^T$ are the fractional orders. If $q_1 = q_2 = \cdots q_n \equiv q$, system (5) is called a commensurate order system, otherwise it is an incommensurate order system.

2.3. Numerical methods

For numerical calculation of the fractional-order derivative we can use the relation (6) derived from the Grünwald–Letnikov definition (1). This approach is based on the fact that for a wide class of functions, two definitions — GL (1), and Caputo's (2) — are equivalent. The relation for the explicit numerical approximation of q-th derivative at the points kh $(k = 1, 2, \ldots)$ has the following form [2,13,9]:

$$_{(k-L/h)}D^q_{t_k} f(t) \approx h^{-q} \sum_{j=0}^{k} (-1)^j \binom{q}{j} f(t_{k-j}), \tag{6}$$

where L is the "memory length", $t_k = kh$, h is the time step of calculation and $(-1)^j \binom{q}{j}$ are binomial coefficients $c_j^{(q)}$ $(j = 0, 1, \ldots)$. For their calculation we can use the following expression [9]:

$$c_0^{(q)} = 1, \qquad c_j^{(q)} = \left(1 - \frac{1+q}{j}\right) c_{j-1}^{(q)}. \tag{7}$$

Then, the general numerical solution of the fractional differential equation

$$_aD^q_t y(t) = f(y(t), t),$$

can be expressed as

$$y(t_k) = f\,(y(t_k), t_k)\, h^q - \sum_{j=v}^{k} c_j^{(q)} y(t_{k-j}). \tag{8}$$

For the *memory term* expressed by a sum, a "short memory" principle can be used. Then the lower index of the sums in the relations (8) will be $v = 1$ for $k < (L/h)$ and $v = k - (L/h)$ for $k > (L/h)$, or without using the "short memory" principle, we put $v = 1$ for all k.

Obviously, for this simplification we pay a penalty in the form of some inaccuracy. If $f(t) \le M$, we can easily establish the following estimate for determining the memory length L, providing the required accuracy ϵ:

$$L \ge \left(\frac{M}{\epsilon|\Gamma(1-q)|}\right)^{1/q}. \tag{9}$$

An evaluation of the short memory effect and the convergence relation of the error between short and long memory were clearly described and also proved in [2].

For a numerical simulation of the fractional order system a method on the basis of the Adams–Bashforth–Moulton type predictor–corrector scheme has also been proposed [22,23]. It is suitable for Caputo's derivative because it just requires the initial conditions and for the unknown function it has a clear physical meaning. The method is based on the fact that the fractional differential equation

$$_0D^q_t y(t) = f(y(t), t), \qquad y^{(k)}(0) = y_0^{(k)}, \quad k = 0, 1, \ldots, m-1$$

is equivalent to the Volterra integral equation

$$y(t) = \sum_{k=0}^{[q]-1} y_0^{(k)} \frac{t^k}{k!} + \frac{1}{\Gamma(q)} \int_0^t (t-\tau)^{q-1} f(\tau, y(\tau))\mathrm{d}\tau. \tag{10}$$

Discretizing the Volterra equation (10) for a uniform grid created by $t_n = nh$ $(n = 0, 1, \ldots, N)$, $h = T_{\mathrm{sim}}/N$ and using the short memory principle (fixed or logarithmic [24]), we obtain a good numerical approximation of the true solution $y(t_n)$ of the fractional differential equation at preserving the order of accuracy. Assume that we have calculated approximations $y_h(t_j)$, $j = 1, 2, \ldots, n$ and we want to obtain $y_h(t_{n+1})$ by means of the equations

$$y_h(t_{n+1}) = \sum_{k=0}^{m-1} \frac{t_{n+1}^k}{k!} y_0^{(k)} + \frac{h^q}{\Gamma(\alpha+2)} f(t_{n+1}, y_h^p(t_{n+1})) + \frac{h^q}{\Gamma(\alpha+2)} \sum_{j=0}^{n} a_{j,n+1} f(t_j, y_n(t_j)), \tag{11}$$

where

$$a_{j,n+1} = \begin{cases} n^{q+1} - (n-q)(n+1)^q, & : \text{if } j = 0, \\ (n-j+2)^{q+1} + (n-j)^{q+1} + 2(n-j+1)^{q+1} & : \text{if } 1 \le j \le n, \\ 1, & : \text{if } j = n+1. \end{cases}$$

The preliminary approximation $y_h^p(t_{n+1})$ is called a predictor and it is given by

$$y_h^p(t_{n+1}) = \sum_{k=0}^{m-1} \frac{t_{n+1}^k}{k!} y_0^{(k)} + \frac{1}{\Gamma(q)} \sum_{j=0}^{n} b_{j,n+1} f(t_j, y_n(t_j)), \tag{12}$$

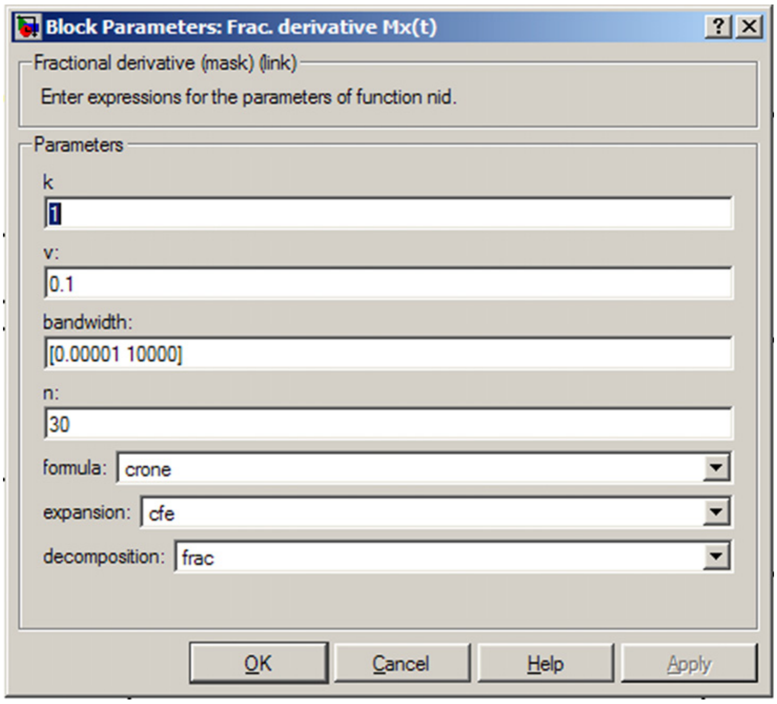

Fig. 1. Properties of the Simulink `nid` block.

where

$$b_{j,n+1} = \frac{h^q}{q}((n+1-j)^q - (n-j)^q). \tag{13}$$

A slightly improved predictor–corrector approach for solving the Fokker–Planck equation has been noted in [22,25]. A collection of the various numerical algorithms was also presented in [26].

A detailed review of the various approximation methods and techniques (Carlson's [8], Charef's [27], CRONE-Oustaloup's [28], etc.) for continuous and discrete fractional-order models in the form of IIR and FIR filters was done in the work [13]. Some other approaches were described in the work [29]. Here, we also should mention the approach proposed by Hwang, which is based on the B-splines function [30] and Podlubny's matrix approach for linear fractional differential equations and a set of such equations [31,32].

For comparison, we can mention methods described in [13,27] which lead to an approximation in the IIR form. Some of the mentioned frequency methods in both forms of approximations have been realized as the Matlab routines in Duarte Valerio's toolbox called `ninteger` (see a detailed review in [33]). In this toolbox was also created a Simulink block `nid` for fractional derivatives and integrals (see Fig. 1), where the order of the derivative/integral and the method of its approximation can be selected. We will use this block for creating the fractional-order system model in Matlab/Simulink (see e.g. [34]).

3. Stability of the fractional-order LTI system

However, we cannot directly use an algebraic tool as for example the Routh–Hurwitz criteria for the fractional order system because we do not have a characteristic polynomial but pseudo-polynomials with rational powers—*multivalued function*.

When dealing with incommensurate fractional order systems (or, in general, with fractional order systems) it is important to bear in mind that $P(s^q)$, $q \in \mathrm{R}$ is a multivalued function of s^q (s is a Laplace operator), $q = \frac{u}{v}$, the domain of which can be viewed as a Riemann surface with a finite number of Riemann sheets v, where the origin is a branch point and the branch cut is assumed at R^-. Function s^q becomes holomorphic in the complement of the branch cut line. It is a fact that in multivalued functions only the first Riemann sheet has its physical significance (see e.g. [35,21]).

As we can see in the previous subsection, in the fractional case, the stability is different from the integer one. An interesting notion is that a stable fractional system may have roots in the right half of the complex w-plane (see Fig. 2). Since the principal sheet of the Riemann surface is defined as $-\pi < \arg(s) < \pi$, by using the mapping $w = s^q$, the corresponding w domain is defined by $-q\pi < \arg(w) < q\pi$, and the w plane region corresponding to the right half plane of this sheet is defined by $-q\pi/2 < \arg(w) < q\pi/2$.

Mapping the poles from the s^q-plane into the w-plane, where $q \in \mathrm{Q}$ such as $q = \frac{k}{m}$ for $k, m \in \mathrm{N}$ and $|\arg(w)| = |\phi|$, can be done by the following rule: if we assume $k = 1$, then the mapping from the s-plane to the w-plane is independent of k. The unstable region from the s-plane transforms to sector $|\phi| < \frac{\pi}{2m}$ and the stable region transforms to sector $\frac{\pi}{2m} < |\phi| < \frac{\pi}{m}$.

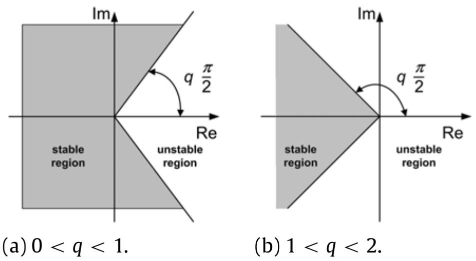

Fig. 2. Stability regions of the fractional-order system in complex w-plane.

The region where $|\phi| > \frac{\pi}{m}$ is not physical. Therefore, the system will be stable if all roots in the w-plane lie in the region $|\phi| > \frac{\pi}{2m}$.

Theorem 1 *([36–39]). It has been shown that commensurate system (5) is stable if the following condition is satisfied (also if the triplet* **A**, **B**, **C** *is minimal):*

$$|\arg(\mathrm{eig}(\mathbf{A}))| > q\frac{\pi}{2}, \tag{14}$$

where $0 < q < 2$ *and* $\mathrm{eig}(\mathbf{A})$ *represents the eigenvalues of matrix* **A**.

Theorem 2 *([40]). Consider the following autonomous system for the internal stability definition:*

$${}_0D_t^{\mathbf{q}}x(t) = \mathbf{A}x(t), \qquad x(0) = x_0, \tag{15}$$

with $\mathbf{q} = [q_1, q_2, \ldots, q_n]^T$ *and its n-dimensional representation:*

$$\begin{aligned}
{}_0D_t^{q_1}x_1(t) &= a_{11}x_1(t) + a_{12}x_2(t) + \cdots + a_{1n}x_n(t)\\
{}_0D_t^{q_2}x_2(t) &= a_{21}x_1(t) + a_{22}x_2(t) + \cdots + a_{2n}x_n(t)\\
&\ldots\\
{}_0D_t^{q_n}x_n(t) &= a_{n1}x_1(t) + a_{n2}x_2(t) + \cdots + a_{nn}x_n(t)
\end{aligned} \tag{16}$$

where all q_i*'s are rational numbers between 0 and 2. Assume m to be the least common multiple of the denominators* u_i*'s of* q_i*'s, where* $q_i = v_i/u_i$, $v_i, u_i \in Z^+$ *for* $i = 1, 2, \ldots, n$ *and we set* $\gamma = 1/m$. *Define:*

$$\det\begin{pmatrix} \lambda^{mq_1} - a_{11} & -a_{12} & \cdots & -a_{1n}\\ -a_{21} & \lambda^{mq_2} - a_{22} & \cdots & -a_{2n}\\ \cdots & & & \\ -a_{n1} & -a_{n2} & \cdots & \lambda^{mq_n} - a_{nn}\end{pmatrix} = 0. \tag{17}$$

The characteristic equation (17) can be transformed to an integer order polynomial equation if all q_i*'s are rational numbers. Then the zero solution of system (16) is globally asymptotically stable if all roots* λ_i*'s of the characteristic (polynomial) equation (17) satisfy*

$$|\arg(\lambda_i)| > \gamma\frac{\pi}{2} \quad \text{for all } i.$$

Denote λ *by* s^γ *in Eq. (17), we get the characteristic equation in the form* $\det(s^\gamma I - A) = 0$.

4. Bloch equations

4.1. Integer-order Bloch equations

In physics and bio-engineering, specifically in NMR or magnetic resonance imaging the Bloch equations are a set of macroscopic equations that are used to calculate the nuclear magnetization $\mathbf{M} = (M_x(t), M_y(t), M_z(t))$ as a function of time when relaxation times are T_1 (spin–lattice) and T_2 (spin–spin). These equations were introduced by Felix Bloch in 1946 and can be expressed in the following form [41]:

$$\begin{aligned}
\frac{\mathrm{d}M_x(t)}{\mathrm{d}t} &= \gamma(\mathbf{M}(t) \times \mathbf{B}(t))_x - \frac{M_x(t)}{T_2},\\
\frac{\mathrm{d}M_y(t)}{\mathrm{d}t} &= \gamma(\mathbf{M}(t) \times \mathbf{B}(t))_y - \frac{M_y(t)}{T_2},\\
\frac{\mathrm{d}M_z(t)}{\mathrm{d}t} &= \gamma(\mathbf{M}(t) \times \mathbf{B}(t))_z - \frac{M_z(t) - M_0}{T_1},
\end{aligned} \tag{18}$$

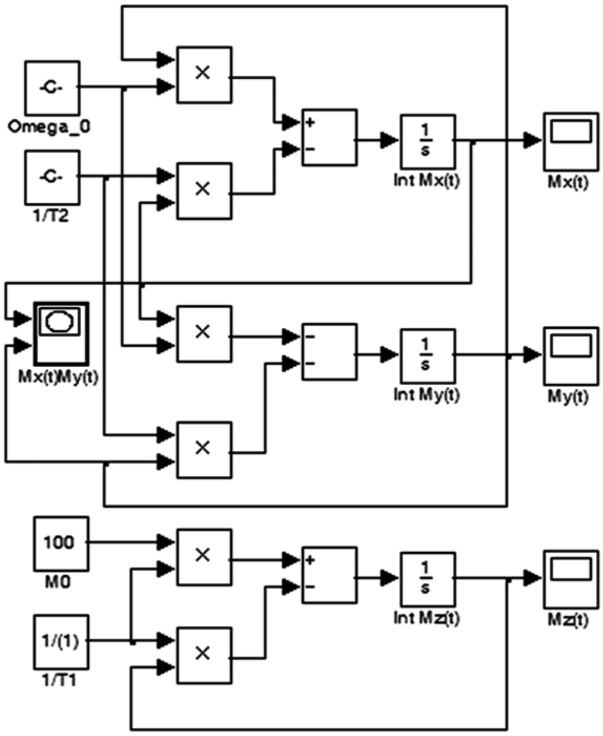

Fig. 3. Simulink model of Eqs. (21).

where $\gamma/2\pi$ is the gyromagnetic ratio, $\mathbf{B}(t) = (B_x(t), B_y(t), B_0 + \Delta B_z(t))$ is the magnetic field experienced by the nuclei, and M_0 is the equilibrium magnetization.

However, the relaxation terms describe the return to equilibrium, but only for a field pointing along the z-axis, the Bloch equations (18) for the constant static magnetic field B_0 (z-component) reduce to the equations [42]

$$\begin{aligned} \frac{\mathrm{d}M_x(t)}{\mathrm{d}t} &= \omega_0 M_y(t) - \frac{M_x(t)}{T_2}, \\ \frac{\mathrm{d}M_y(t)}{\mathrm{d}t} &= -\omega_0 M_x(t) - \frac{M_y(t)}{T_2}, \\ \frac{\mathrm{d}M_z(t)}{\mathrm{d}t} &= \frac{M_0 - M_z(t)}{T_1}, \end{aligned} \tag{19}$$

where $\omega_0 = \gamma B_0$ and $\omega_0 = 2\pi f_0$ (e.g. gyromagnetic ratio $\gamma/2\pi = f_0/B_0 = 42.57$ MHz/T for water protons).

The complete set of analytical solutions is [42]

$$\begin{aligned} M_x(t) &= \mathrm{e}^{-t/T_2}(M_x(0)\cos\omega_0 t + M_y(0)\sin\omega_0 t) \\ M_y(t) &= \mathrm{e}^{-t/T_2}(M_y(0)\cos\omega_0 t - M_x(0)\sin\omega_0 t) \\ M_z(t) &= M_z(0)\mathrm{e}^{-t/T_1} + M_0(1 - \mathrm{e}^{-t/T_1}). \end{aligned} \tag{20}$$

The equilibrium or steady-state solution can be found from the asymptotic limit $t \to \infty$ of (20).

The state Bloch equations (19) are given by using the integration operation and have the form:

$$\begin{aligned} M_x(t) &= \int_0^t \left[\omega_0 M_y(t) - \frac{M_x(t)}{T_2}\right] \mathrm{d}t, \\ M_y(t) &= \int_0^t \left[-\omega_0 M_x(t) - \frac{M_y(t)}{T_2}\right] \mathrm{d}t, \\ M_z(t) &= \int_0^t \left[\frac{M_0 - M_z(t)}{T_1}\right] \mathrm{d}t. \end{aligned} \tag{21}$$

The system model developed from the state equations (21) by using the Matlab/Simulink environment is depicted in Fig. 3.

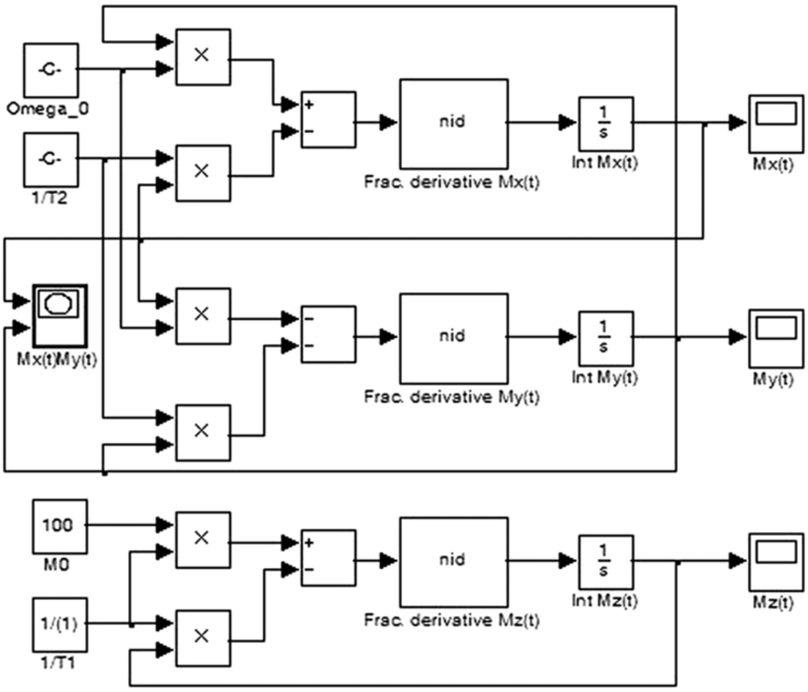

Fig. 4. Simulink model of Eqs. (23).

4.2. Fractional-order Bloch equations

Now, we consider the fractional-order Bloch equations, where integer-order derivatives are replaced by fractional-order ones. A mathematical description of the fractional-order system with Caputo's derivatives is expressed as [43]

$$\begin{aligned} {}_0D_t^{q_1} M_x(t) &= \omega_0' M_y(t) - \frac{M_x(t)}{T_2'}, \\ {}_0D_t^{q_2} M_y(t) &= -\omega_0' M_x(t) - \frac{M_y(t)}{T_2'}, \\ {}_0D_t^{q_3} M_z(t) &= \frac{M_0 - M_z(t)}{T_1'}, \end{aligned} \tag{22}$$

where q_1, q_2, and q_3 are the derivative orders. The total order of the system is $\bar{q} = (q_1, q_2, q_3)$. Here, ω_0', T_1', and T_2' have the units of $(s)^{-q}$ to maintain a consistent set of units for the magnetization.

An analytical solution of the fractional-order Bloch equations (22) based on the Mittag-Leffler function has been derived and discussed in [43].

The state expression of the fractional-order Bloch equations (22) with parameters ω_0', T_1', and T_2' are given by using the integration operation and the properties (3) and (4) and have the form:

$$\begin{aligned} M_x(t) &= {}_0D_t^{1-q_1}\left(\int_0^t \left[\omega_0' M_y(t) - \frac{M_x(t)}{T_2'}\right] \mathrm{d}t\right), \\ M_y(t) &= {}_0D_t^{1-q_2}\left(\int_0^t \left[-\omega_0' M_x(t) - \frac{M_y(t)}{T_2'}\right] \mathrm{d}t\right), \\ M_z(t) &= {}_0D_t^{1-q_3}\left(\int_0^t \left[\frac{M_0 - M_z(t)}{T_1'}\right] \mathrm{d}t\right). \end{aligned} \tag{23}$$

The system model developed from the state equations (23) for system parameters ω_0', T_1', and T_2' by using the Matlab/Simulink environment is depicted in Fig. 4.

5. Simulation results

For simulation purposes, we can use models created for Matlab/Simulink described in the previous section or we can derive a numerical solution of the fractional Bloch equations (22) using one of the methods (Grñwald–Letnikov or Adams–Bashforth–Moulton) described in Section 2. As it has been shown in paper [16], both numerical methods have approximately the same order of accuracy and a good match of numerical solutions. Because of this, we will derive a numerical solution of Bloch equations (22) by using the relationship (8), which leads to an easier numerical solution in

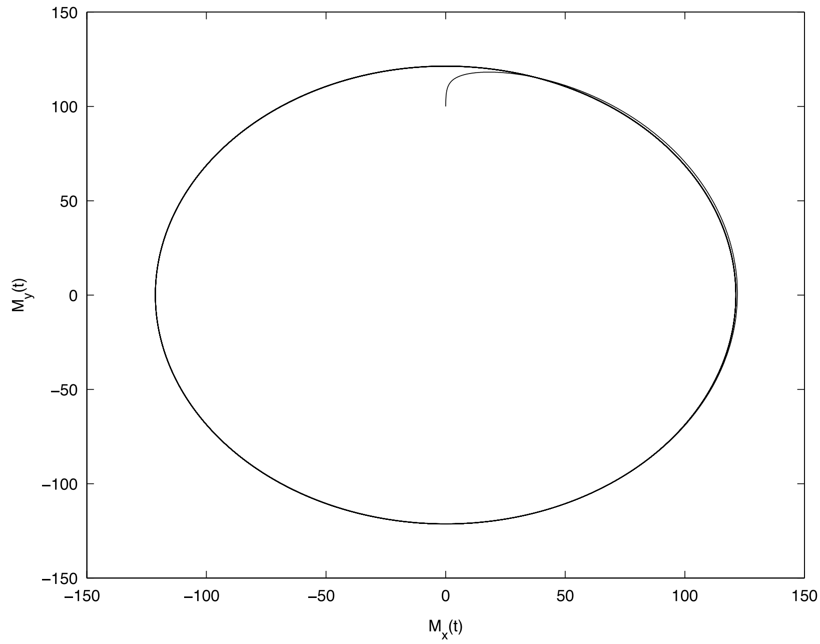

(a) 2D: ($M_x(t)$ vs. $M_y(t)$).

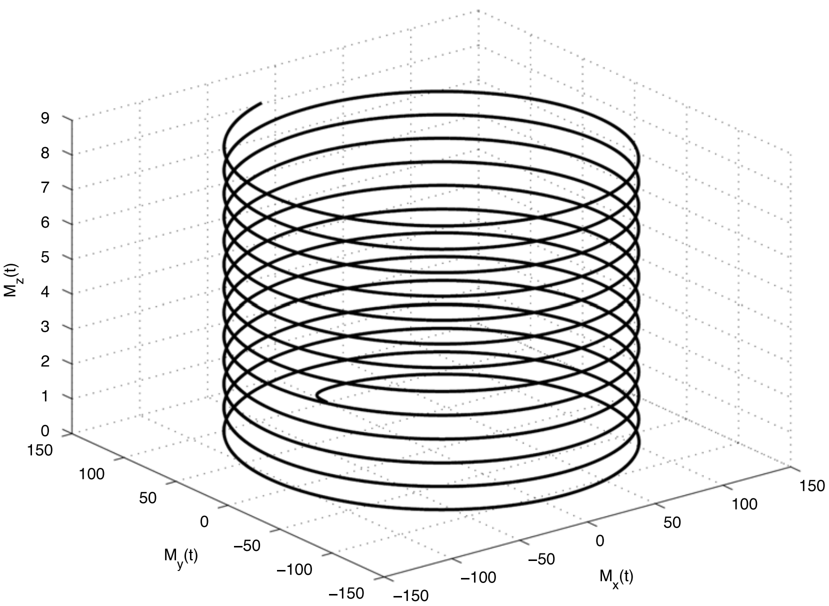

(b) 3D: ($M_x(t)$ vs. $M_y(t)$ vs. $M_z(t)$).

Fig. 5. Numerical solutions of Bloch equations (24) with parameters: $q \equiv q_1 = q_2 \approx 1.03163$, $T_1' = 1\ (\mathrm{s})^q$, $T_2' = 20\ (\mathrm{ms})^q$, $f_0 = 160$ Hz, and initial conditions $M_x(0) = 0$, $M_y(0) = 100$, $M_z(0) = 0$ for $T_{\mathrm{sim}} = 0.1$ s.

the form:

$$
\begin{aligned}
M_x(t_k) &= \left(\omega_0' M_y(t_{k-1}) - \frac{M_x(t_{k-1})}{T_2'}\right) h^{q_1} - \sum_{j=v}^{k} c_j^{(q_1)} M_x(t_{k-j}),\\
M_y(t_k) &= \left(-\omega_0' M_x(t_k) - \frac{M_y(t_{k-1})}{T_2'}\right) h^{q_2} - \sum_{j=v}^{k} c_j^{(q_2)} M_y(t_{k-j}),\\
M_z(t_k) &= \left(\frac{M_0 - M_z(t_{k-1})}{T_1'}\right) h^{q_3} - \sum_{j=v}^{k} c_j^{(q_3)} M_z(t_{k-j}),
\end{aligned}
\tag{24}
$$

where T_{sim} is the simulation time, $k = 1, 2, 3, \ldots, N$, for $N = [T_{\mathrm{sim}}/h]$, and $(M_x(0), M_y(0), M_z(0))$ is the start point (initial conditions). The binomial coefficients $c_j^{(q)}$ are calculated according to the relation (7). All simulations described in this section were performed without using the short memory principle ($v = 1$) for time step $h = 0.00001$.

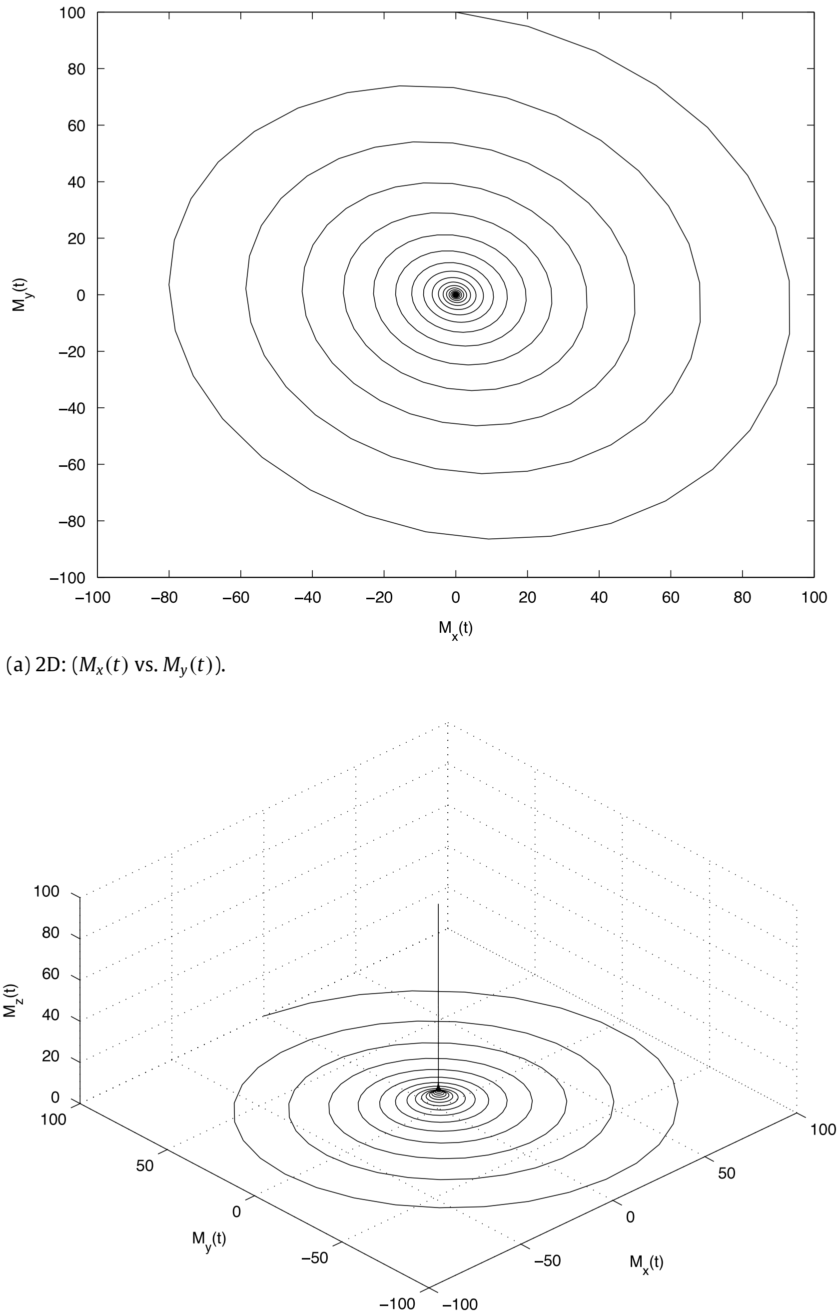

(a) 2D: ($M_x(t)$ vs. $M_y(t)$).

(b) 3D: ($M_x(t)$ vs. $M_y(t)$ vs. $M_z(t)$).

Fig. 6. Numerical solutions of Bloch equations (22) with parameters: $q \equiv q_1 = q_2 = q_3 = 1$, $T_1' = 1$ s, $T_2' = 20$ ms, $f_0 = 160$ Hz, and initial conditions $M_x(0) = 0$, $M_y(0) = 100$, $M_z(0) = 0$ for $T_{\text{sim}} = 1$ s.

For the numerical solution (24) of the Bloch equations (22) was created as a Matlab function `FOBlochEqs()` for which the code and syntax are listed in Appendix.

Stability of the fractional-order Bloch equations (22) can be investigated according to Theorem 1 or 2. The first and second equation of set (22) are a couple and the third one is independent of them. The stability condition is determined from the following expression

$$ {}_0D_t^{\mathbf{q}} \begin{bmatrix} M_x(t) \\ M_y(t) \end{bmatrix} = \begin{bmatrix} -\dfrac{1}{T_2'} & \omega_0' \\ -\omega_0' & -\dfrac{1}{T_2'} \end{bmatrix} \begin{bmatrix} M_x(t) \\ M_y(t) \end{bmatrix}, \tag{25} $$

where $\mathbf{q} = [q_1, q_2]^T$.

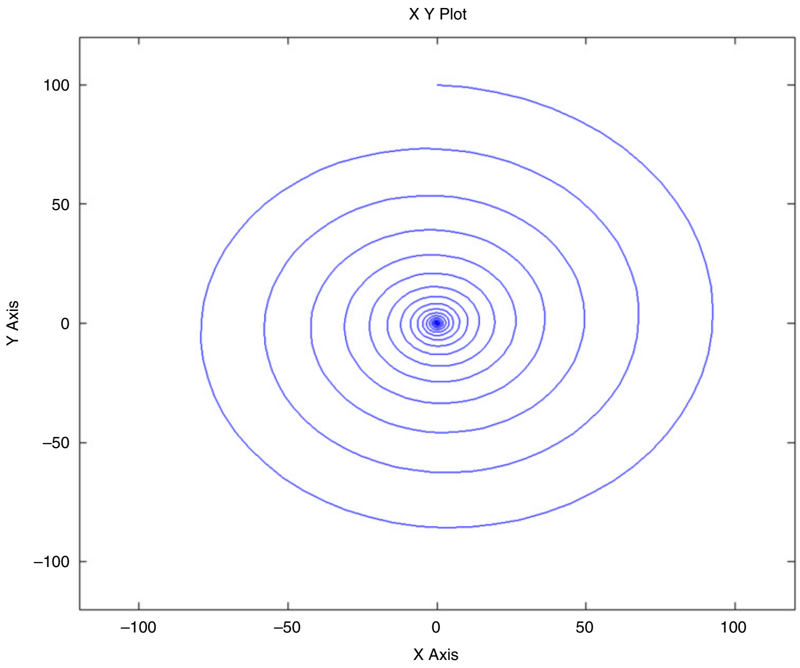

Fig. 7. Numerical solutions of the integer-order Bloch equations in plane ($M_x(t)$ vs. $M_y(t)$) obtained by the Matlab/Simulink model (Fig. 3) for simulation time 1 s.

The system matrix is defined as

$$\mathbf{A} = \begin{bmatrix} -\dfrac{1}{T_2'} & \omega_0' \\ -\omega_0' & -\dfrac{1}{T_2'} \end{bmatrix}. \tag{26}$$

For the following system parameters [43]: $T_2' = 20$ (ms)^q, and $f_0 = 160$ Hz we obtain the eigenvalues eig($\mathbf{A}$) $= -50 \pm 1005.3i$ and $|\arg(\text{eig}(\mathbf{A}))| = 1.6205$. According to the stability condition of Theorem 1, system (25) for the above parameters is *stable* if $q < 1.03163$ in the case $q_1 = q_2$. For $q_1 = q_2 \approx 1.03163$ we get the critical stability border and the solution of the system (25) is depicted in Fig. 5. In Fig. 5(a), we observe a limit cycle and Fig. 5(b) plots a spiral.

In the case, where we consider $q_1 = q_2 = q_3 = 1$ in (22), we have the integer-order (classical) model of the Bloch equations (18), and the numerical solution obtained by (24) is shown in Fig. 6.

The solution of the integer-order Bloch equations (19) with parameters: $T_1 = 1$ s, $T_2 = 20$ ms, $f_0 = 160$ Hz, and initial conditions $M_x(0) = 0$, $M_y(0) = 100$, $M_z(0) = 0$ obtained by the Matlab/Simulink model (see Fig. 3) for $T_{\text{sim}} = 1$ s is depicted in Fig. 7.

When we consider $q_1 = q_2 = q_3 = 0.9$ in (22), we have the fractional-order model of the Bloch equations (18), and the numerical solution obtained by (24) is shown in Fig. 8.

The solution of the fractional-order Bloch equations (22) with parameters: $q \equiv q_1 = q_2 = q_3 = 0.9$, $T_1' = 1$ (s)^q, $T_2' = 20$ (ms)^q, $f_0 = 160$ Hz, and initial conditions $M_x(0) = 0$, $M_y(0) = 100$, $M_z(0) = 0$ obtained by Matlab/Simulink model (see Fig. 4) for $T_{\text{sim}} = 1$ s is depicted in Fig. 10.

In Fig. 9 the comparison of the analytical and numerical solutions of the fractional-order Bloch equations (22) for $M_x(t)$ and $M_y(t)$, respectively is depicted. The analytical solution of the Eq. (22) based on the Mittag-Leffler function was obtained from [43] and for the numerical solution were used the relations (24). For computation of the Mittag-Leffler function was used a Matlab function `mlf()` created by Podlubny and Kačeňák [44]. We can observe a good consistency of both solutions. The same result could be also observed for $M_z(t)$.

When we will consider $q_1 = 0.8$, $q_2 = 0.9$, and $q_3 = 1.0$ in (22), we have the fractional-order model of the Bloch equations (18), and the numerical solution obtained by (24) is shown in Fig. 11.

According to Theorem 2, the stability condition for equation orders $q_1 = 0.8$, $q_2 = 0.9$, $q_3 = 1.0$ of the solution depicted in Fig. 11 is given as $|\arg(\lambda_i)| > \pi/(2m)$ $\forall i$. For $m = 10$ we get the characteristic polynomial in the form

$$\lambda^{17} + 50\lambda^8 + 50\lambda^9 + 2500 + 102\,400\pi^2 = 0.$$

All λ_i ($i = 1, 2, \ldots, 17$) satisfy the condition $|\arg(\lambda_i)| > \pi/20$ and therefore the system is *stable*.

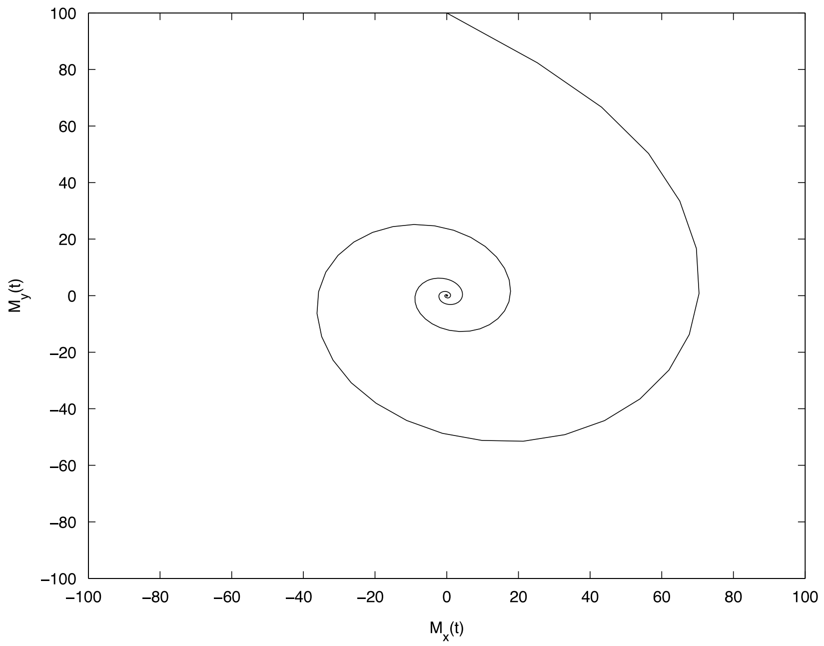

(a) 2D: $(M_x(t)$ vs. $M_y(t))$.

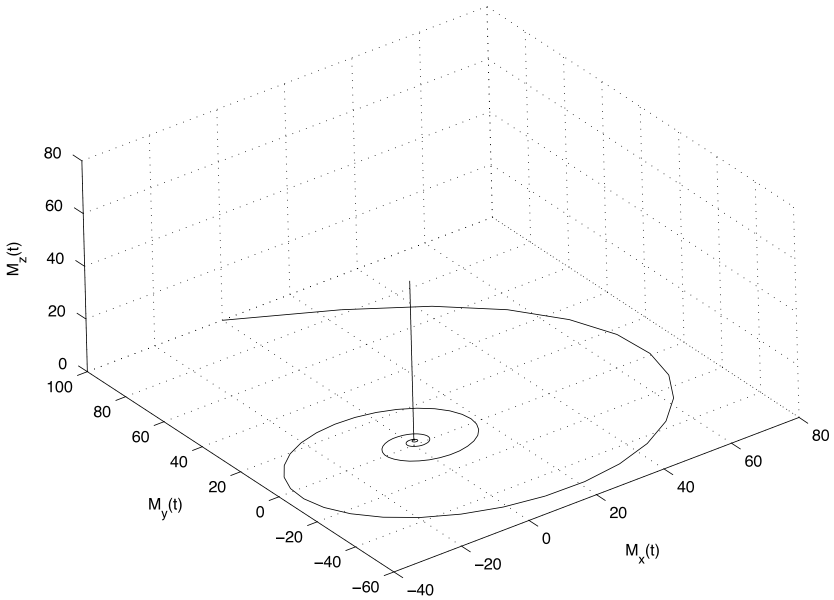

(b) 3D: $(M_x(t)$ vs. $M_y(t)$ vs. $M_z(t))$.

Fig. 8. Numerical solutions of Bloch equations (24) with parameters: $q \equiv q_1 = q_2 = q_3 = 0.9, T_1' = 1\ (\mathrm{s})^q, T_2' = 20\ (\mathrm{ms})^q, f_0 = 160$ Hz, and initial conditions $M_x(0) = 0, M_y(0) = 100, M_z(0) = 0$ for $T_{\mathrm{sim}} = 1$ s.

The solution of the fractional-order Bloch equations (22) with parameters: $q_1 = 0.8, q_2 = 0.9, q_3 = 1.0, T_1' = 1\ (\mathrm{s})^q, T_2' = 20\ (\mathrm{ms})^q, f_0 = 160$ Hz, and initial conditions $M_x(0) = 0, M_y(0) = 100, M_z(0) = 0$ obtained by the Matlab/Simulink model (see Fig. 4) for $T_{\mathrm{sim}} = 1$ s is depicted in Fig. 12.

Figs. 6–12 illustrate dynamic between the $M_x(t)$, $M_x(t)$, and $M_z(t)$, respectively, in 2D and 3D, for the fractional and the integer order relaxation. Entire trajectory of magnetization for both cases is shown also in 3D with the starting at initial conditions $(M_x(0), M_y(0), M_z(0))$ and returning back to its equilibrium value of M_0.

6. Conclusions

In this paper we have presented fractional-order Bloch equations and the method for their numerical solution and simulation. A created mathematical model for NMR allows us to investigate and describe magnetization for spin dynamics

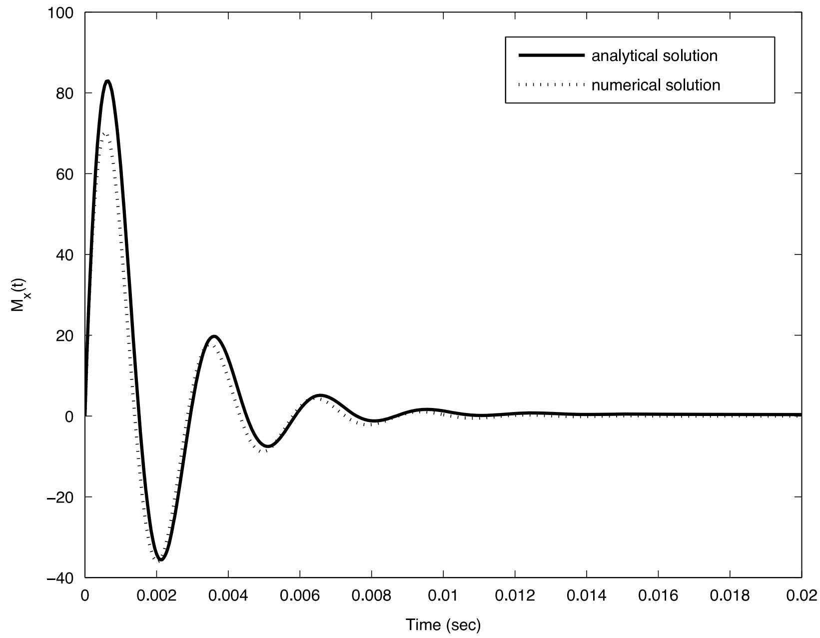

(a) $M_x(t)$ vs. time.

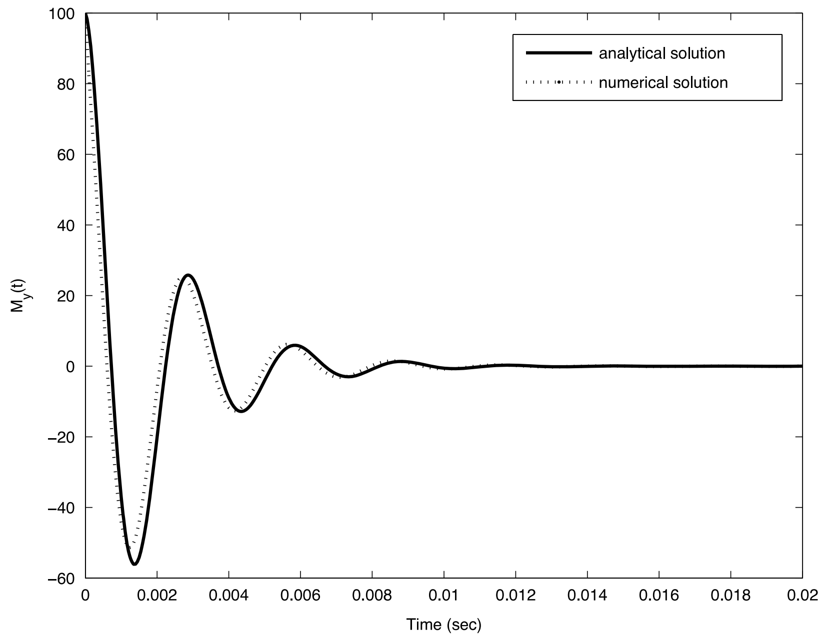

(b) $M_y(t)$ vs. time.

Fig. 9. Comparison of analytical and numerical solutions of Bloch equations (22) with parameters: $q \equiv q_1 = q_2 = q_3 = 0.9, T_1' = 1\ (\mathrm{s})^q, T_2' = 20\ (\mathrm{ms})^q, f_0 = 160$ Hz, and initial conditions $M_x(0) = 0, M_y(0) = 100, M_z(0) = 0$ for $T_{\mathrm{sim}} = 0.02$ s.

(relaxation times T_1 and T_2) at resonance frequency ω_0 in a static magnetic field B_0. By illustrative examples we have shown the behavior of this model for integer and fractional orders of derivatives in the model.

To obtain numerical solutions of the fractional-order Bloch equations a Matlab function and Simulink model was created, which can be used for various equations parameters, initial conditions and desired simulation time.

In further work we will investigate a stability for the interval orders and interval parameters of fractional-order Bloch equations.

Acknowledgement

This work was supported in part by the Slovak Grant Agency for Science under grants VEGA: 1/0390/10, 1/0365/08, 1/0404/08, and grant APVV-0040-07.

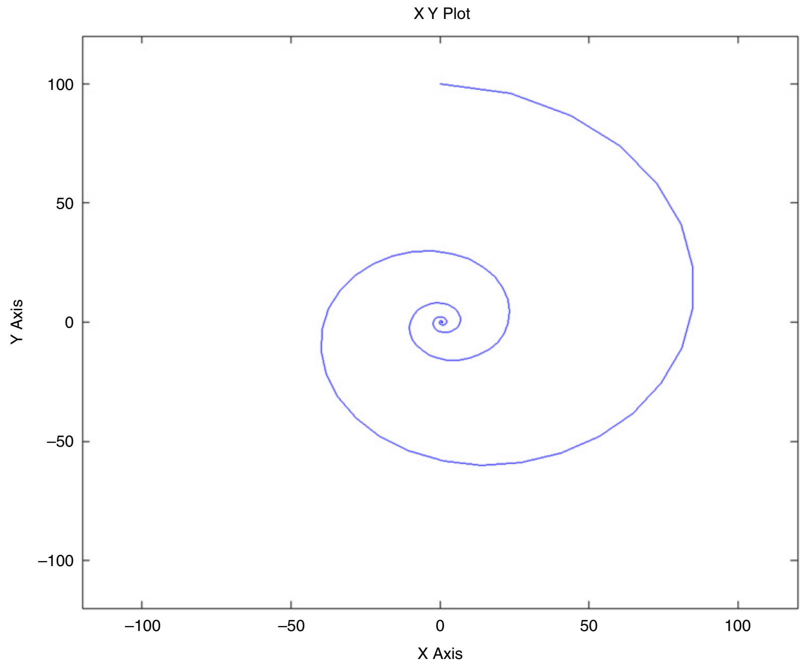

Fig. 10. Numerical solutions of fractional-order ($q_1 = q_2 = q_3 = 0.9$) Bloch equations in plane ($M_x(t)$ vs. $M_y(t)$) obtained by the Matlab/Simulink model (Fig. 4) for simulation time 1 s.

Appendix. Matlab function

```
function [T, Y]=FOBlochEqs(parameters, orders, TSim, Y0)
%
% Numerical Solution of the Fractional-Order Bloch's System
%
%   D^q1 Mx(t) =  omega_0 My(t) - Mx(t)/T2
%   D^q2 My(t) = -omega_0 Mx(t) - My(t)/T2
%   D^q3 Mz(t) =  (M0 - Mz(t))/T1
%
% function [T, Y] = FOBlochEqs(parameters, orders, TSim, Y0)
%
% Input:    parameters - model parameters [omega_0, T1, T2, M0]
%           orders - derivatives orders [q1, q2, q3]
%           TSim - simulation time (0 - TSim) in sec
%           Y0 - initial conditions [Y0(1), Y0(2), Y0(3)]
%
% Output:   T - simulation time (0 : Tstep: TSim)
%           Y - solution of the system (Mx=Y(1), My=Y(2), Mz=Y(3))
%
% Author:  (c) Ivo Petras (ivo.petras@tuke.sk), 2010.

% time step:
h=0.00001;
% number of calculated mesh points:
n=round(TSim/h);
%orders of derivatives, respectively:
q1=orders(1); q2=orders(2); q3=orders(3);
% constants of Bloch's system:
omega_0=parameters(1); T1=parameters(2);
T2=parameters(3); M0=parameters(4);
% binomial coefficients calculation:
cp1=1; cp2=1; cp3=1;
for j=1:n
    c1(j)=(1-(1+q1)/j)*cp1;
```

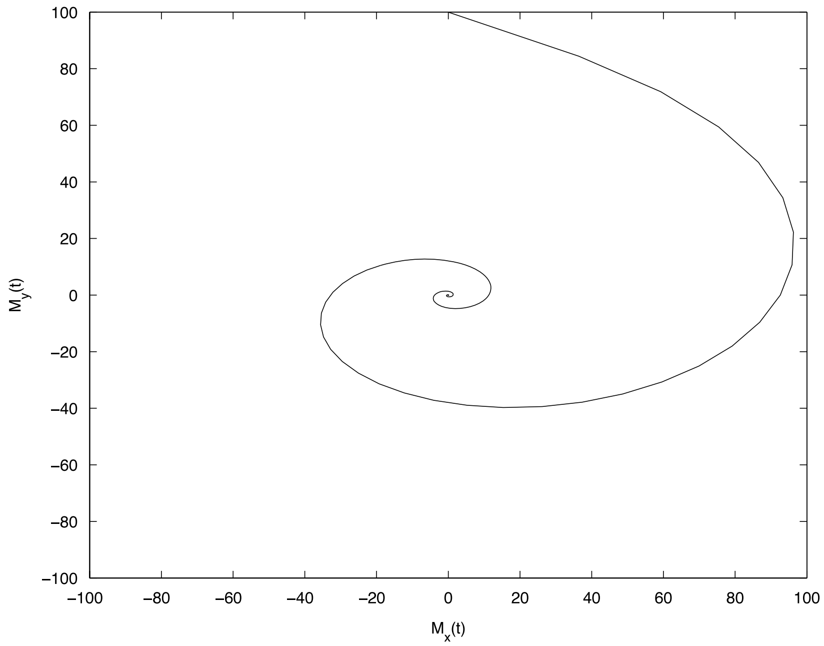

(a) 2D: ($M_x(t)$ vs. $M_y(t)$).

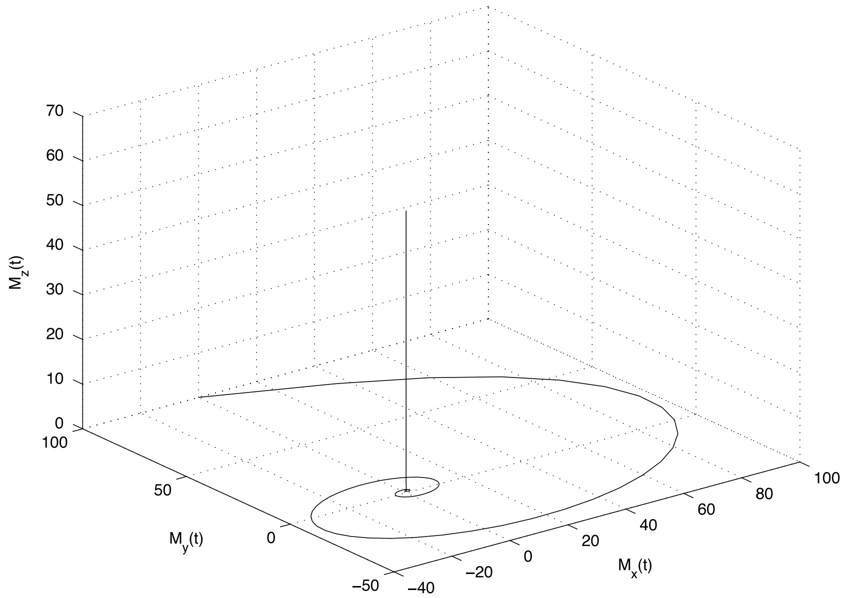

(b) 3D: ($M_x(t)$ vs. $M_y(t)$ vs. $M_z(t)$).

Fig. 11. Numerical solutions of Bloch equations (24) with parameters: $q_1 = 0.8$, $q_2 = 0.9$, $q_3 = 1.0$, $T_1' = 1\ (\mathrm{s})^q$, $T_2' = 20\ (\mathrm{ms})^q$, $f_0 = 160$ Hz, and initial conditions $M_x(0) = 0$, $M_y(0) = 100$, $M_z(0) = 0$ for $T_{\mathrm{sim}} = 1$ s.

```
    c2(j)=(1-(1+q2)/j)*cp2;
    c3(j)=(1-(1+q3)/j)*cp3;
    cp1=c1(j); cp2=c2(j); cp3=c3(j);
end
% initial conditions setting:
Mx(1)=Y0(1); My(1)=Y0(2); Mz(1)=Y0(3);
% calculation of numerical solution:
for i=2:n
    Mx(i)=(omega_0*My(i-1)-Mx(i-1)/T2)*h^q1 - memo(Mx, c1, i);
    My(i)=(-omega_0*Mx(i)-My(i-1)/T2)*h^q2 - memo(My, c2, i);
    Mz(i)=((M0-Mz(i-1))/T1)*h^q3 - memo(Mz, c3, i);
end
for j=1:n
```

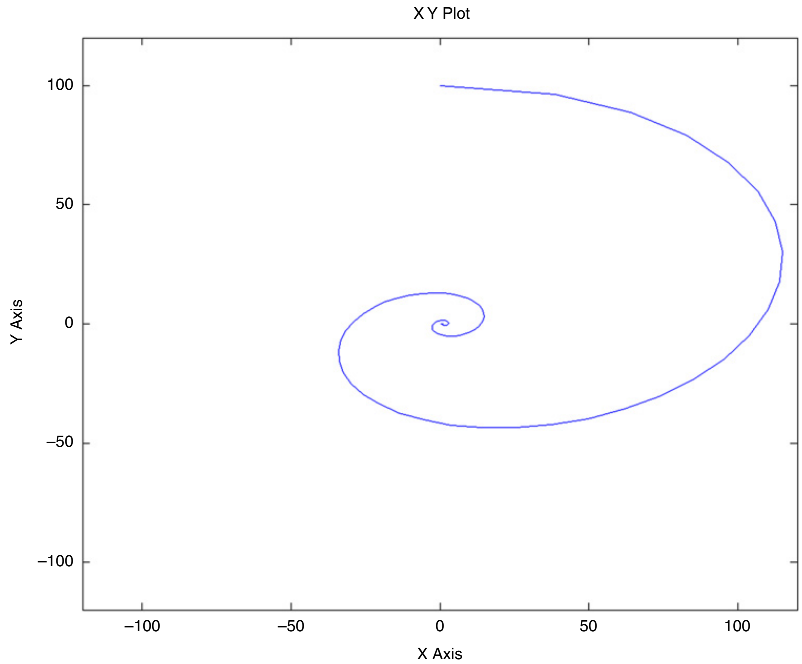

Fig. 12. Numerical solutions of fractional-order ($q_1 = 0.8, q_2 = 0.9, q_3 = 1.0$) Bloch equations in plane ($M_x(t)$ vs. $M_y(t)$) obtained by the Matlab/Simulink model (Fig. 4) for simulation time 1 s.

```
    Y(j,1)=Mx(j); Y(j,2)=My(j); Y(j,3)=Mz(j);
end
T=0:h:TSim;
%
function [yo] = memo(r, c, k)
%
temp = 0;
for j=1:k-1
   temp = temp + c(j)*r(k-j);
end
yo = temp;
%
```

References

[1] A. Oustaloup, La Derivation Non Entiere: Theorie, Synthese et Applications, Hermes, Paris, France, 1995.
[2] I. Podlubny, Fractional Differential Equations, Academic Press, San Diego, 1999.
[3] S. Westerlund, Dead Matter Has Memory!, Causal Consulting, Kalmar, Sweden, 2002.
[4] J.C. Wang, Realizations of generalized Warburg impedance with RC ladder networks and transmission lines, Journal of the Electrochemical Society 134 (8) (1987) 1915–1920.
[5] F.J. Valdes-Parada, J.A. Ochoa-Tapia, J. Alvarez-Ramirez, Effective medium equations for fractional Fick's law in porous media, Physica A 373 (2007) 339–353.
[6] P.J. Torvik, R.L. Bagley, On the appearance of the fractional derivative in the behavior of real materials, Transactions of the ASME 51 (1984) 294–298.
[7] M. Nakagava, K. Sorimachi, Basic characteristics of a fractance device, IEICE Transactions on Fundamentals of Electronics, Communications and Computer Sciences E75-A (12) (1992) 1814–1818.
[8] G.E. Carlson, C.A. Halijak, Approximation of fractional capacitors $(1/s)^{1/n}$ by a regular Newton process, in: Proc. of the Sixth Midwest Symposium on Circuit Theory, Madison, Wisconsin, May 6–7, 1963.
[9] Ľ. Dorčák, Numerical models for the simulation of the fractional-order control systems, in: UEF-04-94, The Academy of Sciences, Institute of Experimental Physics, Košice, Slovakia, 1994.
[10] I. Petráš, Ľ. Dorčák, Fractional-order control systems: modelling and simulation, Fractional Calculus and Applied Analysis 6 (2) (2003) 205–232.
[11] I. Podlubny, Fractional-order systems and $PI^{\lambda}D^{\mu}$-controllers, IEEE Transactions on Automatic Control 44 (1) (1999) 208–213.
[12] Maria da Graca Marcos, F.B.M. Duarte, J.A. Tenreiro Machado, Fractional dynamics in the trajectory control of redundant manipulators, Communications in Nonlinear Science and Numerical Simulations 13 (2008) 1836–1844.
[13] B.M. Vinagre, Y.Q. Chen, I. Petráš, Two direct Tustin discretization methods for fractional-order differentiator/integrator, Journal of the Franklin Institute 340 (2003) 349–362.
[14] Ch.-Ch. Tseng, Design of FIR and IIR fractional order Simpson digital integrators, Signal Processing 87 (2007) 1045–1057.
[15] K.B. Oldham, J. Spanier, The Fractional Calculus, Academic Press, New York, 1974.
[16] I. Petráš, Chaos in the fractional-order Volta's system: modeling and simulation, Nonlinear Dynamics 57 (1–2) (2009) 157–170.
[17] M.S. Tavazoei, M. Haeri, Chaotic attractors in incommensurate fractional order systems, Physica D 237 (2008) 2628–2637.
[18] R. Magin, Fractional Calculus in Bioengineering, Begell House Publishers, 2006.

[19] I. Podlubny, Geometric and physical interpretation of fractional integration and fractional differentiation, Fractional Calculus and Applied Analysis 5 (4) (2002) 367–386.
[20] D. Matignon, Stability result on fractional differential equations with applications to control processing, in: IMACS-SMC Proceedings, Lille, France, July, 1996, pp. 963–968.
[21] I. Petráš, Stability of fractional-order systems with rational orders: a survey, Fractional Calculus and Applied Analysis 12 (3) (2009) 269–298.
[22] W. Deng, Short memory principle and a predictor–corrector approach for fractional differential equations, Journal of Computational and Applied Mathematics 206 (2007) 174–188.
[23] W.H. Deng, C.P. Li, Chaos synchronization of the fractional Lu system, Physica A 353 (2005) 61–72.
[24] N. Ford, A. Simpson, The numerical solution of fractional differential equations: speed versus accuracy, Numerical Analysis Report 385, Manchester Centre for Computational Mathematics, Manchester, 2001.
[25] W. Deng, Numerical algorithm for the time fractional Fokker–Planck equation, Journal of Computational Physics 227 (2007) 1510–1522.
[26] K. Diethelm, N.J. Ford, A.D. Freed, Yu. Luchko, Algorithms for the fractional calculus: a selection of numerical methods, Computer Methods in Applied Mechanics and Engineering 194 (2005) 743–773.
[27] A. Charef, H.H. Sun, Y.Y. Tsao, G. Onaral, Fractal systems as represented by singularity function, IEEE Transactions on Automatic Control 37 (9) (1992) 1465–1470.
[28] A. Oustaloup, F. Levron, F. Nanot, B. Mathieu, Frequency-band complex non integer differentiator: characterization and synthesis, IEEE Transactions on Circuits and Systems 47 (1) (2000) 25–40.
[29] I. Podlubny, I. Petráš, B.M. Vinagre, P. O'Leary, Ľ. Dorčák, Analogue realization of fractional-order controllers, Nonlinear Dynamics 29 (1–4) (2002) 281–296.
[30] Ch. Hwang, J.F. Leu, S.Y. Tsay, A note on time-domain simulation of feedback fractional-order systems, IEEE Transactions on Automatic Control 47 (4) (2002) 625–631.
[31] I. Podlubny, Matrix approach to discrete fractional calculus, Fractional Calculus and Applied Analysis 3 (4) (2000) 359–386.
[32] I. Podlubny, A. Chechkin, T. Skovranek, Y.Q. Chen, B.M. Vinagre Jara, Matrix approach to discrete fractional calculus II: partial fractional differential equations, Journal of Computational Physics 228 (8) (2009) 3137–3153.
[33] D. Valerio, Toolbox `ninteger` for Matlab, v. 2.3, September 2005. http://web.ist.utl.pt/duarte.valerio/ninteger/ninteger.htm , visited: May 23, 2008).
[34] I. Petráš, Method for simulation of the fractional order chaotic systems, Acta Montanistica Slovaca 11 (4) (2006) 273–277.
[35] W.R. LePage, Complex Variables and the Laplace Transform for Engineers, McGraw-Hill, 1961.
[36] D. Matignon, Stability properties for generalized fractional differential systems, in: Proc. of Fractional Differential Systems: Models, Methods and Applications, 5, 1998, pp. 145–158.
[37] M.S. Tavazoei, M. Haeri, Unreliability of frequency-domain approximation in recognising chaos in fractional-order systems, IET Signal Processing 1 (4) (2007) 171–181.
[38] M.S. Tavazoei, M. Haeri, A necessary condition for double scroll attractor existence in fractional-order systems, Physics Letters A 367 (2007) 102–113.
[39] M.S. Tavazoei, M. Haeri, Limitations of frequency domain approximation for detecting chaos in fractional order systems, Nonlinear Analysis 69 (2008) 1299–1320.
[40] W. Deng, Ch. Li, J. Lu, Stability analysis of linear fractional differential system with multiple time delays, Nonlinear Dynamics 48 (2007) 409–416.
[41] F. Bloch, Nuclear induction, Physical Review 70 (1946) 460–473.
[42] E.M. Haacke, R.W. Brown, M.R. Thompson, R. Venkatesan, Magnetic Resonance Imaging: Physical Principles and Sequence Design, Wiley, New York, 1999.
[43] R. Magin, X. Feng, D. Baleanu, Solving the fractional order Bloch equation, Concepts in Magnetic Resonance Part A 34A (1) (2009) 16–23.
[44] I. Podlubny, M. Kačeňák, Mittag-Leffler function, MathWorks, Inc., 2009. http://www.mathworks.com/matlabcentral/fileexchange/8738.

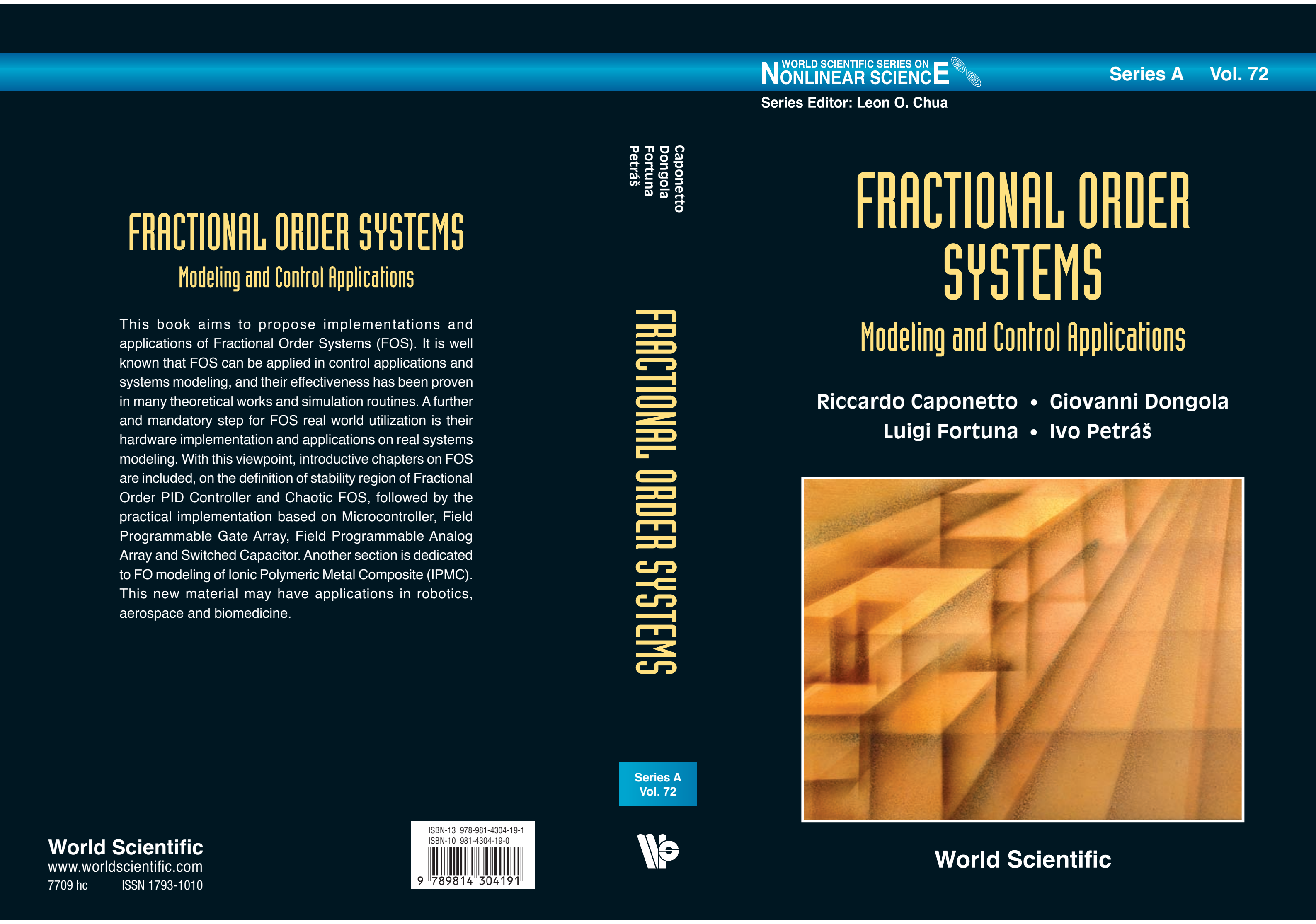
WORLD SCIENTIFIC SERIES ON NONLINEAR SCIENCE
Series A Vol. 72
Series Editor: Leon O. Chua
FRACTIONAL ORDER SYSTEMS
Modeling and Control Applications
Riccardo Caponetto • Giovanni Dongola
Luigi Fortuna • Ivo Petráš
World Scientific
Caponetto
Dongola
Fortuna
Petráš
FRACTIONAL ORDER SYSTEMS
Series A
Vol. 72
FRACTIONAL ORDER SYSTEMS
Modeling and Control Applications
This book aims to propose implementations and applications of Fractional Order Systems (FOS). It is well known that FOS can be applied in control applications and systems modeling, and their effectiveness has been proven in many theoretical works and simulation routines. A further and mandatory step for FOS real world utilization is their hardware implementation and applications on real systems modeling. With this viewpoint, introductive chapters on FOS are included, on the definition of stability region of Fractional Order PID Controller and Chaotic FOS, followed by the practical implementation based on Microcontroller, Field Programmable Gate Array, Field Programmable Analog Array and Switched Capacitor. Another section is dedicated to FO modeling of Ionic Polymeric Metal Composite (IPMC). This new material may have applications in robotics, aerospace and biomedicine.
World Scientific
www.worldscientific.com
7709 hc
ISSN 1793-1010
ISBN-13 978-981-4304-19-1
ISBN-10 981-4304-19-0
9 789814 304191

WORLD SCIENTIFIC SERIES ON NONLINEAR SCIENCE Series A Vol. 72
Series Editor: Leon O. Chua

FRACTIONAL ORDER SYSTEMS

Modeling and Control Applications

Riccardo Caponetto
Giovanni Dongola
Luigi Fortuna
University of Catania, Italy

Ivo Petráš
Technical University of Košice, Slovakia

World Scientific

NEW JERSEY • LONDON • SINGAPORE • BEIJING • SHANGHAI • HONG KONG • TAIPEI • CHENNAI

Published by

World Scientific Publishing Co. Pte. Ltd.
5 Toh Tuck Link, Singapore 596224
USA office: 27 Warren Street, Suite 401-402, Hackensack, NJ 07601
UK office: 57 Shelton Street, Covent Garden, London WC2H 9HE

British Library Cataloguing-in-Publication Data
A catalogue record for this book is available from the British Library.

World Scientific Series on Nonlinear Science, Series A — Vol. 72
FRACTIONAL ORDER SYSTEMS
Modeling and Control Applications

ISBN-13 978-981-4304-19-1
ISBN-10 981-4304-19-0

Printed in Singapore.

IEEE TRANSACTIONS ON CIRCUITS AND SYSTEMS—II: EXPRESS BRIEFS, VOL. 57, NO. 12, DECEMBER 2010 975

Fractional-Order Memristor-Based Chua's Circuit

Ivo Petráš, *Member, IEEE*

***Abstract*—This express brief deals with the memristor-based Chua's circuit. For the first time, the fractional-order model for such system is presented. A numerical solution of the fractional-order memristor-based Chua's equations is derived for simulations. The dynamical behavior and stability analysis of this system are described and investigated as well.**

***Index Terms*—Chaos, Chua's circuit, fractional calculus, fractional-order Chua's equations, memristive systems, memristor.**

I. Introduction

FRACTIONAL calculus is a topic that is more than 300 years old. These mathematical phenomena attracted many scientists and engineers in various areas of applications such as (e.g., [1]–[4], etc.) physics, chemistry, bioengineering, signal processing, control systems, etc. A very important area of applications is the chaos theory, where the new mathematical models were already proposed and used (e.g., [5]–[7]).

In this brief, we offer an application of fractional calculus in a nonlinear electrical circuit, which is modeled by fractional-order equations. This brief is organized as follows.

Basic facts of fractional calculus, fractional-order dynamic systems, numerical methods, and models of basic electrical elements are first presented in Section II. Then, stability conditions for the fractional-order dynamical systems are introduced in Section III. The integer-order and fractional-order equations of memristor-based Chua's oscillators and their numerical solution are described, analyzed, and illustrated in Section IV. In Section V, the simulation examples are presented. Some conclusion remarks are mentioned in Section VI.

II. Fractional Calculus

A. Basic Facts

Fractional calculus is a generalization of integration and differentiation to non-integer-order fundamental operator ${}_aD_t^q$, where a and t are the bounds of the operation, and $q \in \mathrm{R}$.

The most frequently used definitions for the general fractional differintegral are [2], [3] the Grünwald–Letnikov (GL), the Riemann–Liouville (RL), and Caputo's definition.

In this brief, we will consider with the GL definition. If we assume that $n = (t-a)/h$, where a is a real constant, which expresses a limit value, we can write the GL definition as

$$ {}_aD_t^q f(t) = \lim_{h\to 0} \frac{1}{h^q} \sum_{i=0}^{[n]} (-1)^i \binom{q}{i} f(t-ih) \qquad (1)$$

where [.] means the integer part.

B. Numerical Methods

For numerical calculation of the fractional-order derivative, we use the relation (2) derived from the GL definition (1). This approach is based on the fact that, for a wide class of functions, the well-known definitions—GL (1), RL, and Caputo's—are equivalent. The relation for the explicit numerical approximation of the qth derivative at the points kh $(k = 1, 2, \ldots)$ has the following form [3], [8]:

$$ {}_{(k-L_m/h)}D_{t_k}^q f(t) \approx h^{-q} \sum_{i=0}^{k} c_i^{(q)} f(t_{k-i}) \qquad (2)$$

where L_m is the "memory length," $t_k = kh$, h is the time step of calculation, and $c_i^{(q)}$ $(i = 0, 1, \ldots)$ are binomial coefficients. For their calculation, we can use the following expression [8]:

$$ c_0^{(q)} = 1, \qquad c_i^{(q)} = \left(1 - \frac{1+q}{i}\right) c_{i-1}^{(q)}. \qquad (3)$$

Then, general numerical solution of the fractional differential equation

$$ {}_aD_t^q y(t) = f\left(y(t), t\right)$$

can be expressed as

$$ y(t_k) = f\left(y(t_k), t_k\right) h^q - \sum_{i=v}^{k} c_i^{(q)} y(t_{k-i}). \qquad (4)$$

For the *memory term* expressed by the sum in (4), a "short-memory" principle can be used. Then, the lower index of the sums in relations (4) will be $v = 1$ for $k < (L_m/h)$ and $v = k - (L_m/h)$ for $k > (L_m/h)$, or without using a "short-memory" principle, we put $v = 1$ for all k.

C. Fractional Calculus and Electricity

There are a large number of electric and magnetic phenomena where the fractional calculus can be used [4]. We will consider three of them—capacitor, inductor, and memristor.

Westerlund and Ekstam in 1994 proposed a new linear capacitor model [9]. For a general input voltage $V(t)$, the current is

$$ I(t) = C\frac{d^\alpha V(t)}{dt^\alpha} \equiv C_0 D_t^\alpha V(t) \qquad (5)$$

Manuscript received June 1, 2010; revised August 17, 2010; accepted September 13, 2010. Date of publication November 9, 2010; date of current version December 15, 2010. This work was supported in part by Grant VEGA: 1/0390/10, 1/0365/08, 1/0404/08, Grant APVV-0040-07, and Grant SK-PL-0052-09. This paper was recommended by Associate Editor A. Brambilla.

The author is with Institute of Control and Informatization of Production Processes, Faculty of Mining, Ecology, Process Control and Geotechnologies (BERG), Technical University of Košice, 042 00 Košice, Slovakia (e-mail: ivo.petras@tuke.sk).

Digital Object Identifier 10.1109/TCSII.2010.2083150

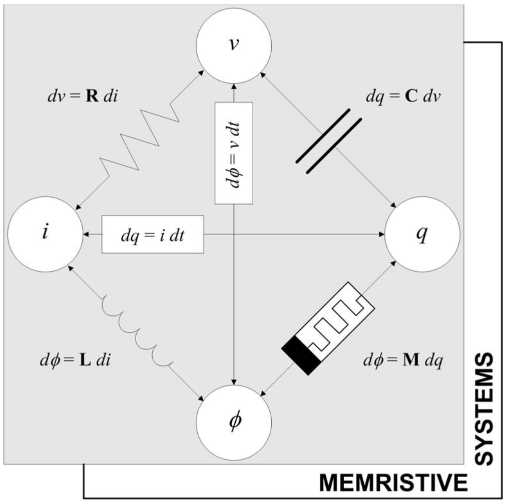

Fig. 1. Connection of the four basic electrical elements (inspired by [13]).

where C is the capacitance of the capacitor. It is related to the kind of dielectric. Another constant α (order) is related to the losses of the capacitor. Westerlund provided in his work the table of various capacitor dielectrics with appropriated constant α, which has experimentally been obtained by measurements.

Westerlund also described the behavior of a real inductor [4]. For a general current in the inductor, the voltage is

$$V(t) = L\frac{d^\alpha I(t)}{dt^\alpha} \equiv L_0 D_t^\alpha I(t) \qquad (6)$$

where L is inductance of the inductor, and the constant α (order) is related to the "proximity effect." Some coefficients α for real inductors can be found in [10].

Prof. Leon O. Chua in 1971 predicted a new circuit element—called memristor—characterized by a relationship between the charge $q(t)$ and the flux $\phi(t)$. Chua extrapolated the conceptual symmetry between the resistor, inductor, and capacitor and inferred that the memristor is a similarly fundamental device [11], which belongs to a class of the memristive systems [12]. This relation is illustrated in Fig. 1.

The memristor used in this brief is a flux-controlled memristor that is characterized by

$$I(t) = W(\phi(t))V(t), \quad \text{for} \quad W(\phi(t)) = dq(\phi)/d\phi \qquad (7)$$

where $W(\phi(t))$ is an incremental memductance of the memristor. Similar to a capacitor and an inductor, the memristor is also not an ideal circuit element, and we can predict the fractional-order model of this basic *fourth element* [14].

D. Fractional-Order Nonlinear System

In this brief, we consider the following general incommensurate fractional-order nonlinear system:

$$\begin{aligned} {}_0D_t^{q_i} x_i(t) &= f_i\left(x_1(t), x_2(t), \dots, x_n(t), t\right) \\ x_i(0) &= c_i, \qquad i = 1, 2, \dots, n \end{aligned} \qquad (8)$$

where c_i are initial conditions. The vector representation of (8) is

$$D^{\mathbf{q}}\mathbf{x} = \mathbf{f}(\mathbf{x}) \qquad (9)$$

where $\mathbf{q} = [q_1, q_2, \dots, q_n]^T$ for $0 < q_i < 2$, $(i = 1, 2, \dots, n)$, and $\mathbf{x} \in \mathrm{R}^n$.

The equilibrium points of (9) are calculated via solving the following equation:

$$\mathbf{f}(\mathbf{x}) = 0 \qquad (10)$$

and we suppose that $E^* = (x_1^*, x_2^*, \dots, x_n^*)$ is its equilibrium point.

III. Stability of a Fractional-Order Nonlinear System

The stability of the fractional-order nonlinear system is very complex, and it is different from the fractional-order linear system because nonlinear systems have several equilibrium points. This topic is still open [15]. Some known results are the following.

Theorem 1

The equilibrium points are asymptotically stable for $q_1 = q_2 = \dots = q_n \equiv q$ if all the eigenvalues λ_i $(i = 1, 2, \dots, n)$ of the Jacobian matrix $\mathbf{J} = \partial\mathbf{f}/\partial\mathbf{x}$, where $\mathbf{f} = [f_1, f_2, \dots, f_n]^T$, evaluated at the equilibrium E^*, satisfy the following condition [7], [16], [17]:

$$|\arg(\mathrm{eig}(\mathbf{J}))| = |\arg(\lambda_i)| > q\frac{\pi}{2}, \qquad i = 1, 2, \dots, n. \qquad (11)$$

When we consider the incommensurate fractional-order system $q_1 \neq q_2 \neq \dots \neq q_n$ and suppose that m is the least common multiple (LCM) of the denominators u_i's of q_i's, where $q_i = v_i/u_i$, v_i, $u_i \in Z^+$ for $i = 1, 2, \dots, n$, and we set $\gamma = 1/m$, (9) is asymptotically stable if [18]

$$|\arg(\lambda)| > \gamma\frac{\pi}{2}$$

for all roots λ of the following equation:

$$\det\left(\mathrm{diag}\left([\lambda^{mq_1}\lambda^{mq_2}\dots\lambda^{mq_n}]\right) - \mathbf{J}\right) = 0. \qquad (12)$$

A necessary stability condition for fractional-order systems (9) to remain chaotic is keeping at least one eigenvalue λ in the unstable region [16]. The number of equilibrium points and eigenvalues for one-scroll, double-scroll, and multiscroll attractors was exactly described in this brief [19]. For instance, assume that a 3-D chaotic system has only three equilibria. Therefore, if a system has a double-scroll attractor, it may have two saddle–focus points surrounded by scrolls and one additional saddle point, etc.

Theorem 2

Suppose that the unstable eigenvalues of scroll saddle points are $\lambda_{1,2} = r_{1,2} \pm j\omega_{1,2}$. The necessary condition to exhibit the double-scroll attractor of (9) is the eigenvalues $\lambda_{1,2}$ remaining in the unstable region. The condition for the commensurate derivatives order is

$$q > \frac{2}{\pi}\mathrm{atan}\left(\frac{|\omega_i|}{r_i}\right), \qquad i = 1, 2. \qquad (13)$$

This condition can be used to determine the minimum order for which a nonlinear system can generate chaos [16]. In other

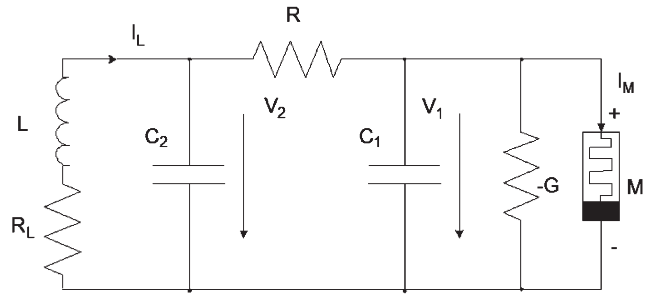

Fig. 2. Chua's circuit with a memristor and negative conductance.

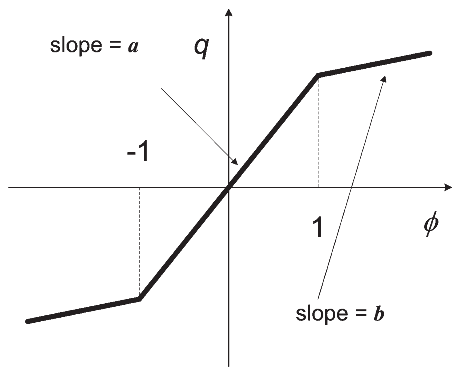

Fig. 3. Characteristic of a piecewise-linear flux-controlled memristor.

words, when the instability measure $\pi/2m - \min(|\arg(\lambda)|)$ is negative, the system cannot be chaotic [19].

IV. Concept of the New Chua's Circuit

The well-known classical Chua's circuit was proposed in [20]. It is a simple electronic circuit that exhibits nonlinear dynamical phenomena such as bifurcation and chaos.

The fractional-order Chua's system was described and investigated in many works [3], [6], [21]. Similar to the classical one, it contains a capacitor C, an inductor L, a resistor R, and a nonlinear resistor, which is known as the Chua's diode.

Since the memristor was postulated by Prof. L. O. Chua in 1971 and discovered by Williams *et al.* (HP laboratory) in 2008, it has become the fourth circuit element. This fact allows us to use a memristor as a nonlinear element in a circuit that exhibits chaos. In the case of Chua's circuit, the nonlinear resistor is replaced by a memristor (M).

The memristor in Fig. 2 is a flux-controlled memristor whose characteristic is given by [11]

$$I_M(t) = W(\phi(t))\, V_1(t) \tag{14}$$

where $W(\phi(t))$ is called the incremental memductance defined by (7). For the flux-controlled memristor, a monotonically increasing piecewise-linear characteristic was assumed [22]. The memristor constitutive relation is shown in Fig. 3 and can be expressed as

$$q(\phi) = b\phi + 0.5(a-b) \times (|\phi+1| - |\phi-1|) \tag{15}$$

where $a,\ b > 0$. The memductance function that is obtained from the $q(\phi)$ function is

$$W(\phi) = \frac{dq(\phi)}{d\phi}\begin{cases} a & : \quad |\phi| < 1, \\ b & : \quad |\phi| > 1. \end{cases} \tag{16}$$

The dynamics of the Chua's circuit with a passive memristor (flux-controlled memristor and negative conductance [23]) depicted in Fig. 2 is given by the following set of differential equations:

$$\begin{aligned} \frac{dV_1(t)}{dt} &= \frac{1}{C_1}\left[\frac{(V_2(t)-V_1(t))}{R} + V_1(t)\left(G - W(\phi(t))\right)\right], \\ \frac{dV_2(t)}{dt} &= \frac{1}{C_2}\left[\frac{(V_1(t)-V_2(t))}{R} + I_L(t)\right], \\ \frac{dI_L(t)}{dt} &= \frac{1}{L}\left[-V_2(t) - R_L I_L(t)\right], \\ \frac{d\phi(t)}{dt} &= V_1(t) \end{aligned} \tag{17}$$

where functions $q(\phi)$ and $W(\phi)$ are given by (15) and (16), respectively.

When we set

$$\begin{aligned} &x = V_1, \quad y = V_2, \quad z = I_L, \quad w = \phi, \quad C_2 = 1, \\ &\alpha = 1/C_1, \quad \beta = 1/L, \quad \gamma = R_L/L, \quad \zeta = G, \quad R = 1, \end{aligned} \tag{18}$$

then (17) can be transformed into the dimensionless form [22]

$$\begin{aligned} \frac{dx(t)}{dt} &= \alpha\left(y(t) - x(t) + \zeta x(t) - W(w)x(t)\right), \\ \frac{dy(t)}{dt} &= x(t) - y(t) + z(t), \\ \frac{dz(t)}{dt} &= -\beta y(t) - \gamma z(t), \\ \frac{dw(t)}{dt} &= x(t) \end{aligned} \tag{19}$$

where the piecewise-linear function $W(w)$ is given as

$$W(w) = \begin{cases} a & : \quad |w| < 1, \\ b & : \quad |w| > 1. \end{cases} \tag{20}$$

The equilibrium points of the system (19) are given by setting the left side of the equations to zero, except the last one. We set $w =$ constant, which corresponds to the w-axis [22]. The Jacobian matrix at this equilibrium state E^* is

$$\mathbf{J}_W = \begin{bmatrix} \alpha(-1+\zeta-W(w)) & \alpha & 0 & 0 \\ 1 & -1 & 1 & 0 \\ 0 & -\beta & -\gamma & 0 \\ 1 & 0 & 0 & 0 \end{bmatrix}. \tag{21}$$

If we consider a fractional-order model for each electrical element in the circuit depicted in Fig. 2, we can write a more general mathematical model for this circuit. As it was already mentioned, a real capacitor and a real inductor are "fractional," and for a real memristor, we postulated a fractional-order model as well ($d^\alpha \phi(t)/dt^\alpha = V(t)$). By using a technique of fractional calculus, we obtain the following equations:

$$\begin{aligned} {}_0D_t^{q_1} x(t) &= \alpha\left(y(t) - x(t) + \zeta x(t) - W(w)x(t)\right), \\ {}_0D_t^{q_2} y(t) &= x(t) - y(t) + z(t), \\ {}_0D_t^{q_3} z(t) &= -\beta y(t) - \gamma z(t), \\ {}_0D_t^{q_4} w(t) &= x(t) \end{aligned} \tag{22}$$

where function $W(w)$ is given by (20), and q_1, q_2, q_3, and q_4 are the fractional orders of the real electrical elements (memristive systems): capacitor C_1, capacitor C_2, inductor L, and memristor M, respectively.

The stability of the new fractional-order memristor-based Chua's system can be investigated by using Theorem 1. For the fractional-incommensurate-order system (22), we can rewrite the real order as $q_i = v_i/u_i$, $v_i, u_i \in Z^+$ for $i = 1, 2, 3, 4$, and if we set $\gamma = 1/m$, where m is the LCM of the denominators, the characteristic equation of the system (22) for Jacobian matrix $\mathbf{J}_W$ is

$$\det\left(\mathrm{diag}\left([\lambda^{mq_1}\ \lambda^{mq_2}\ \lambda^{mq_3}\ \lambda^{mq_4}]\right) - \mathbf{J}_W\right) = 0$$

and the stability condition is defined as

$$|\arg(\lambda_i)| > \gamma\frac{\pi}{2}$$

for all eigenvalues λ_i.

When we consider a simple case where the fractional-order memristor-based Chua's system has a commensurate order, which means that $q_1 = q_2 = q_3 = q_4 \equiv q$, the stability can be investigated according to Theorem 1, where the condition is

$$|\arg\left(\mathrm{eig}(\mathbf{J}_W)\right)| = |\arg(\lambda_i)| > q\frac{\pi}{2}$$

for all eigenvalues λ_i.

In the case of the piecewise nonlinearity depicted in Fig. 3, we should investigate the characteristic equation for the linear part with slope a and for the linear part with slope b, respectively.

A necessary stability condition for fractional-order systems (22) to remain chaotic is keeping at least one eigenvalue λ in the unstable region. According to condition (13) of Theorem 2, we can also determine a minimal order q for which a nonlinear system has chaotic behavior.

Because the frequency approximation techniques are unreliable in recognizing chaos in fractional-order nonlinear systems [17], for simulation purposes, we use a numerical solution of the memristor-based Chua's equations (22) obtained by the method described in [24]. That is, a time-domain method is derived by using relationship (2), which leads to equations in the form

$$\begin{aligned} x(t_k) &= \left(\alpha\left(y(t_{k-1}) - x(t_{k-1}) + \zeta x(t_{k-1})\right.\right.\\ &\qquad \left.\left. - W\left(w(t_{k-1})\right)x(t_{k-1})\right)\right)h^{q_1} - \sum_{i=v}^{k} c_i^{(q_1)}x(t_{k-i}),\\ y(t_k) &= \left(x(t_k) - y(t_{k-1}) + z(t_{k-1})\right)h^{q_2}\\ &\qquad - \sum_{i=v}^{k} c_i^{(q_2)}y(t_{k-i}),\\ z(t_k) &= \left(-\beta y(t_k) - \gamma z(t_{k-1})\right)h^{q_3} - \sum_{i=v}^{k} c_i^{(q_3)}z(t_{k-i}),\\ w(t_k) &= x(t_k)h^{q_4} - \sum_{i=v}^{k} c_i^{(q_4)}w(t_{k-i}) \end{aligned} \tag{23}$$

where

$$\begin{aligned} W\left(w(t_{k-1})\right) &= a, \quad \text{for} \quad |w(t_{k-1})| < 1,\\ W\left(w(t_{k-1})\right) &= b, \quad \text{for} \quad |w(t_{k-1})| > 1 \end{aligned} \tag{24}$$

and where T_{sim} is the simulation time, $k = 1, 2, 3, \ldots, N$, for $N = [T_{sim}/h]$, and $(x(0), y(0), z(0), w(0))$ is the start point (initial conditions). The binomial coefficients $c_i^{(q)}$ are calculated according to relation (3).

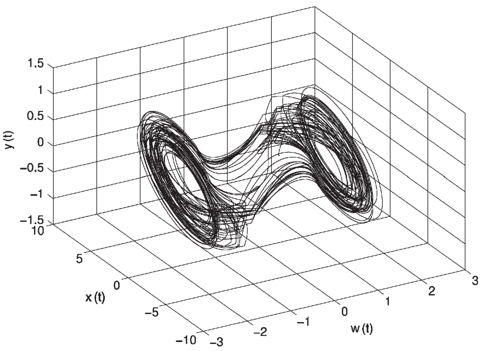

Fig. 4. Strange attractor of the memristor-based Chua's system (22) in the wxy state space for parameters $\alpha = 10$, $\beta = 13$, $\gamma = 0.1$, $\zeta = 1.5$, $a = 0.3$, and $b = 0.8$ and orders $q_1 = q_2 = q_3 = q_4 = 0.97$.

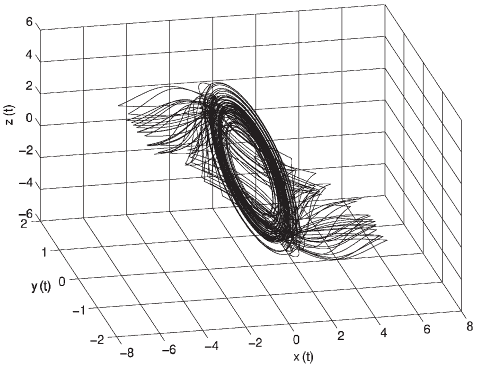

Fig. 5. Strange attractor of the memristor-based Chua's system (22) in the xyz state space for parameters $\alpha = 10$, $\beta = 13$, $\gamma = 0.1$, $\zeta = 1.5$, $a = 0.3$, and $b = 0.8$ and orders $q_1 = q_2 = q_3 = q_4 = 0.97$.

V. Illustrative Examples

Let us consider the following parameter set:

$$\alpha=10 \quad \beta=13 \quad \gamma=0.1 \quad \zeta=1.5 \quad a=0.3 \quad b=0.8. \tag{25}$$

For these parameters, a minimal commensurate order given by Theorem 2 is $q > 0.95$ because the eigenvalues are $\lambda_{1,2} \approx 0.2228154143 \pm 2.8941365766j$. We performed a simulation for the aforementioned parameters and commensurate order $q = 0.97$ ($q_1 = q_2 = q_3 = q_4 = 0.97$). It means that the total order is 3.88.

In Figs. 4 and 5, chaotic attractors in the 3-D state space for $T_{sim} = 200$ s are depicted. Both simulations were performed without using the short-memory principle ($v = 1$) for time step $h = 0.005$ with the following initial conditions: $x(0) = 0.8$, $y(0) = 0.05$, $z(0) = 0.007$, and $w(0) = 0.6$.

When we consider real orders of capacitor models [9], i.e., $q_1 = q_2 = 0.98$, and a real order of the inductor model [10], i.e., $q_3 = 0.99$, and we assume a real order of the memristor model, i.e., $q_4 = 0.97$, for the parameters in (25) with initial conditions $x(0) = 0.8$, $y(0) = 0.05$, $z(0) = 0.007$, and $w(0) = 0.6$, simulation time $T_{sim} = 100$ s, and time step $h = 0.005$, we get the chaotic double-scroll attractor as well for the total system order 3.92.

In Figs. 6 and 7, chaotic attractors in the 3-D state space for $T_{sim} = 100$ s are depicted. The simulations were performed

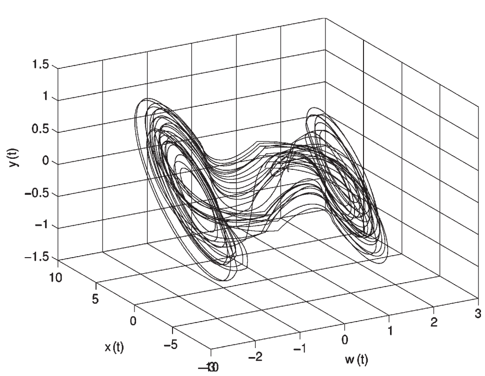

Fig. 6. Strange attractor of the memristor-based Chua's system (22) in the wxy state space for parameters $\alpha = 10$, $\beta = 13$, $\gamma = 0.1$, $\zeta = 1.5$, $a = 0.3$, and $b = 0.8$ and orders $q_1 = q_2 = 0.98$, $q_3 = 0.99$, and $q_4 = 0.97$.

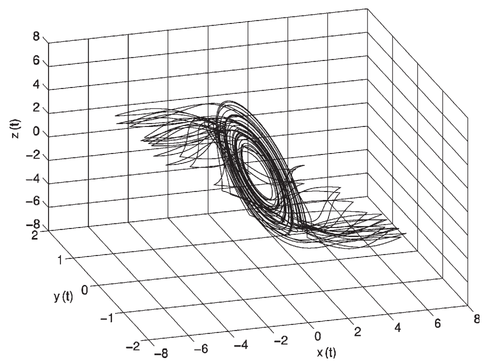

Fig. 7. Strange attractor of the memristor-based Chua's system (22) in the xyz state space for parameters $\alpha = 10$, $\beta = 13$, $\gamma = 0.1$, $\zeta = 1.5$, $a = 0.3$, and $b = 0.8$ and orders $q_1 = q_2 = 0.98$, $q_3 = 0.99$, and $q_4 = 0.97$.

without using the short-memory principle $(v = 1)$ for time step $h = 0.005$ with the following initial conditions: $x(0) = 0.8$, $y(0) = 0.05$, $z(0) = 0.007$, and $w(0) = 0.6$. In this case, we just estimated the real order of the memristor. Simulations show the double-scroll atractors, and we can observe a chaotic behavior. It can also be confirmed by using Theorem 1. The characteristic equation of the system (22) with the parameters in (25), orders $q_1 = q_2 = 0.98 = 98/100$, $q_3 = 0.99 = 99/100$, and $q_4 = 0.97 = 97/100$, with $m = 100$, for Jacobian matrix (21) and slope a is

$$\lambda^{392} - \lambda^{294} + 0.1\lambda^{293} - 12\lambda^{196} + 12.9\lambda^{195} - 27.2\lambda^{97} = 0$$

and for Jacobian matrix (21) and slope b, it has the following form:

$$\lambda^{392} + 4\lambda^{294} + 0.1\lambda^{293} - 7\lambda^{196} + 13.4\lambda^{195} + 38.3\lambda^{97} = 0.$$

Both of the aforementioned characteristic equations are polynomials of very high order, and it is difficult to analytically find the roots of such polynomials. Because of this, we have used a MATLAB routine `roots()`. For the system to remain chaotic, there should be at least one root λ in the unstable region; it means that $|\arg(\lambda)| < \pi/(2m) = \pi/200$. This condition is satisfied for roots $\lambda_1 = 0$ and $\lambda_2 \approx 1.0120565137$ of slope a and $\lambda_1 = 0$ and $\lambda_{2,3} \approx 1.0107809162 \pm 0.0153011315j$ of slope b. Such equilibrium point is the unstable focus node. These results confirm the results obtained via simulations.

VI. Conclusion

In this brief, we have presented the fractional-order memristor-based Chua's equations and methods for their numerical solution, simulation, and stability analysis.

The results show that fractional calculus is a very useful tool even in nonlinear circuit analysis. By using the fractional differential equations, we get a total order of the system that is less than the number of differential equations. In the case of a chaotic system usually described by three equations, we obtain a total order of less than three, and chaos still can be observed. In the case of a hyperchaotic system, the situation is similar. It opens a new area of applications for the proposed chaotic system.

References

[1] R. L. Magin, *Fractional Calculus in Bioengineering*. Redding, CT: Begell House Publishers, 2006.
[2] K. B. Oldham and J. Spanier, *The Fractional Calculus*. New York: Academic, 1974.
[3] I. Podlubny, *Fractional Differential Equations*. San Diego, CA: Academic, 1999.
[4] S. Westerlund, *Dead Matter Has Memory!* Kalmar, Sweden: Causal Consulting, 2002.
[5] R. Caponetto, G. Dongola, L. Fortuna, and I. Petráš, *Fractional Order Systems: Modeling and Control Applications*. Singapore: World Scientific, 2010.
[6] T. T. Hartley, C. F. Lorenzo, and H. K. Qammer, "Chaos on a fractional Chua's system," *IEEE Trans. Circuits Syst. I, Fundam. Theory Appl.*, vol. 42, no. 8, pp. 485–490, Aug. 1995.
[7] M. S. Tavazoei and M. Haeri, "Chaotic attractors in incommensurate fractional order systems," *Phys. D*, vol. 237, no. 20, pp. 2628–2637, Oct. 2008.
[8] L. Dorčák, "Numerical models for simulation the fractional-order control systems," Acad. Sci., Inst. Exp. Phys., Košice, Slovakia, UEF-04-94, 1994.
[9] S. Westerlund and L. Ekstam, "Capacitor theory," *IEEE Trans. Dielectr. Elect. Insul.*, vol. 1, no. 5, pp. 826–839, Oct. 1994.
[10] I. Schafer and K. Kruger, "Modelling of lossy coils using fractional derivatives," *J. Phys. D, Appl. Phys.*, vol. 41, no. 4, pp. 1–8, Feb. 2008.
[11] L. O. Chua, "Memristor—The missing circuit element," *IEEE Trans. Circuit Theory*, vol. CT-18, no. 5, pp. 507–519, Sep. 1971.
[12] L. O. Chua and M. K. Sung, "Memristive devices and systems," *Proc. IEEE*, vol. 64, no. 2, pp. 209–223, Feb. 1976.
[13] D. B. Strukov, G. S. Snider, D. R. Stewart, and R. S. Williams, "The missing memristor found," *Nature*, vol. 453, no. 7191, pp. 80–83, May 2008.
[14] C. Coopmans, I. Petráš, and Y. Q. Chen, "Analogue fractional-order generalized memristive devices," in *Proc. ASME Conf.*, San Diego, CA, Aug. 30–Sep. 2, 2009.
[15] W. Deng, "Smoothness and stability of the solutions for nonlinear fractional differential equations," *Nonlinear Anal.*, vol. 72, no. 3/4, pp. 1768–1777, Feb. 2010.
[16] M. S. Tavazoei and M. Haeri, "A necessary condition for double scroll attractor existence in fractional-order systems," *Phys. Lett. A*, vol. 367, no. 1/2, pp. 102–113, Jul. 2007.
[17] M. S. Tavazoei and M. Haeri, "Unreliability of frequency-domain approximation in recognising chaos in fractional-order systems," *IET Signal Process.*, vol. 1, no. 4, pp. 171–181, Dec. 2007.
[18] W. Deng, C. Li, and J. Lu, "Stability analysis of linear fractional differential system with multiple time delays," *Nonlinear Dyn.*, vol. 48, no. 4, pp. 409–416, Jun. 2007.
[19] M. S. Tavazoei and M. Haeri, "Limitations of frequency domain approximation for detecting chaos in fractional order systems," *Nonlinear Anal.*, vol. 69, no. 4, pp. 1299–1320, Aug. 2008.
[20] T. Matsumoto, "A chaotic attractor from Chua's circuit," *IEEE Trans. Circuits Syst.*, vol. CAS-31, no. 12, pp. 1055–1058, Dec. 1984.
[21] I. Petráš, "A note on the fractional-order Chua's system," *Chaos Solitons Fractals*, vol. 38, no. 1, pp. 140–147, Oct. 2008.
[22] M. Itoh and L. O. Chua, "Memristor oscillation," *Int. J. Bifurcat. Chaos Appl. Sci. Eng.*, vol. 18, no. 11, pp. 3183–3206, 2008.
[23] R. Riaza, "Nondegeneracy conditions for active memristive circuits," *IEEE Trans. Circuits Syst. II, Exp. Briefs*, vol. 57, no. 3, pp. 223–227, Mar. 2010.
[24] I. Petráš, "A note on the fractional-order Volta's system," *Commun. Nonlinear Sci. Numer. Simul.*, vol. 15, no. 2, pp. 384–393, Feb. 2010.

Journal of ELECTRICAL ENGINEERING, VOL. 60, NO. 3, 2009, 117–128

FRACTIONAL – ORDER FEEDBACK CONTROL OF A DC MOTOR

Ivo Petráš *

This paper deals with the feedback control of a DC motor speed with using the fractional-order controller. The permanent-magnet DC motor is often used in mechatronic and other fields of control theory and therefore its control is very important. The mathematical description of the fractional - order controller and its implementation in the analogue and the discrete domains is presented. An example of simulation and possible realization of the particular case of digital fractional-order $PI^{\lambda}D^{\delta}$ controller are shown as well. The hardware realization is proposed in digital form with the microprocessor and in analogue form with the fractance circuits.

K e y w o r d s: fractional calculus, fractional-order controller, microprocessor, fractance, DC motor

1 INTRODUCTION

The DC motor is a power actuator, which converts direct current electrical energy into rotational mechanical energy. The DC motors are still often used in industry and in numerous control applications, robotic manipulators and commercial applications such as disk drive, tape motor as well.

We will consider the armature - controlled DC motor utilizes a constant field current. This kind of the DC motor will be controlled by a nonconventional control technique which is known as a fractional-order control. Mentioned technique was developed during last few decades and there are various practical applications as for example flexible spacecraft attitude control [25], car suspension control [29], temperature control [32], motor control [51], etc. This idea of the fractional calculus application to control theory was described in many other works (*eg*: [4], [15], [31], [38], *etc*) and its advantages were proved as well. All these works used the continuous models based on fractional differential equations or transfer function. For practical application of the fractional-order models in control and for realization of the fractional-order controllers (FOC), we need discrete fractional-order models. It is also well known that the fractional-order systems have an unlimited memory (infinite dimensional) while the integer-order systems have a limited memory (finite dimensional). It is important to approximately describe the fractional-order systems using a finite difference equations. We will consider new discretization technique proposed by Chen *et al* in [12]. Obtained discrete version of fractional order controller will be implemented by a microprocessor and proposed to the DC motor control.

This article is organized as follow: In section 2, we present a brief introduction to fractional calculus and its approximation. Section 3 presents mathematical model of DC motor as a controlled object. Section 4 deals with fractional order control. Section 5 presents some simulation results. Section 6 treats of proposal to digital and analogue realization of the FOC. Section 7 concludes this paper by some remarks and conclusions.

2 FUNDAMENTALS OF FRACTIONAL CALCULUS

2.1 A bit of history and definitions

Fractional calculus is a generalization of integration and differentiation to non-integer (fractional) order fundamental operator ${}_aD_t^r$, where a and t are the limits and $(r \in R)$ is the order of the operation. There are several definition of fractional integration and differentiation (see [28], [29], [39]). The most often used are the Grünwald-Letnikov (GL) definition and the Riemann-Liuville definition (RL). For a wide class of functions, the two definitions – GL and RL – are equivalent [39].

The GL is given as

$$ {}_aD_t^r f(t) = \lim_{h\to 0} h^{-r} \sum_{j=0}^{[\frac{t-a}{h}]} (-1)^j \binom{r}{j} f(t-jh), \qquad (1)$$

where $[\cdot]$ means the integer part. The RL definition is given as

$$ {}_aD_t^r f(t) = \frac{1}{\Gamma(n-r)} \frac{\mathrm{d}^n}{\mathrm{d}t^n} \int_a^t \frac{f(\tau)}{(t-\tau)^{r-n+1}} \mathrm{d}\tau\,, \qquad (2)$$

for $(n-1 < r < n)$ and where $\Gamma(\cdot)$ is the *Gamma* function.

For many engineering applications the Laplace transform methods are often used. The Laplace transform of the GL and RL fractional derivative/integral, under zero initial conditions for order r is given by [28]:

$$ \mathcal{L}\{{}_aD_t^{\pm r} f(t); s\} = s^{\pm r} F(s)\,. \qquad (3)$$

* Institute of Control and Informatization of Production Processes, Faculty of BERG, Technical University of Košice, B. Němcovej 3, 042 00 Košice, Slovakia, ivo.petras@tuke.sk

ISSN 1335-3632

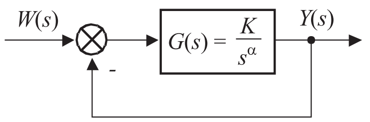

Fig. 1. Bode's ideal loop

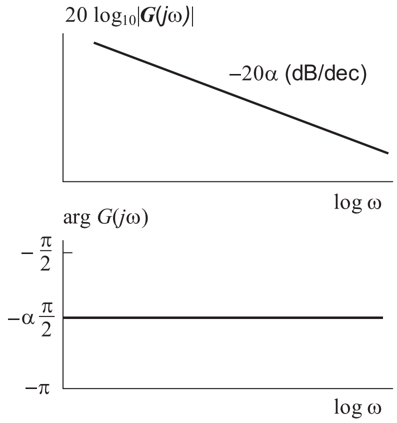

Fig. 2. Bode plots of transfer function $G_o(s)$ in (5)

Some other important properties of the fractional derivatives and integrals can be found in several works ([28],[29], [39], *etc*).

Geometric and physical interpretation of fractional integration and fractional differentiation were exactly described in [40].

2.2 Bode's ideal loop as a reference model

H. W. Bode suggested an ideal shape of the loop transfer function in his work on design of feedback amplifiers in 1945. Ideal loop transfer function has form [7]:

$$L(s) = \left(\frac{s}{\omega_{gc}}\right)^{\alpha}, \tag{4}$$

where ω_{gc} is desired crossover frequency and α is slope of the ideal cut-off characteristic.

Phase margin is $\Phi_m = \pi(1+\alpha/2)$ for all values of the gain. The amplitude margin A_m is infinity. The constant phase margin 60^o, 45^o and 30^o correspond to the slopes $\alpha = -1.33$, -1.5 and -1.66.

The Nyquist curve for ideal Bode transfer function is simply a straight line through the origin with $\arg(L(j\omega)) = \alpha\pi/2$.

Bode's transfer function (4) can be used as a reference system in the following form [3], [24], [36], [41], [50]:

$$G_c(s) = \frac{K}{s^\alpha + K}, \quad G_o(s) = \frac{K}{s^\alpha}, \quad (0 < \alpha < 2), \tag{5}$$

where $G_c(s)$ is transfer function of closed loop and $G_o(s)$ is transfer function in open loop.

General characteristics of Bode's ideal transfer function are:

(a) Open loop:
- Magnitude: constant slope of $-\alpha 20$ dB/dec;
- Crossover frequency: a function of K;
- Phase: horizontal line of $-\alpha\frac{\pi}{2}$;
- Nyquist: straight line at argument $-\alpha\frac{\pi}{2}$.

(b) Closed loop:
- Gain margin: $A_m = \infty$;
- Phase margin: constant : $\Phi_m = \pi\left(1 - \frac{\alpha}{2}\right)$;
- Step response:

$$y(t) = Kt^\alpha E_{\alpha,\alpha+1}\left(-Kt^\alpha\right),$$

where $E_{a,b}(z)$ is the Mittag-Leffler function of two parameters [38].

2.3 Continuous time approximation of fractional calculus

A detailed review of the various approximation methods and techniques for continuous and discrete fractional-order models in form of IIR and FIR filters was done in work [45].

For simulation purpose, here we present the Oustaloup's approximation algorithm [29], [30]. The method is based on the approximation of a function of the form:

$$H(s) = s^r, \qquad r \in R, \qquad r \in [-1;1] \tag{6}$$

for the frequency range selected as (ω_b, ω_h) by a rational function:

$$\widehat{H}(s) = C_o \prod_{k=-N}^{N} \frac{s + \omega'_k}{s + \omega_k} \tag{7}$$

using the following set of synthesis formulas for zeros, poles and the gain:

$$\omega'_k = \omega_b \left(\frac{\omega_h}{\omega_b}\right)^{\frac{k+N+0.5(1-r)}{2N+1}},$$

$$\omega_k = \omega_b \left(\frac{\omega_h}{\omega_b}\right)^{\frac{k+N+0.5(1-r)}{2N+1}}, \tag{8}$$

$$C_o = \left(\frac{\omega_h}{\omega_b}\right)^{-\frac{r}{2}} \prod_{k=-N}^{N} \frac{\omega_k}{\omega'_k}, \tag{9}$$

where ω_h, ω_b are the high and low transitional frequencies. An implementation of this algorithm in Matlab as a function script `ora_foc()` is given in [14].

Using the described Oustaloup-Recursive-Approximation (ORA) method with:

$$\omega_h = 10^3, \quad \omega_b = 10^{-3}, \tag{10}$$

the obtained approximation for fractional function $H(s) = s^{-\frac{1}{2}}$ is:

$$\widehat{H_5}(s) = \frac{s^5 + 74.97s^4 + 768.5s^3 + 1218s^2 + 298.5s + 10}{10s^5 + 298.5s^4 + 1218s^3 + 768.5s^2 + 74.97s + 1}. \tag{11}$$

The Bode plots and the unit step response of the approximated fractional order integrator (11) are depicted in Fig. 3. Bode plots can be compared with the ideal plots depicted in Fig. 2.

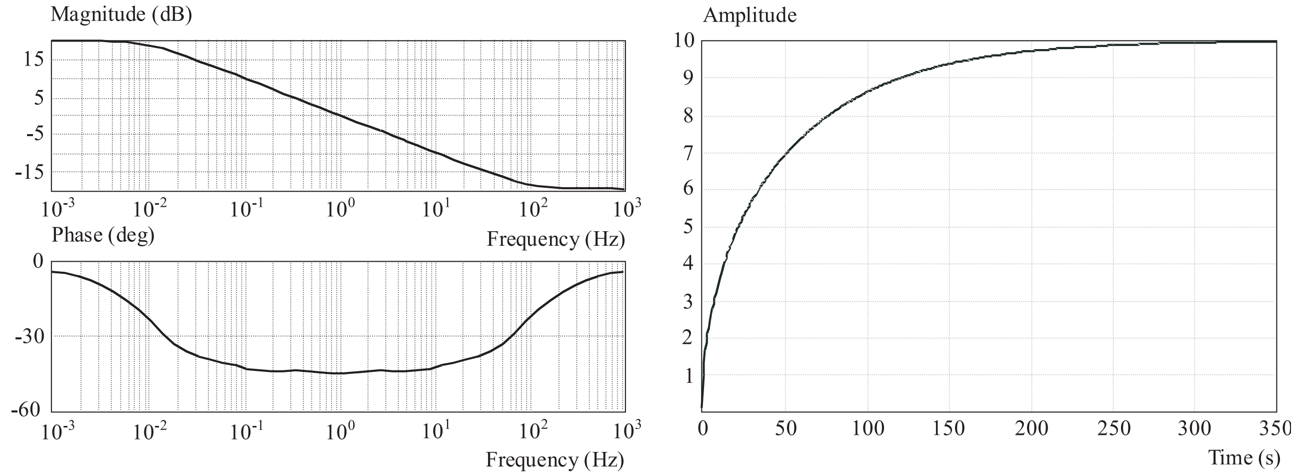

Fig. 3. Characteristics of approximated fractional order integrator (11): Bode plots for $r = -0.5$ and $N = 5$ (left), Unit step response for $r = -0.5$ and $N = 5$ (right)

2.4 Discrete time approximation of fractional calculus

In general, the discretization of fractional-order differentiator/integrator $s^{\pm r}$ $(r \in R)$ can be expressed by the so-called *generating function* $s \approx \omega(z^{-1})$. This generating function and its expansion determine both the form of the approximation and the coefficients [19].

As a generating function $\omega(z^{-1})$ can be used in generally the following formula [6]:

$$\omega(z^{-1}) = \Big(\frac{1}{\beta T}\frac{1-z^{-1}}{\gamma + (1-\gamma)z^{-1}}\Big), \tag{12}$$

where β and γ are denoted the gain and phase tuning parameters, respectively. For example, when $\beta = 1$ and $\gamma = \{0,\ 1/2,\ 7/8,\ 1,\ 3/2\}$, the generating function (12) becomes the forward Euler, the Tustin, the Al-Alaoui, the backward Euler, the implicit Adams rules, respectively. In this sense the generating formula can be tuned precisely.

The expansion of the generating functions can be done by Power Series Expansion (PSE) or Continued Fraction Expansion (CFE).

It is very important to note that PSE scheme leads to approximations in the form of polynomials, that is, the discretized fractional order derivative is in the form of FIR filters, which have only zeros.

Taking into account that our aim is to obtain discrete equivalents to the fractional integrodifferential operators in the Laplace domain, $s^{\pm r}$, the following considerations have to be made [46]:

1. s^r, $(0 < r < 1)$, viewed as an operator, has a branch cut along the negative real axis for arguments of s on $(-\pi, \pi)$ but is free of poles and zeros.
2. It is well known that, for interpolation or evaluation purposes, rational functions are sometimes superior to polynomials, roughly speaking, because of their ability to model functions with zeros and poles. In other words, for evaluation purposes, rational approximations frequently converge much more rapidly than PSE and have a wider domain of convergence in the complex plane.

In this paper, for directly discretizing s^r, $(0 < r < 1)$, we shall concentrate on the IIR form of discretization where as a generating function we will adopt an Al-Alaoui idea on mixed scheme of Euler and Tustin operators [1], [2] but we will use a different ration between both operators. The mentioned new operator, raised to power $\pm r$, has the form [34]:

$$(\omega(z^{-1}))^{\pm r} = \Big(\frac{1+a}{T}\frac{1-z^{-1}}{1+az^{-1}}\Big)^{\pm r}, \tag{13}$$

where a is ratio term and r is fractional order. The ratio term a is the amount of phase shift and this tuning knob is sufficient for most solved engineering problems.

In expanding the above in rational functions, we will use the CFE. It should be pointed out that, for control applications, the obtained approximate discrete-time rational transfer function should be stable and minimum phase. Furthermore, for a better fit to the continuous frequency response, it would be of high interest to obtain discrete approximations with poles an zeros interlaced along the line $z \in (-1, 1)$ of the z plane. The direct discretization approximations proposed in this paper enjoy the desirable properties.

The result of such approximation for an irrational function, $\widehat{G}(z^{-1})$, can be expressed by $G(z^{-1})$ in the CFE form [46]:

$$G(z^{-1}) \simeq$$
$$a_0(z^{-1}) + \cfrac{b_1(z^{-1})}{a_1(z^{-1}) + \cfrac{b_2(z^{-1})}{a_2(z^{-1}) + \cfrac{b_3(z^{-1})}{a_3(z^{-1}) + \dots}}}$$
$$= a_0(z^{-1}) + \frac{b_1(z^{-1})}{a_1(z^{-1})+}\ \frac{b_2(z^{-1})}{a_2(z^{-1})+}\ \cdots \frac{b_3(z^{-1})}{a_3(z^{-1})+} \dots \tag{14}$$

where a_i and b_i are either rational functions of the variable z^{-1} or constants. The application of the method

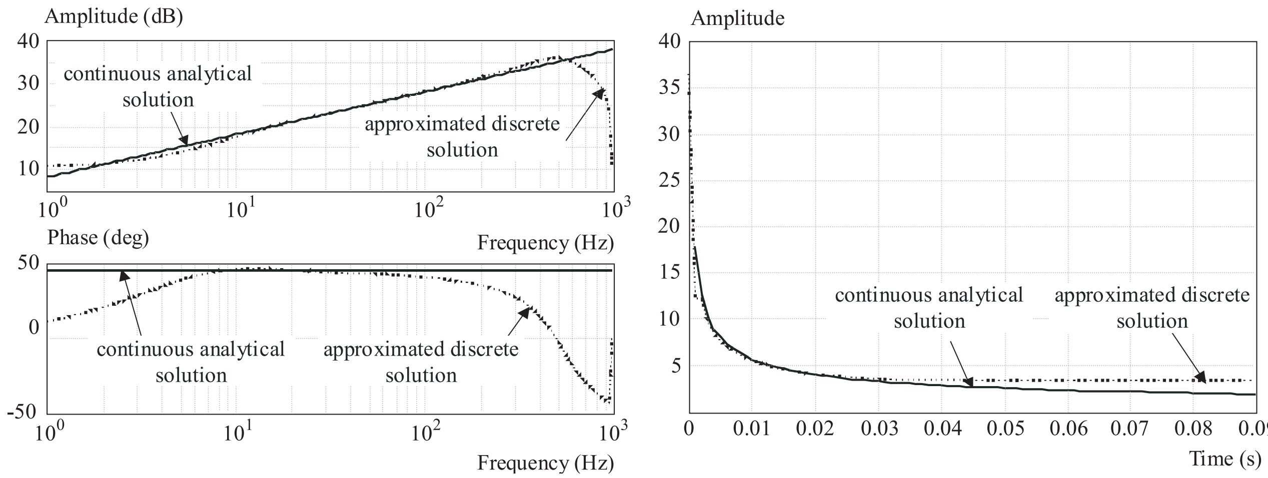

Fig. 4. Characteristics of approximated fractional order differentiator (16): Bode plots for $r = 0.5$, $n = 5$, $a = 1/3$, and $T = 0.001$ s in (15) (left), Unit step responses for $r = 0.5$, $n = 5$, $a = 1/3$, and $T = 0.001$ s in (15) (right)

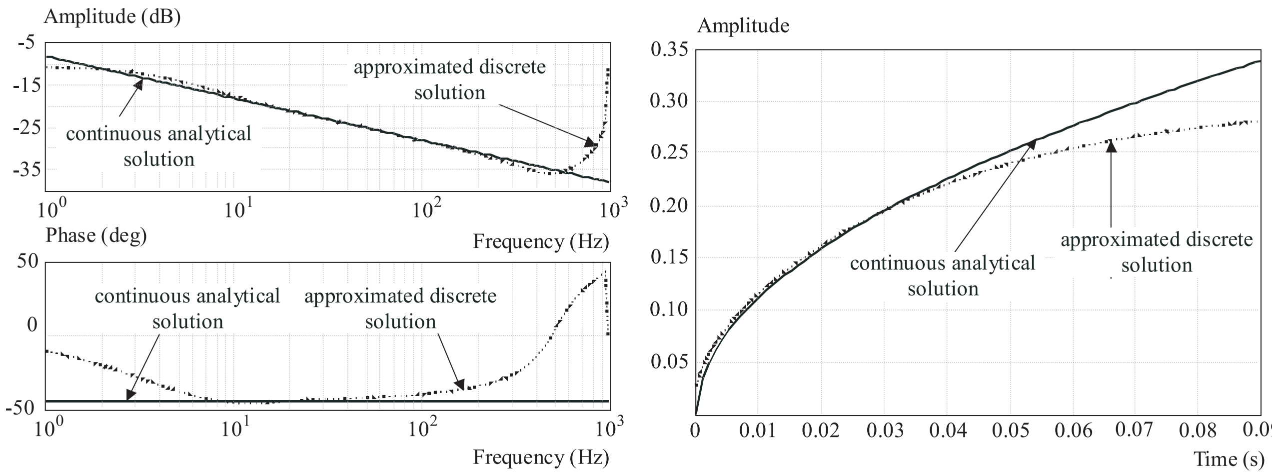

Fig. 5. Characteristics of approximated fractional order integrator (17): Bode plots for $r = -0.5$, $n = 5$, $a = 1/3$, and $T = 0.001$ s in (15) (left), Unit step responses for $r = -0.5$, $n = 5$, $a = 1/3$, and $T = 0.001$ s in (15) (right)

yields a rational function, $G(z^{-1})$, which is an approximation of the irrational function $\widehat{G}(z^{-1})$.

The resulting discrete transfer function, approximating fractional-order operators, can be expressed as:

$$
\begin{aligned}
(\omega(z^{-1}))^{\pm r} &\approx \Big(\frac{1+a}{T}\Big)^{\pm r} \mathrm{CFE}\Big\{\Big(\frac{1-z^{-1}}{1+az^{-1}}\Big)^{\pm r}\Big\}_{p,q} \\
&= \Big(\frac{1+a}{T}\Big)^{\pm r} \frac{P_p(z^{-1})}{Q_q(z^{-1})}, \\
&= \Big(\frac{1+a}{T}\Big)^{\pm r} \frac{p_0 + p_1 z^{-1} + \dots + p_m z^{-p}}{q_0 + q_1 z^{-1} + \dots + q_n z^{-q}},
\end{aligned}
\tag{15}
$$

where $\mathrm{CFE}\{u\}$ denotes the continued fraction expansion of u; p and q are the orders of the approximation and P and Q are polynomials of degrees p and q. Normally, we can set $p = q = n$.

In Matlab Symbolic Toolbox, by the following script, for a given n we can easily get the approximated direct discretization of fractional order derivative (let us denote that $x = z^{-1}$):

```
syms r a x;maple('with(numtheory)');
f = ((1-x)/(1+a*x))^r;;
n=5; n2=2*n;
maple(['cfe := cfrac(' char(f) ',x,n2);'])
pq=maple('P_over_Q := nthconver','cfe',n2)
p0=maple('P := nthnumer','cfe',n2)
q0=maple('Q := nthdenom','cfe',n2)
p=(p0(5:length(p0)));q=(q0(5:length(q0)));
p1=collect(sym(p),x)
q1=collect(sym(q),x)
```

Modified and improved digital fractional-order differentiator using fractional sample delay and digital integrator using recursive Romberg integration rule and fractional order delay as well has been described in [42].

Some others solutions for design IIR approximation using least-squares *eg*: the Padé approximation, the Prony's method and the Shranks' method were described in [6]. The Prony and Shranks methods can produce better approximations the widely used CFE method. The Padé and the CFE methods yield the same approximation (causal,

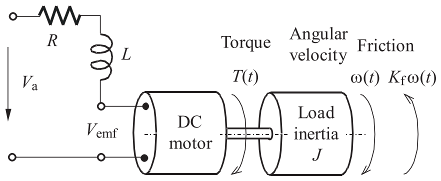

Fig. 6. General model of a DC motor

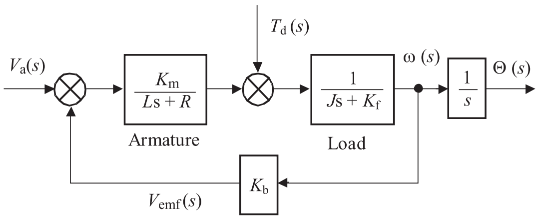

Fig. 7. Mathematical model of a DC motor

stable and minimum phase). Different approach of the CFE method was used in [23].

Here we present some results for fractional order $r = \pm 0.5$ (half order derivative/integral). The value of approximation order n is truncated to $n = 5$ and weighting factor a was chosen $a = 1/3$. Assume sampling period $T = 0.001$ s.

For $r = 0.5$ we have the following approximation of the fractional half-order derivative:

$$G(z^{-1}) = \frac{985.9 - 1315z^{-1} + 328.6z^{-2} + 36.51z^{-3}}{27 - 18z^{-1} - 3z^{-2} + z^{-3}} \tag{16}$$

The Bode plots and unit step response of the digital fractional order differentiator (16) and the analytical continuous solution of a fractional semi-derivative are depicted in Fig. 4. Poles and zeros of the transfer function (16) lie in a unit circle.

For $r = -0.5$ we have the following approximation of the fractional half-order integral:

$$G(z^{-1}) = \frac{0.739 - 0.493z^{-1} - 0.0822z^{-2} + 0.0274z^{-3}}{27 - 36z^{-1} + 9z^{-2} + z^{-3}} \tag{17}$$

The Bode plots and unit step response of the digital fractional order integrator (17) and the analytical continuous solution of a fractional semi-derivative are depicted in Fig. 5. Poles and zeros of the transfer function (17) lie in a unit circle.

3 MODEL OF A DC MOTOR

We will consider the general model of the DC motor (DCM) which is depicted in Fig. 6. The applied voltage V_a controls the angular velocity $\omega(t)$.

The relations for the armature controlled DC motor are shown schematically in Fig. 7. Transfer function (with $T_d(s) = 0$) has the form [16]:

$$G_{DCM}(s) = \frac{\theta(s)}{V_a(s)} = \frac{K_m}{s[(Ls+R)(Js+K_f)+K_bK_m]}. \tag{18}$$

However, for many DCM the time constant of the armature is negligible and therefore we can simplify model (18). A simplified continuous mathematical model has the following form:

$$G_{DCM}(s) = \frac{\theta(s)}{V_a(s)} = \frac{K_m}{s[R(Js+K_f)+K_bK_m]} = \frac{[K_m/(RK_f+K_bK_m)]}{s(\tau s+1)} = \frac{K_{DCM}}{s(\tau s+1)}, \tag{19}$$

where the time constant $\tau = RJ/(RK_f + K_bK_m)$ and $K_{DCM} = K_m/(RK_f + K_bK_m)$. It is of interest to note that $K_m = K_b$.

This mini DC motor with model number PPN13KA12C is great for robots, remote control applications, CD and DVD mechanics, etc. Specifications are [21]: min. voltage 1.5 V, nominal voltage 2 V, max. voltage 2.5 V, max. rated current 0.08 A, no load speed 3830 r/min and rated load speed 3315 r/min. For our mini DC motor the physical constants are: $R = 6\,\Omega$, $K_m = K_b = 0.1$, $K_f = 0.2$ N m s and $J = 0.01\,\mathrm{kg\,m^2/s^2}$. For these motor constants the transfer function (19) of the DC motor has the form:

$$G_{DCM}(s) = \frac{0.08}{s(0.05s+1)}. \tag{20}$$

Discrete mathematical model of the DC motor (20) obtained via new discretization method (13), for sampling period $T = 0.001$ s and $a = 1/3$, has the following form:

$$G_{DCM}(z^{-1}) = \frac{8.89\times10^{-3}z^{-2} + 0.053z^{-1} + 0.08}{8.844\times10^{4}z^{-2} - 1.787\times10^{5}z^{-1} + 9.022\times10^{4}}. \tag{21}$$

In Fig. 8 is depicted the comparison of the continues (20) and dicsrete (21) model of the DC motor. As we can observe in figures, both models have a good agreement.

4 FRACTIONAL–ORDER CONTROL

4.1 Preliminary consideration

As we mentioned in introduction, we can also find works dealing with the application of the fractional calculus tool in control theory, but these works have usually theoretical character, whereas the number of works, in which a real object is analyzed and the fractional - order controller is designed and implemented in practice, is very small. The main reason for this fact is the difficulty of controller implementation. This difficulty arises from the mathematical nature of fractional operators, which, defined by convolution and implying a non-limited memory, demand hard requirements of processors memory and velocity capacities.

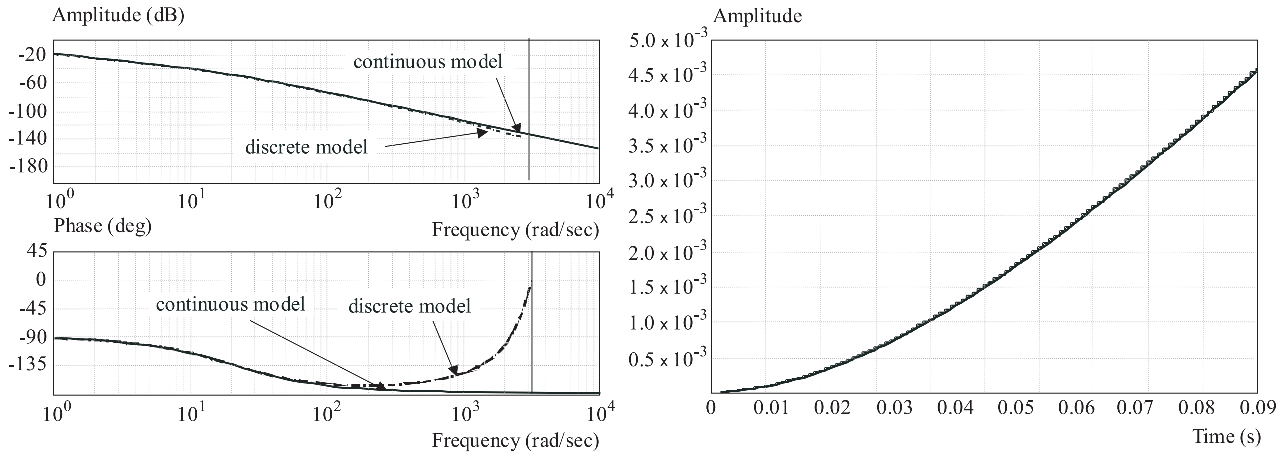

Fig. 8. Comparison of characteristics for both models of a DC motor: Bode plots of the motor models (left), Comparison of characteristics for both models of a DC motor (right)

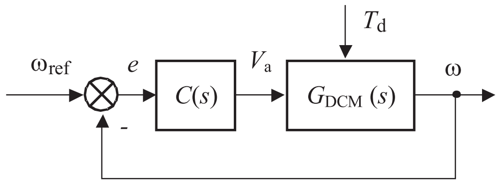

Fig. 9. Feedback control loop

4.2 Fractional-order controllers

The fractional-order $PI^\lambda D^\delta$ controller was proposed as a generalization of the PID controller with integrator of real order λ and differentiator of real order δ. The transfer function of such type the controller in Laplace domain has form [38]:

$$C(s) = \frac{U(s)}{E(s)} = K_p + K_i\, s^{-\lambda} + K_d\, s^{\delta}, \quad (\lambda, \delta > 0)\,, \tag{22}$$

where K_p is the proportional constant, K_i is the integration constant and K_d is the differentiation constant.

Transfer function (22) corresponds in discrete domain with the discrete transfer function in the following expression [46]:

$$C(z^{-1}) = \frac{U(z^{-1})}{E(z^{-1})} = K_p + K_i(\omega(z^{-1}))^{-\lambda} + K_d(\omega(z^{-1}))^{\delta}, \tag{23}$$

where λ and δ are arbitrary real numbers.

Taking $\lambda = 1$ and $\delta = 1$, we obtain a classical PID controller. If $\delta = 0$ and $K_d = 0$, we obtain a PI^λ controller, *etc.* All these types of controllers are particular cases of the $PI^\lambda D^\delta$ controller, which is more flexible and gives an opportunity to better adjust the dynamical properties of the fractional-order control system.

There are many another considerations of the fractional-order controller. For example we can notice the $CRONE$ controller [29], the non-integer integral and its application to control [24] or the TID compensator [20], which has a similar structure as a PID controller but the proportional component is replaced with a tilted component having a transfer function s to the power of $(-1/n)$.

All those fractional-order controllers are sometimes called optimal phase controllers because only with non-integer order we can get a constant phase somewhere between 0^o and -180^o depending on the parameters λ and δ.

4.3 Fractional-order controller design

For the FOC design we will use an idea which was proposed by Bode [7] and for first time used to the motion control described by Tustin [43]. This principle was also used by Manabe to induction motor speed control [25].

The several methods and tuning techniques for the FOC parameters were developed during the past ten years. They are based on various approaches (see [5], [13], [22], [26], [31], [49], [52]).

In Fig. 9 is depicted feedback control loop, where C(s) is transfer function of controller and $G_{DCM}(s)$ is transfer function of the DC motor.

We will design the controller, which give us a step response of feedback control loop with overshoot independent of payload changes (iso-damping). In the frequency domain point of view it means phase margin independent of the payload changes.

Phase margin of controlled system is [9], [48]

$$\Phi_m = \arg\left[C(j\omega_g)G_{DCM}(j\omega_g)\right] + \pi\,, \tag{24}$$

where $j\omega_g$ is the crossover frequency. Independent phase margin means in other words constant phase. This can be accomplished by controller of the form

$$C(s) = k_1 \frac{k_2 s + 1}{s^{\mu}}\,, \quad k_1 = 1/K_{DCM}\,, \quad k_2 = \tau\,. \tag{25}$$

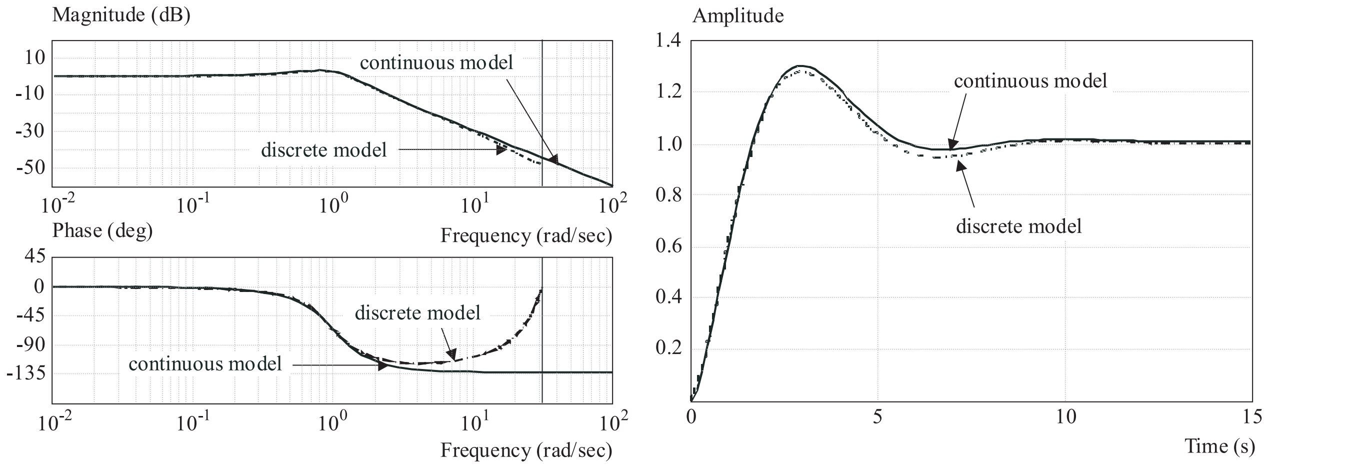

Fig. 10. Characteristics of fractional order transfer function (28): Bode plots – continuous and discrete models $n = 5$, $a = 1/3$, and $T = 0.1$ s (left), Unit step responses –continuous and discrete models $n = 5$, $a = 1/3$, and $T = 0.1$ s (right)

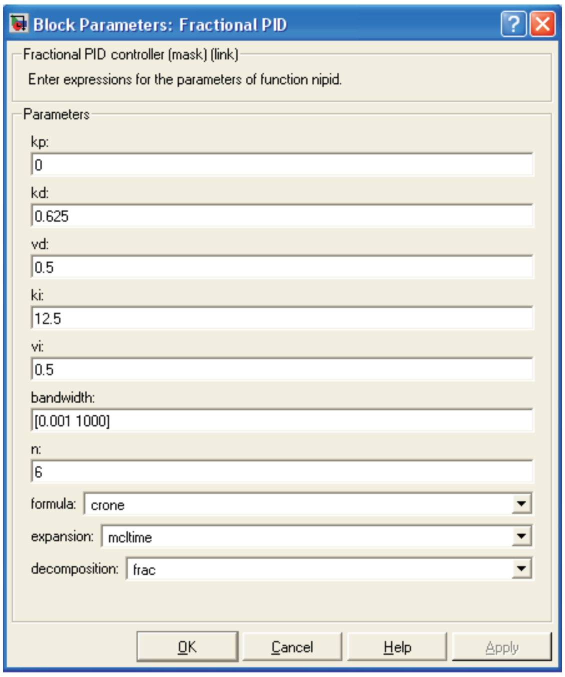

Fig. 11. Simulink block **nipid** - fractional order controller

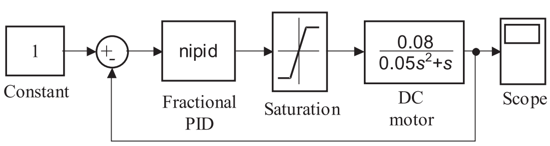

Fig. 12. Simulink model for feedback control of the DC motor

Such controller gives a constant phase margin and obtained phase margin is

$$\begin{aligned}\Phi_m &= \arg\left[C(j\omega)G_{DCM}(j\omega)\right] + \pi \\ &= \arg\left[\frac{k_1 K_{DCM}}{(j\omega)^{(1+\mu)}}\right] + \pi \\ &= \arg\left[(j\omega)^{-(1+\mu)}\right] + \pi = \pi - (1+\mu)\frac{\pi}{2}\,. \end{aligned} \tag{26}$$

For our parameters of controlled object (20) and desired phase margin $\Phi_m = 45^o$, we get the following constants of the fractional order controllres (25): $k_1 = 12.5$, $k_2 = 0.05$ and $\mu = 0.5$. With these constants we obtain a fractional $I^\lambda D^\delta$ controller, which is a particular case of the $PI^\lambda D^\delta$ controller and has the form

$$\begin{aligned} C(s) &= \frac{\tau}{K_{DCM}} s^{0.5} + \frac{1}{K_{DCM} s^{0.5}} \\ &= K_d s^{0.5} + K_i s^{-0.5} = 0.625\sqrt{s} + \frac{12.5}{\sqrt{s}}\,, \end{aligned} \tag{27}$$

where $K_i = 12.5$, $K_d = 0.625$ and $\delta = \lambda = 0.5$.

According to relation (26), by using a controller (27), we can obtain a phase margin

$$\Phi_m = \arg\left[C(j\omega)G_{DCM}(j\omega)\right] + \pi = \pi - (1.5)\,\frac{\pi}{2} = 45°,$$

which was desired phase margin specification.

5 SIMULATION RESULTS

The transfer function of the closed feedback control loop with the fractional-order controller (27) and the DC motor (20) has the following form:

$$\begin{aligned} G_c(s) &= \frac{G_o(s)}{1+G_o(s)} = \frac{G_{DCM}(s)C(s)}{1+G_{DCM}(s)C(s)} \\ &= \frac{0.05s+1}{0.05s^{2.5}+s^{1.5}+0.05s+1}\,, \end{aligned} \tag{28}$$

where $G_o(s)$ is the transfer function of the open control loop with

$$G_o(s) = \frac{0.05s+1}{0.05s^{2.5}+s^{1.5}}\,.$$

The feedback control loop described above can be simulated in Matlab environment with using the approximation technique described before, namely Oustaloup's re-

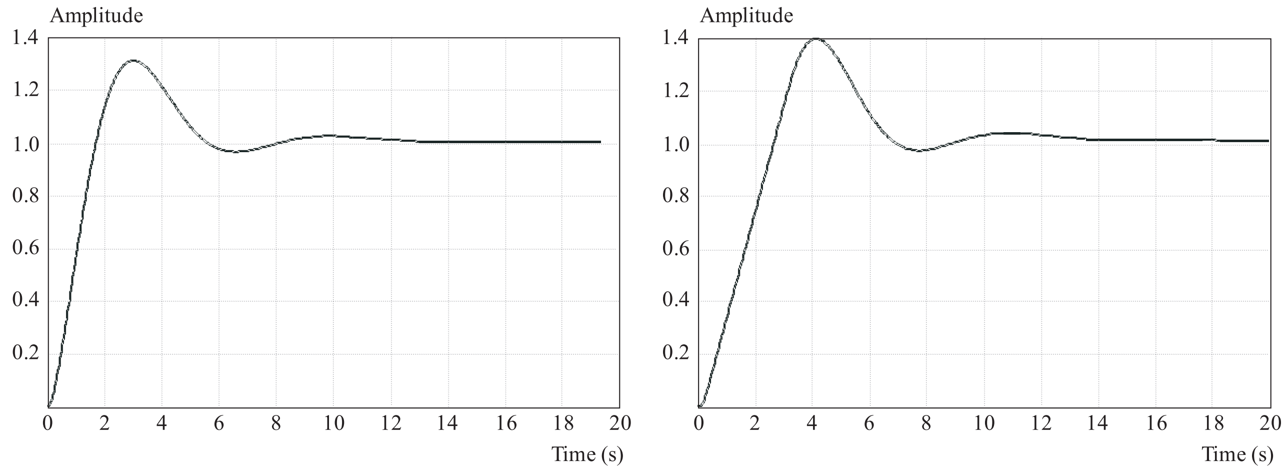

Fig. 13. Comparison of unit step responses of a feedback control loop: Unit step response without actuator saturation overshoot ≈ 30 %, set. time ≈ 11 s (left), Unit step response with actuator saturation overshoot ≈ 40 %, settling time ≈ 14 s (right)

cursive approximation function `ora_foc()` for the desired frequency range given in (10).

```
close all; clear all;
Gs_DCM=tf([0.08],[0.05 1 0]);
Cs=(0.625*ora_foc(0.5,6,0.001,1000))
       +(12.5*ora_foc(-0.5,6,0.001,1000));
Gs_close=(Gs_DCM*Cs)/(1+(Gs_DCM*Cs));
step(Gs_close,15);
Gs_open=(Gs_DCM*Cs);
bode(Gs_open);
[Gm,Pm] = margin(Gs_open);
```

The results obtained via described Matlab scripts are depicted in Fig. 10. Continues model is shown with solid line. Phase margin is $\Phi_m \approx 44.9^\circ$ and gain margin is infinite.

The disrete version of the continues fractional order transfer function can be obtained with using the digital operator (13) and Matlab function for approximation of digital fractional order derivative/integral `dfod1()`. Assume that $T = 0.1$ s and $a = 1/3$.

```
close all; clear all;
T=0.1;
a=1/3;
z=tf('z',T,'variable','z^-1')
Hz=((1+a)/T)*((1-z^-1)/(1+a*z^-1));
Gz_DCM=0.08/(Hz*(0.05*Hz+1));
Cz=0.625*dfod1(5,T,a,0.5)+12.5*dfod1(5,T,a,-0.5);
Gz_close=(Gz_DCM*Cz)/(1+(Gz_DCM*Cz));
step(Gz_close,15);
Gz_open=(Gz_DCM*Cz);
bode(Gz_open);
[Gm,Pm] = margin(Gz_open);
```

The results obtained via described Matlab scripts are depicted in Fig. 10. Discrete model is shown with dashed line. Phase margin is $\Phi_m \approx 45.1^\circ$ and gain margin is infinite.

Simulation of the closed feedback loop can also be dome in Matlab/Simulink environment, where fractional - order controller is realized via `nipid` block proposed by D. Valerio [44], where block parameters are depicted in Fig. 11.

General Simulink model is shown in Fig. 12. Block constants were set according to parameters of DC motor and fractional-order controller.

Time domain simulation results for fractional order feedback loop are depicted in Fig. 13. Obtained results are comparable with the results obtained with simulation in Matlab by routines.

Stability analysis is investigated by solving the characteristic equation of transfer function (28) with using Matlab function `solve()`

```
s=solve('0.05*s^2.5 + s^1.5 + 0.05*s + 1 = 0','s')
```

with the following results: $s_{1,2} = -0.5 \pm 0.86602j$ and $s_3 = -20$. It means that feedback control loop is stable.

As we can observe in Fig. 13, the quality indexes (overshoot and settling time) are worse in the case of control loop with saturation, because of controller power limitations.

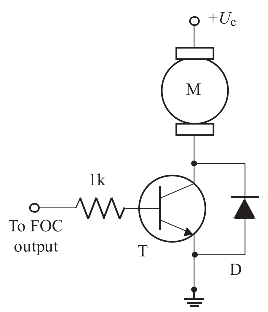

Fig. 14. Actuator for the DC motor

6 PROPOSED REALIZATIONS OF FOC

Basically, there are two methods for realization of the FOC. One is a digital realization based on processor devices and appropriate control algorithm and the second

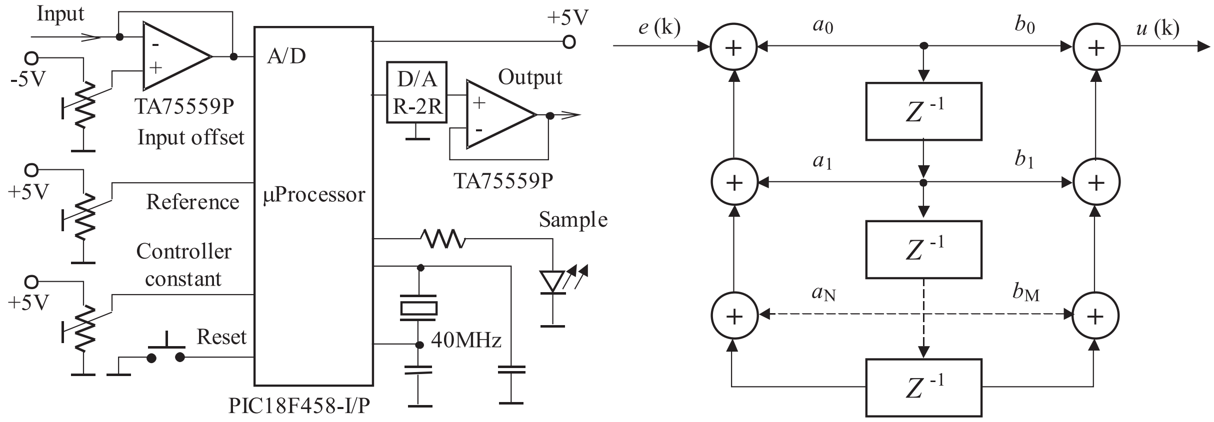

Fig. 15. Proposal for digital implementation of the FOC: Block diagram of the digital fractional-order controller based on PIC processor (left), Block diagram of the canonical representation of IIR filter form (right)

one is an analogue realization based on analogue circuits so-called *fractance*. In this section is described both of them.

In Fig. 14 is depicted the actuator for connection the DC motor to the FOC.

6.1 Digital realization: Control algorithm and HW

This realization can be based on implementation of the control algorithm in the processor devices, e.g.: PLC controller [35], processor C51 or PIC [33], PCL IO card [47], etc. Suppose that processor PIC18F458 is used [55]. Some experimental measurements with this processor were already done in [33].

Generally, the control algorithm is be based on canonical form of IIR filter, which can be expressed as follow

$$F(z^{-1}) = \frac{U(z^{-1})}{E(z^{-1})} = \frac{b_0 + b_1 z^{-1} + b_2 z^{-2} + \cdots + b_M z^{-M}}{a_0 + a_1 z^{-1} + a_2 z^{-2} + \cdots + a_N z^{-N}}, \quad (29)$$

where $a_0 = 1$ for compatible with the definitions used in Matlab. Normally, we choose $M = N$.

For designed fractional-order controller (27) we can use the half-order approximations (16) and (17), respectively. The resulting discrete transfer function of the fractional-order controller arranged to canonical form (29) is represented as

$$C(z^{-1}) = \big(23.17 - 61.33z^{-1} + 55.87z^{-2} - 18.52z^{-3} + 0.268z^{-4} + 0.560z^{-5} + 0.032z^{-6}\big) \Big/ \big(1.00 - 2.00z^{-1} + 1.11z^{-2} - 0.111z^{-4} + 0.0082z^{-5} + 0.0014z^{-6}\big) \quad (30)$$

This controller can be directly implemented to any processor based devices as for instance PLC or PIC depicted in Fig. 15 left. A direct form of such implementation using canonical form shown in Fig. 15 right with input $e(k)$ and output $u(k)$ range mapping to the interval $0 - U_{FOC}$ [V] is divided into two sections: initialization code and cyclic code. Pseudocode has the following syntax

```
(* initialization code *)
scale := 32752; % input and output
order := 6; % order of approximation
U_FOC := 5; % input and output voltage range: 5[V], 10[V],
...
a[0] := 1.0; a[1] := -2.0; a[2] := 1.11; a[3] := 0.0;
a[4] := -0.111; a[5] := 0.0082; a[6] := 0.0014;
b[0] := 23.17; b[1] := -61.33; b[2] := 55.87; b[3] := -18.52;
b[4] := 0.268; b[5] := 0.560; b[6] := 0.032;

loop i := 0 to order do
s[i] := 0;
endloop

(* cyclic code *)
in := (REAL(input)/scale) * U_FOC;
feedback := 0; feedforward := 0;
loop i:=1 to order do
feedback := feedback - a[i] * s[i];
feedforward := feedforward + b[i] * s[i];
endloop
s[0] := in + a[0] * feedback;
out := b[0] * s[1] + feedforward;
loop i := order downto 1 do
s[i] := s[i-1];
endloop output := INT(out*scale)/U_FOC;
```

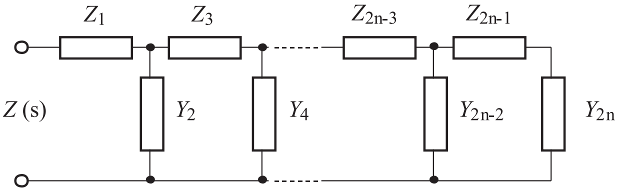

Fig. 16. Finite ladder circuit

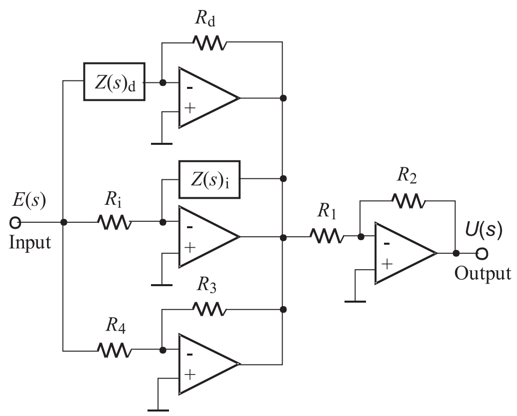

Fig. 17. Analogue fractional-order $PI^{\lambda}D^{\delta}$ controller

The disadvantage with this solution is that the complete controller is calculated using floating point arithmetic.

There are many softwares for PIC programming. As for example: Microchip MPLAB, HiTech C Compiler, PICBasic Pro, *etc.*

6.2 Analogue realization: Fractance circuits and fractor

A circuit exhibiting fractional-order behavior is called a *fractance* [39]. The fractance devices have the following characteristics [27], [28], [18]. First the phase angle is constant independent of the frequency within a wide frequency band. Second it is possible to construct a filter which has moderated characteristics which can not be realized by using the conventional devices.

Generally speaking, there are three basic fractance devices. The most popular is a domino ladder circuit network. Very often used is a tree structure of electrical elements and finally, we can find out also some transmission line circuit. Here we must mention that all basic electrical elements (resistor, capacitor and coil) are not ideal [10], [54].

Design of fractances can be done easily using any of the rational approximations [36] or a truncated CFE, which also gives a rational approximation.

Truncated CFE does not require any further transformation; a rational approximation based on any other methods must be transformed to the form of a continued fraction. The values of the electric elements, which are necessary for building a fractance, are then determined from the obtained finite continued fraction. If all coefficients of the obtained finite continued fraction are positive, then the fractance can be made of classical passive elements (resistors and capacitors). If some of the coefficients are negative, then the fractance can be made with the help of negative impedance converters [37].

Domino ladder lattice networks can approximate fractional operator more effectively than the lumped networks [17].

Let us consider the circuit depicted in Fig. 16, where $Z_{2k-1}(s)$ and $Y_{2k}(s)$, $k = 1, \dots, n$, are given impedances of the circuit elements. The resulting impedance $Z(s)$ of the entire circuit can be found easily, if we consider it in the right-to-left direction:

$$Z(s) = Z_1(s) + \cfrac{1}{Y_2(s) + \cfrac{1}{Z_3(s) + \cfrac{1}{Y_4(s) + \cfrac{1}{\cfrac{\cdots\cdots\cdots\cdots}{\cfrac{1}{Y_{2n-2}(s) + \cfrac{1}{Z_{2n-1}(s) + \cfrac{1}{Y_{2n}(s)}}}}}}}} \tag{31}$$

The relationship between the finite domino ladder network, shown in Fig. 16, and the continued fraction (31) provides an easy method for designing a circuit with a given impedance $Z(s)$. For this one has to obtain a continued fraction expansion for $Z(s)$. Then the obtained particular expressions for $Z_{2k-1}(s)$ and $Y_{2k}(s)$, $k = 1, \dots, n$, will give the types of necessary components of the circuit and their nominal values.

Rational approximation of the fractional integrator/differentiator can be formally expressed as

$$s^{\pm\alpha} \approx \left\{ \frac{P_p(s)}{Q_q(s)} \right\}_{p,q} = Z(s) , \tag{32}$$

where p and q are the orders of the rational approximation, P and Q are polynomials of degree p and q, respectively.

For direct calculation of circuit elements was proposed method by Wang [53]. This method was designed for constructing resistive-capacitive ladder network and transmission lines that have a generalized Warburg impedance $As^{-\alpha}$, where A is independent of the angular frequency and $0 < \alpha < 1$. This impedance may appear at an electrode/electrolyte interface, etc. The impedance of the ladder network (or transmission line) can be evaluated and rewritten as a continued fraction expansion:

$$Z(s) = R_0 + \frac{1}{C_0 s +} \frac{1}{R_1 +} \frac{1}{C_1 s +} \frac{1}{R_2 +} \frac{1}{C_2 s +} \dots \tag{33}$$

If we consider that $Z_{2k-1} \equiv R_{k-1}$ and $Y_{2k} \equiv C_{k-1}$ for $k = 1, \dots, n$ in Fig. 16, then the values of the resistors and capacitors of the network are specified by

$$\begin{aligned} R_k &= 2h^{\alpha} P(\alpha) \frac{\Gamma(k+\alpha)}{\Gamma(k+1-\alpha)} - h^{\alpha}\delta_{ko} \\ C_k &= h^{1-\alpha}(2k+1) \frac{\Gamma(k+1-\alpha)}{P(\alpha)\Gamma(k+1+\alpha)} , \\ P(\alpha) &= \frac{\Gamma(1-\alpha)}{\Gamma(\alpha)} , \end{aligned} \tag{34}$$

where $0 < \alpha < 1$, h is an arbitrary small number, δ_{ko} is the Kronecker delta, and k is an integer, $k \in [0, \infty)$.

In Fig. 17 is depicted an analogue implementation of fractional-order $PI^{\lambda}D^{\delta}$ controller. Fractional order differentiator is approximated by general Warburg impedance $Z(s)_d$ and fractional order integrator is approximated by impedance $Z(s)_i$, where orders of both approximations are $0 < \alpha < 1$. For orders greater than 1, the Warburg impedance can be combined with classical integer order one. Usually we suppose $R_2 = R_1$ in Fig. 17. For proportional gain K_p we can write the formula

$$K_p = \frac{R_3}{R_4}.$$

The integration and derivation constants K_i and K_d can be computed from relationships

$$K_i = \frac{Z(s)_i}{R_i}, \qquad K_d = \frac{R_d}{Z(s)_d}.$$

In the case, if we use identical resistors (R-series) and identical capacitors (C-shunt) in the fractances, then the behavior of the circuit will be as a half-order integrator/differentiator. Realization and measurements of such kind controllers were done in [36]. Some others experimental results we can find in [11].

Instead fractance circuit the new electrical element introduced by G. Bohannan which is so-called *fractor* can be used as well [8]. This element — fractor made from a material with the properties of $LiN_2H_5SO_4$ has been already used for temperature control [5].

7 CONCLUSION

In this paper was presented a case study of fractional order feedback control of a DC motor. Described method is based on Bode's ideal control loop. Design algorithm for fractional-order $PI^{\lambda}D^{\delta}$ controller parameters uses a phase margin specification of open control loop. Another very important advantage is an iso-damping property of such control loop. Simulation results obtained via Matlab/Simulink confirm the described theoretical suggestion. This article also proposed digital and analogue realization of fractional-order controller. Described techniques are useful for practical implementation of fractional-order controllers as the non-conventional control techniques. However this approach also gave a good start for analysis and design of the analog fractional order controller. The fractional-order controller gives us an insight into the concept of memory of the fractional order operator. The design, realization, and implementation of the fractional order control systems also became possible and much easier than before.

Acknowledgment

This work was supported in part by the Slovak Grant Agency for Science under grants VEGA: 1/4058/07, 1/0365/08 and 1/0404/08, and grant APVV-0040-07.

References

[1] Al-ALAOUI, M. A.: Novel Digital Integrator and Differentiator, Electron. Lett. **29** No. 4 (1993), 376-378.

[2] Al-ALAOUI, M. A.: Filling the Gap between the Bilinear and the Backward Difference Transforms: An Interactive Design Approach, Int. J. Elect. Eng. Edu. **34** No. 4 (1997), 331-337.

[3] ASTROM, K. J.: Model Uncertainty and Robust Control, COSY project, 2000.

[4] AXTELL, M.—BISE, E. M.: Fractional Calculus Applications in Control Systems, Proc. of the IEEE 1990 Nat. Aerospace and Electronics Conf, New York, 1990, pp. 563–566.

[5] BASHKARAN, T.—CHEN, Y. Q.—BOHANNAN, G.: Practical Tuning of Fractional Order Proportional and Integral Controller (II): Experiments, Proc. of the ASME 2007 International Design Engineering Technical Conferences & Computers and Information in Engineering Conference, Las Vegas, Nevada, USA, September 4-7, 2007.

[6] BARBOSA, R. S.—MACHADO, J. A. T.—SILVA, M. F.: Time Domain Design of Fractional Differintegrators using Least-Squares, Signal Processing **86** (2006), 2567–2581.

[7] BODE, H. W.: Network Analysis and Feedback Amplifier Design, Tung Hwa Book Company, 1949.

[8] BOHANNAN, G.: Analog Realization of a Fractional Control Element – Revisited, Proc. of the 41st IEEE Int. Conf. on Decision and Control, Tutorial Workshop 2: Fractional Calculus Applications in Automatic Control and Robotics, Las Vegas, USA, December 9, 2002.

[9] BIDAN, P.: Commande diffusive d'une machine électrique: une introduction, ESAIM Proceedings, vol. 5, France, 1998, pp. 55–68.

[10] CARLSON, G. E.—HALIJAK, C. A.: Approximation of Fractional Capacitors $(1/s)^{1/n}$ by a Regular Newton Process, IEEE Trans. on Circuit Theory **11** No. 2 (1964), 210–213.

[11] CHAREF, A.: Analogue Realisation of Fractional-Order Integrator, Differentiator and Fractional $PI^{I}D^{m}$ Controller, IEEE Proc.-Control Theory Appl. **153** No. 6 (Nov 2006), 714–720.

[12] CHEN, Y. Q.—MOORE, K. L.: Discretization Schemes for Fractional-Order Differentiators and Integrators, IEEE Trans. On Circuits and Systems - I: Fundamental Theory and Applications **.49** No. 3 (2002), 363–367.

[13] CHEN, Y. Q.: Tuning Method for Fractional-Order Controllers, United States Patent, US2006/0265085 A1, USA, 2006.

[14] CHEN, Y. Q.: Oustaloup-Recursive-Approximation for Fractional Order Differentiators, MathWorks Inc, August 2003: *http://www.mathworks.com/matlabcentral/fileexchange/3802.*

[15] DORČÁK, Ľ.: Numerical Models for Simulation the Fractional-Order Control Systems, UEF-04-94, Slovak Acad. Sci., Košice, 1994.

[16] DORF, R. C.—BISHOP, R. H.: Modern Control Systems, Addison-Wesley, New York, 1990.

[17] DUTTA ROY, S. C.: On the Realization of a Constant-Argument Immitance of Fractional Operator, IEEE Transactions on Circuit Theory **14** No. 3 (1967), 264–374.

[18] ICHISE, M.—NAGAYANAGI, Y.—KOJIMA, T.: An Analog Simulation of Non-Integer Order Transfer Functions for Analysis of Electrode Processes, J. Electroanal. Chem. **33** (1971), 253–265.

[19] LUBICH, C.: Discretized Fractional Calculus, SIAM J. Math. Anal. **17** No. 3 (1986), 704–719.

[20] LURIE, B. J.: Three-Parameter Tunable Tilt-Integral-Derivative (TID) Controller, United States Patent, 5 371 670, USA, 1994.

[21] Manual for DC motor PPN13: Minebea Motor Manufacturing Corporation, *http://www.eMinebea.com/.*

[22] MACHADO, J. A. T. : Analysis and Design of Fractional-Order Digital Control Systems, J. Syst. Anal. Modeling-Simulation **27** (1997), 107-122.

[23] MAIONE, G. : Continued Fractions Approximation of the Impulse Response of Fractional-Order Dynamic Systems, IET Control Theory Appl. **2** No. 7 (2008), 564–572.

[24] MANABE, S. : The Non-Integer Integral and its Application to Control Systems, ETJ of Japan **6** No. 3-4 (1961), 83–87.

[25] MANABE, S. : A Suggestion of Fractional-Order Controller for Flexible Spacecraft Attitude Control, Nonlinear Dynamics **29** (2002), 251–268.

[26] MONJE, C. A.—VINAGRE, B. M.—FELIU, V.—CHEN, Y. Q. : Tuning and Auto-Tuning of Fractional Order Controllers for Industry Application, Control Engineering Practice **16** (2008), 798–812.

[27] NAKAGAVAM.—SORIMACHI, K. : Basic Characteristics of a Fractance Device, IEICE Trans. fundamentals **E75-A** No. 12 (1992), 1814–1818.

[28] OLDHAM, K. B.—SPANIER, J. : The Fractional Calculus, Academic Press, NY, 1974.

[29] OUSTALOUP, A. : La Dérivation non Entière, Hermes, Paris, 1995.

[30] OUSTALOUP, A.—LEVRON, F.—MATHIEU, B.—NANOT, F. M. : Frequency-Band Complex Noninteger Differentiator: Characterization and Synthesis, IEEE Trans. on Circuits and Systems I: Fundamental Theory and Applications I **47** No. 1 (2000), 25–39.

[31] PETRÁŠ, I. The fractional-Order Controllers: Methods for their Synthesis and Application : Journal of Electrical Engineering **50** No. 9-10 (1999), 284–288.

[32] PETRÁŠ, I.—VINAGRE, B. M. Practical Application of Digital Fractional-Order Controller to Temperature Control : Acta Montanistica Slovaca **7** No. 2 (2002), 131–137.

[33] PETRÁŠ, I.—GREGA, Š. : Digital Fractional Order Controllers Realized by PIC Microprocessor: Experimental Results,, Proceedings of the ICCC2003, High Tatras, Slovak Republic, May 26-29, pp. 873–876.

[34] PETRÁŠ, I. : Digital Fractional Order Differentiator/Integrator – IIR type, MathWorks, Inc.: *http://www.mathworks.com/matlabcentral/fileexchange/3672*, July 2003.

[35] PETRÁŠ, I.—Dorčák, Ľ.—PODLUBNY, I.—TERPÁK, J.—O'LEARY, P. : Implementation of Fractional-Order Controllers on PLC B&R 2005, Proceedings of the ICCC2005 Miskolc-Lillafured, Hungary, May 24-27, pp. 141–144.

[36] PETRÁŠ, I.—PODLUBNY, I.—;O'LEARY, P.—DORČÁK, Ľ.—VINAGRE, B.M. : Analog Realizations of Fractional Order Controllers, Faculty of BERG, TU Košice, 2002.

[37] PODLUBNY, I.—PETRÁŠ, I.—VINAGRE, B.M.—O'LEARY, P.—DORČÁK, Ľ. : Analogue Realization of Fractional-Order Controllers, Nonlinear Dynamics **29** No. 1-4 (2002), 281–296.

[38] PODLUBNY, I. : Fractional-Order Systems and $PI^{\lambda}D^{\mu}$-Controllers, IEEE Transactions on Automatic Control **44** No. 1 (1999), 208–214.

[39] PODLUBNY, I. : Fractional Differential Equations, Academic Press, San Diego, 1999.

[40] PODLUBNY, I. : Geometric and Physical Interpretation of Fractional Integration and Fractional Differentiation, Fractional Calculus and Applied Analysis **5** No. 4 (2002), 367-386.

[41] TAKYAR, M. S.—GEORGIU, T. T. : The Fractional Integrator as a Control Design Element, Proc. of the 46th IEEE Conf. on Decision and Control, New Orleans, USA, Dec. 12-14, 2007, pp. 239–244.

[42] TSENG, C. C.—LEE, S. L. : Digital IIR Integrator Design using Recursive Romberg Integration Rule and Fractional Sample Delay, Signal Processing **88** (2008), 2222–2233.

[43] TUSTIN, A.—ALLANSON, J. T.—LAYTON, J. M.—JAKEWAYS, R. J. : The Design of Systems for Automatic Control of the Position of Massive Objects,, The Proceedings of the Institution of Electrical Engineers **105C** (1) (1958).

[44] VALERIO, D. : Toolbox *ninteger* for Matlab, v. 2.3 (September 2005) *http://web.ist.utl.pt/duarte.valerio/ninteger/ninteger.htm*, visited: May 23, 2008.

[45] VINAGRE, B. M.—PODLUBNY, I.—HERNÁNDEZ, A.—FELIU, V. : Some Approximations of Fractional Order Operators used in Control Theory and Applications, Fractional Calculus and Applied Analysis **3** No. 3 (2000), 231–248.

[46] VINAGRE, B. M.—CHEN, Y. Q.—PETRÁŠ, I. : Two Direct Tustin Discretization Methods for Fractional-Order Differentiator/Integrator, Journal of Franklin Institute **340** (2003), 349–362.

[47] VINAGRE, B. M.—CHEN, Y. Q.—PETRÁŠ, I.—MERCHANT, P.—DORČÁK, Ľ. : Two Digital Realization of Fractional Controllers: Application to Temperature Control of a Solid, Proc. Eur. Control Conf. (ECC01), Porto, Portugal, Sep 2001, pp. 1764-1767.

[48] VINAGRE, B. M.—PODLUBNY, I.—DORČÁK, Ľ.—FELIU, V. : On Fractional PID Controllers: A Frequency Domain Approach,, Proc. of the IFAC Workshop on Digital Control – PID'00, Terrassa, Spain, 2000, pp. 53–55.

[49] VINAGRE, B. M.—MONJE, C. A.—CALDERON, A. J.—SUÁREZ, J. I. : Fractional PID Controllers for Industry Application. A Brief Introduction, Journal of Vibration and Control **13** No. 9-10 (2007), 1419–1429.

[50] VINAGRE, B. M.—MONJE, C. A.—CALDERON, A. J.—CHEN, Y. Q.—FELIU, V. The Fractional Integrator as Reference Function : Proc. of the First IFAC Symposium on Fractional Differentiation and its Application, Bordeaux, France, July 19-20, 2004.

[51] XUE, D.—ZHAO, C.—CHEN, Y. Q. : Fractional Order PID Control of a DC-Motor with Elastic Shaft: A Case Study, Proc. of the 2006 American Control Conference, Minneapolis, Minnesota, USA, June 14-16, 2006, pp. 3182–3187.

[52] ZHAO, C.—XUE, D.—CHEN, Y. Q. : A Fractional Order PID Tuning Algorithm for a Class of Fractional Order Plants, Proc. of the IEEE Int. Conf. Mechatronics and Automation, Niagara Falls, Canada, July 2005, pp. 216–221.

[53] WANG, J. C. : Realizations of Generalized Warburg Impedance with RC Ladder Networks and Transmission Lines, J. of Electrochem. Soc. **134** No. 8 (1987), 1915–1920.

[54] WESTERLUND, S. : Dead Matter Has Memory!, Kalmar, Sweden: Causal Consulting, 2002.

[55] Web site of Microchip Technology corporation. PIC18F458 processor *documentation, http://www.microchip.com/.*

Received 9 December 2008

Ivo Petráš received MSc (1997) degree and PhD (2000) degree in process control at the Technical university of Košice. He works at the Institute of Control and Informatization of Production Processes, Faculty of BERG, Technical university of Košice as an Associate professor and institute director. His research interests include control systems, automation and applied mathematics. He is a member of the IEEE and the SSAKI. In 2005 he received Award from Ministry of Education in Slovak republic in category young scientist to 35 years. In 2008 he became a member of Editorial board in the Journal of Advanced Research in Dynamical and Control Systems. During last 10 years he spent time abroad in the research visits at several institutions (in Canada, Austria, Spain, *etc*).

Available at WWW.MATHEMATICSWEB.ORG POWERED BY SCIENCE @ DIRECT®

PERGAMON Journal of the Franklin Institute 340 (2003) 349–362

Journal of The Franklin Institute

www.elsevier.com/locate/jfranklin

Two direct Tustin discretization methods for fractional-order differentiator/integrator

Blas M. Vinagre[a], Yang Quan Chen[b,*], Ivo Petráš[c]

[a] *Department of Electronic and Electromechanical Engineering, Industrial Engineering School, University of Extremadura, Avda. De Elvas s/n, 06071-Badajoz, Spain*

[b] *Center for Self-Organizing and Intelligent System, Department of Electrical and Computer Engineering, Utah State University, UMC 4160, College of Engineering, 4160 Old Main Hill, Logan, UT 84322-4160, USA*

[c] *Department of Informatics and Process Control, BERG Faculty, Technical University of Kosice, B. Nemcovej 3, 042 00 Kosice, Slovak Republic*

Received 10 February 2003; received in revised form 19 July 2003; accepted 6 August 2003

Abstract

This paper deals with fractional calculus and its approximate discretization. Two direct discretization methods useful in control and digital filtering are presented for discretizing the fractional-order differentiator or integrator. Detailed mathematical formulae and tables are given. An illustrative example is presented to show the practically usefulness of the two proposed discretization schemes. Comparative remarks between the two methods are also given.

Keywords: Fractional differentiator; Fractional-order controllers; Tustin operator; Power series expansion; Continued fraction expansion; Discretization

1. Introduction

The idea of fractional calculus has been known since the development of the regular calculus, with the first reference probably being associated with correspondence between Leibniz and L'Hospital in 1695. There are many applications of the fractional-order calculus such as physical system modeling [1], control theory (e.g.

*Corresponding author. Tel.: +1-435-7970148(O); fax: +1-435-7973054.

E-mail address: yqchen@ieee.org (Y.Q. Chen).

URL: http://www.csois.usu.edu/people/yqchen.

0016-0032/$30.00 © 2003 The Franklin Institute. Published by Elsevier Ltd. All rights reserved.
doi:10.1016/j.jfranklin.2003.08.001

[2–8]), to name a few. For the latest development of fractional calculus in automatic control and robotics, we cite [9]. For practical application of the fractional-order models (e.g. for realization of fractional-order controllers (FOC)), one needs to discretize the FOC. It is well known that the fractional-order systems involve unlimited memory (infinite dimensional) while the integer-order systems are with limited memory (finite dimensional). It is important to approximately describe the fractional-order system using a finite difference equation. To do so, rational approximations [10] are often used mainly in continuous-time domain. In practice, direct discretization is more preferred. The work of this paper provides a way to achieve direct discretization of fractional-order operator using Tustin operator.

In this paper, two practically useful direct discretization methods are presented and compared by some illustrative examples. The first one is the recursive Tustin discretization scheme based on Muir's recursion (`Tustin+Muir`). The other scheme is the continued fraction expansion (CFE) of the Tustin operator (`Tustin+CFE`). Two direct discretization schemes are then applied, as an illustrative example, to a double integrator plant with an uncertain gain. The robustness of FOC is demonstrated and the two direct discretization schemes are compared. It is found that `Tustin+CFE` scheme is better in terms of accuracy while `Tustin+Muir` is attractive for its nice closed-form recursion. Both schemes presented are applicable in FOC implementation. Note that the discretization schemes presented in [11] were based on different operators and therefore, the reported results were hard to compare. In this paper, based on the *same* Tustin operator, the two discretization schemes are now comparable. Moreover, in this paper, an illustrative example is included to demonstrate how a fractional-order controller can be applied to a double integrator plant with an uncertain gain.

This paper is organized as follows: in Section 2, fractional-order derivative and its discretization are briefly reviewed; Section 3 presents a new direct discretization scheme based on Tustin operator and Muir recursion; Section 4 details another direct discretization scheme based on the Tustin operator and the continued fraction expansion method; Section 5 presents a fractional-order control of a double integrator plant with possible uncertainty in the plant gain. Section 6 concludes this paper with some remarks.

2. Fractional-order derivative and its discretization

Fractional calculus is a generalization of integration and differentiation to a fractional, or non-integer, order fundamental operator ${}_aD_t^r$, where a and t are the limits and r, ($r \in \mathbb{R}$) the order of the operation. Two commonly used definitions for the general fractional integrodifferential are the Grünwald–Letnikov (GL) definition and the Riemann–Liouville (RL) definition [8,12]. The GL definition is that

$$ {}_aD_t^r f(t) = \lim_{h \to 0} h^{-r} \sum_{j=0}^{[(t-a)/h]} (-1)^j \binom{r}{j} f(t-jh), \tag{1} $$

where $[\cdot]$ means the integer part, $\binom{r}{j}$ is the fractional binomial coefficient. while the RL definition is

$$ {}_aD_t^r f(t) = \frac{1}{\Gamma(n-r)} \frac{\mathrm{d}^n}{\mathrm{d}t^n} \int_a^t \frac{f(\tau)}{(t-\tau)^{r-n+1}} \mathrm{d}\tau \tag{2} $$

for $(n-1<r<n)$ and where $\Gamma(\cdot)$ is the Euler's *gamma* function.

For convenience, Laplace domain notion is usually used to describe the fractional integro-differential operation [8]. The Laplace transform of the RL fractional derivative/integral (2) under zero initial conditions for order r, $(0<r<1)$ is given by [12]:

$$ \pounds\{ {}_aD_t^{\pm r} f(t); s\} = s^{\pm r} F(s), \tag{3} $$

where $F(s)$ is the normal Laplace transform of $f(t)$ and $a=0$.

The key point in digital implementation of an FOC is the numerical evaluation or discretization of the fractional-order differentiator s^r. In general, there are two discretization methods: *direct discretization* and *indirect discretization*. In *indirect discretization* methods, two steps are required, i.e., frequency domain fitting in continuous time domain first and then discretizing the fit s-transfer function. In this paper, we focus on the *direct discretization* method.

The simplest and most straightforward method is the direct discretization using finite memory length expansion from GL definition (1). This approach is based on the fact that, for a wide class of functions, the two definitions—GL (1) and RL (2)—are equivalent [8]. In general, the discretization of fractional-order differentiator/integrator $s^{\pm r}$, $(r \in \mathbb{R})$ can be expressed by the so-called generating function $s = \omega(z^{-1})$. This generating function and its expansion determine both the form of the approximation and the coefficients [13]. For example, when a backward difference rule is used, i.e., $\omega(z^{-1}) = (1-z^{-1})/T$, performing the power series expansion (PSE) of $(1-z^{-1})^{\pm r}$ gives the discretization formula for the GL definition (1). By using the short memory principle [8], the discrete equivalent of the fractional-order integro-differential operator, $(\omega(z^{-1}))^{\pm r}$, is given by

$$ D^{\pm(r)}(z) = (\omega(z^{-1}))^{\pm r} = T^{\mp r} z^{-[L/T]} \sum_{j=0}^{[L/T]} (-1)^j \binom{\pm r}{j} z^{[L/T]-j}, \tag{4} $$

where T is the sampling period, L is the memory length and $(-1)^j \binom{\pm r}{j}$ are binomial coefficients $c_j^{(r)}$, $(j = 0, 1, \ldots)$ where

$$ c_0^{(r)} = 1, \qquad c_j^{(r)} = \left(1 - \frac{1 + (\pm r)}{j}\right) c_{j-1}^{(r)}. \tag{5} $$

It is very important to note that the PSE scheme leads to approximations in the form of polynomials, that is, the discretized fractional-order derivative is in the form of FIR (finite impulse response) filters. Taking into account that our aim is to obtain discrete equivalents to the fractional integrodifferential operators in the Laplace domain, $s^{\pm r}$, the following considerations have to be made:

(1) s^r, $(0<r<1)$, viewed as an operator, has a branch cut along the negative real axis for arguments of s on $(-\pi, \pi)$ but is free of poles and zeros.

(2) A dense interlacing of simple poles and zeros along a line in the s plane is, in some way, equivalent to a branch cut.
(3) It is well known that, for interpolation or evaluation purposes, rational functions are sometimes superior to polynomials, roughly speaking, because of their ability to model functions with zeros and poles. In other words, for evaluation purposes, compared to PSE, the rational approximation usually converges much more rapidly and has a wider domain of convergence in the complex plane.
(4) The Tustin transformation or the trapezoidal rule maps adequately the stability regions of the s plane on the z plane, and maps the points $s = 0$, $s = -\infty$ to the points $z = 1$ and -1, respectively.

Therefore, in this paper, for the direct discretization of s^r, $(0<r<1)$, we shall concentrate on the trapezoidal rule or Tustin operator as the generating function as follows:

$$(\omega(z^{-1}))^{\pm r} = \left(\frac{2}{T}\frac{1-z^{-1}}{1+z^{-1}}\right)^{\pm r}. \tag{6}$$

In expanding the above into a rational function, we shall use two techniques. The first one is based on Muir-recursion applied to numerator and denominator of the Tustin operator and the second one is by the continued fraction expansion. It should be pointed out that, for control applications, the obtained approximate discrete-time rational transfer function should be stable and minimum phase. Furthermore, for a better fit to the continuous frequency response, it would be of high interest to obtain discrete approximations with poles an zeros interlaced along the line $z \in (-1, 1)$ of the z plane. As it will be shown later, the two direct discretization approximations proposed in this paper enjoy the above desirable properties. In the next sections, we first introduce the new direct discretization scheme by recursive Tustin transformation followed by the second direct discretization scheme by continued fraction expansion of the Tustin operator.

3. Direct discretization by recursive Tustin transformation

One of the key points of Tustin discretization of fractional-order differentiator is how to get a recursive formula similar to (5) in the preceeding subsection. Here, we introduce the so-called Muir-recursion scheme, which was originally used in geophysical data processing with applications to petroleum prospecting [14]. The Muir-recursion was motivated in computing the vertical plane wave reflection response via the impedance of a stack of n-layered earth. This scheme can be used in recursive discretization of fractional-order differentiator of Tustin generating function. In the following, without loss of generality, assume that $r \in [-1, 1]$. In order to simplify the presentation, we only give the recursive formula for positive r

$$(\omega(z^{-1}))^{r} = \left(\frac{2}{T}\right)^{r}\left(\frac{1-z^{-1}}{1+z^{-1}}\right)^{r} = \left(\frac{2}{T}\right)^{r}\lim_{n\to\infty}\frac{A_n(z^{-1}, r)}{A_n(z^{-1}, -r)}, \tag{7}$$

where

$$A_0(z^{-1}, r) = 1, \quad A_n(z^{-1}, r) = A_{n-1}(z^{-1}, r) - c_n z^n A_{n-1}(z, r) \tag{8}$$

and

$$c_n = \begin{cases} r/n, & n \text{ is odd}, \\ 0, & n \text{ is even}. \end{cases} \tag{9}$$

For any given order of approximation n, we can use MATLAB symbolic toolbox to generate an expression for $A_n(z^{-1}, r)$. Therefore,

$$s^r \approx \left(\frac{2}{T}\right)^r \frac{A_n(z^{-1}, r)}{A_n(z^{-1}, -r)}.$$

For a ready reference, we listed $A_n(z^{-1}, r)$ in Table 1 up to $n = 9$, which should be sufficient in many applications.

Remark 3.1. To examine the correctness of the Muir-recursion used for the recursive discretization of the fractional-order derivative operator, one can compare the symbolic Taylor expansion of (6). It has been verified that the proposed recursive formula is as correct as Taylor series expansion till the order of approximation.

As an example, using the recursive method described in this section, the discretization of $s^{0.5}$ sampled at 0.001 s is studied numerically, and the approximate models are

$$G_1(z) = \frac{44.72z - 22.36}{z + 0.5}, \quad G_3(z) = \frac{44.72z^3 - 22.36z^2 + 3.727z - 7.454}{z^3 + 0.5z^2 + 0.08333z + 0.1667},$$

Table 1
Table of formulae $A_n(z^{-1}, r)$ for $n = 1, \ldots, 9$

n	$A_n(z^{-1}, r)$
0	1
1	$-rz^{-1} + 1$
3	$-\frac{1}{3}rz^{-3} + \frac{1}{3}r^2z^{-2} - rz^{-1} + 1$
5	$-\frac{1}{5}rz^{-5} + \frac{1}{5}r^2z^{-4} - \left(\frac{1}{3}r + \frac{1}{15}r^3\right)z^3 + \frac{2}{5}r^2z^{-2} - rz^{-1} + 1$
7	$-\frac{1}{7}rz^{-7} + \frac{1}{7}r^2z^{-6} - \left(\frac{1}{5}r + \frac{2}{35}r^3\right)z^{-5} + \left(\frac{26}{105}r^2 + \frac{1}{105}r^4\right)z^{-4}$ $-\left(\frac{1}{3}r + \frac{2}{21}r^3\right)z^{-3} + \frac{3}{7}r^2z^{-2} - rz^{-1} + 1$
9	$-\frac{1}{9}rz^{-9} + \frac{1}{9}r^2z^{-8} - \left(\frac{1}{7}r + \frac{1}{21}r^3\right)z^{-7} + \left(\frac{34}{189}r^2 + \frac{2}{189}r^4\right)z^{-6}$ $-\left(\frac{1}{5}r + \frac{16}{189}r^3 + \frac{1}{945}r^5\right)z^{-5} + \left(\frac{17}{63}r^2 + \frac{1}{63}r^4\right)z^{-4}$ $-\left(\frac{1}{3}r + \frac{1}{9}r^3\right)z^{-3} + \frac{4}{9}r^2z^{-2} - rz^{-1} + 1$

$$G_7(z) = \frac{44.72z^7 - 22.36z^6 + 4.792z^5 - 7.986z^4 + 2.795z^3 - 4.792z^2 + 1.597z - 3.194}{z^7 + 0.5z^6 + 0.1071z^5 + 0.1786z^4 + 0.0625z^3 + 0.1071z^2 + 0.0357z + 0.07143},$$

$$G_9(z) = \frac{\begin{array}{c}44.72z^9 - 22.36z^8 + 4.969z^7 - 8.075z^6 + 3.061z^5 - 4.947z^4 + \\ 2.041z^3 - 3.461z^2 + 1.242z - 2.485\end{array}}{\begin{array}{c}z^9 + 0.5z^8 + 0.1111z^7 + 0.1806z^6 + 0.06845z^5 + 0.1106z^4 + \\ 0.04563z^3 + 0.07738z^2 + 0.02778z + 0.05556\end{array}}.$$

We present four plots as shown in Fig. 1 and to show the effectiveness of the approximate discretization with Z-transfer function given above, the approximations are compared with the exact solution (straight lines).

It should be pointed out that the direct discretization method introduced above always gives a Z-transfer function with stable minimum phase characteristics.

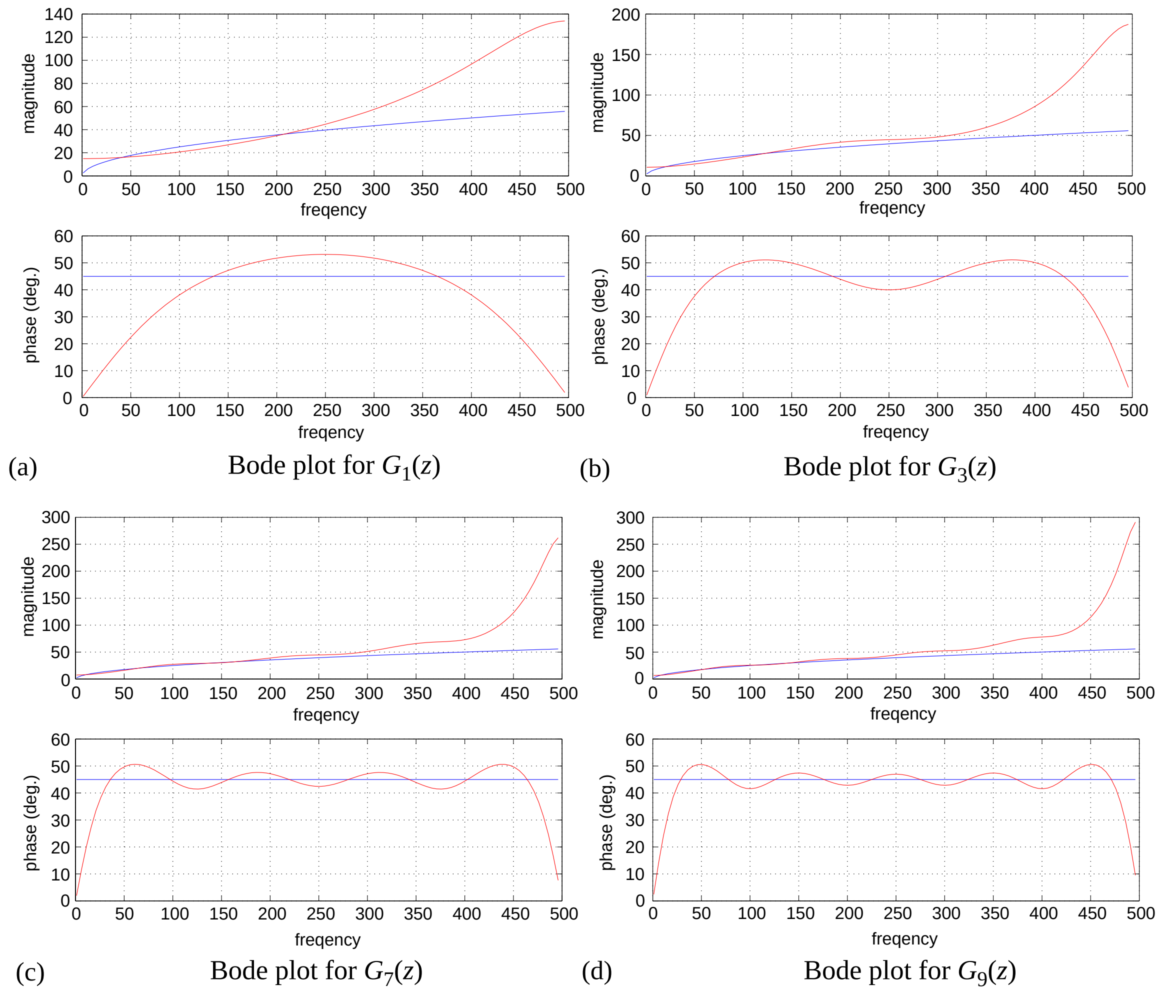

Fig. 1. Approximate discretization of $s^{0.5}$ at $T = 0.001$ s.

4. Direct discretization by continued fraction expansion of Tustin transformation

It is well known that, compared to the power series expansion method, the continued fraction expansion (CFE) is a method for evaluation of functions with faster convergence and larger domain of convergence in the complex plane [15,16]. Using CFE, an approximation for any irrational function $G(z)$ can be expressed in the form

$$G(z) \simeq a_0(z) + \cfrac{b_1(z)}{a_1(z) + \cfrac{b_2(z)}{a_2(z) + \cfrac{b_3(z)}{a_3(z)+\cdots}}}$$
$$= a_0(z) + \frac{b_1(z)}{a_1(z)+}\frac{b_2(z)}{a_2(z)+}\frac{b_3(z)}{a_3(z)+}\cdots, \tag{10}$$

where a_i's and b_i's are either rational functions of the variable z or constants. The application of the method yields a rational function, $\hat{G}(z)$, which is an approximation of the irrational function $G(z)$.

The resulting discrete transfer function, approximating fractional-order operators, can be expressed as

$$D_{\pm r}(z) = \frac{Y(z)}{F(z)} = \left(\frac{2}{T}\right)^{\pm r} \mathrm{CFE}\left\{\left(\frac{1-z^{-1}}{1+z^{-1}}\right)^{\pm r}\right\}_{p,q}$$
$$= \left(\frac{2}{T}\right)^{\pm r} \frac{P_p(z^{-1})}{Q_q(z^{-1})}, \tag{11}$$

where T is the sampling period, $\mathrm{CFE}\{u\}$ denotes the function from applying the continued fraction expansion to the function u, $Y(z)$ is the Z transform of the output sequence $y(nT)$, $F(z)$ is the Z transform of the input sequence $f(nT)$, p and q are the orders of the approximation, and P and Q are polynomials of degrees p and q, correspondingly, in the variable z^{-1}.

By using MAPLE or MATLAB Symbolic Math Toolbox, the obtained symbolic approximation has the following form:

$$D_r(z) = 1 + \cfrac{z^{-1}}{-\frac{1}{2}\frac{1}{r} + \cfrac{z^{-1}}{-2 + \cfrac{z^{-1}}{\frac{3}{2}\frac{r}{r^2-1} + \cfrac{z^{-1}}{2 + \cfrac{z^{-1}}{-\frac{5}{2}\frac{r^2-1}{r(-4+r^2)} + \cfrac{z^{-1}}{-2+\cdots}}}}}}. \tag{12}$$

In Table 2, the general expressions for numerator and denominator of $D_r(z)$ in (11) are listed for $p = q = 1, 3, 5, 7, 9$.

Table 2
Numerators and denominators of $D_r(z)$ (12) for different r

$p = q$	$P_p(z^{-1})$ $(k = 1)$, and $Q_q(z^{-1})(k = 0)$
1	$(-1)^k z^{-1} r + 1$
3	$(-1)^k(r^3 - 4r)z^{-3} + (6r^2 - 9)z^{-2} + (-1)^k 15z^{-1}r + 15$
5	$(-1)^k(r^5 - 20r^3 + 64r)z^{-5} + (-195r^2 + 15r^4 + 225)z^{-4} + (-1)^k(105r^3 - 735r)z^{-3} + (420r^2 - 1050)z^{-2} + (-1)^k 945z^{-1}r + 945$
7	$(-1)^k(784r^3 + r^7 - 56r^5 - 2304r)z^{-7} + (10612r^2 - 1190r^4 - 11025 + 28r^6)z^{-6} + (-1)^k(53487r + 378r^5 - 11340r^3)z^{-5} + (99225 - 59850r^2 + 3150r^4)z^{-4} + (-1)^k(17325r^3 - 173250r)z^{-3} + (-218295 + 62370r^2)z^{-2} + (-1)^k 135135z^{-1}r + 135135$
9	$(-1)^k(-52480r^3 + 147456r + r^9 - 120r^7 + 4368r^5)z^{-9} + (45r^8 + 120330r^4 - 909765r^2 - 4410r^6 + 893025)z^{-8} + (-1)^k(-5742495r - 76230r^5 + 1451835r^3 + 990r^7)z^{-7} + (-13097700 + 9514890r^2 - 796950r^4 + 13860r^6)z^{-6} + (-1)^k(33648615r - 5405400r^3 + 135135r^5)z^{-5} + (-23648625r^2 + 51081030 + 945945r^4)z^{-4} + (-1)^k(-61486425r + 4729725r^3)z^{-3} + (16216200r^2 - 72972900)z^{-2} + (-1)^k 34459425z^{-1}r + 34459425$

With $r = 0.5$ and $T = 0.001$ s, the approximate models for $p = q = 1, 3, 7, 9$ are

$$G_1(z) = 44.72\frac{z-0.5}{z+0.5}, \quad G_3(z) = 44.72\frac{z^3-0.5z^2-0.5z+0.125}{z^3+0.5z^2-0.5z-0.125},$$

$$G_7(z) = 44.72\frac{\begin{array}{c} z^7-0.5z^6-1.5z^5+0.625z^4+0.625z^3-0.1875z^2 \\ -0.0625z+0.007813 \end{array}}{\begin{array}{c} z^7+0.5z^6-1.5z^5-0.625z^4+0.625z^3+0.1875z^2 \\ -0.0625z-0.007813 \end{array}},$$

$$G_9(z) = 44.72\frac{\begin{array}{c} z^9-0.5z^8-2z^7+0.875z^6+1.313z^5-0.4688z^4-0.3125z^3 \\ +0.07813z^2+0.01953z-0.001953 \end{array}}{\begin{array}{c} z^9+0.5z^8-2z^7-0.875z^6+1.313z^5+0.4688z^4-0.3125z^3 \\ -0.07813z^2+0.01953z+0.001953 \end{array}}.$$

In Figs. 2 and 3, the Bode plots and the distributions of zeros and poles of the approximations are presented. In Fig. 2, the effectiveness of the approximations fitting the ideal responses in a wide range of frequencies, in both magnitude and phase, can be observed. In Fig. 3, it can be observed that the approximations fulfill the two desired properties: (i) all the poles and zeros lie inside the unit circle, and

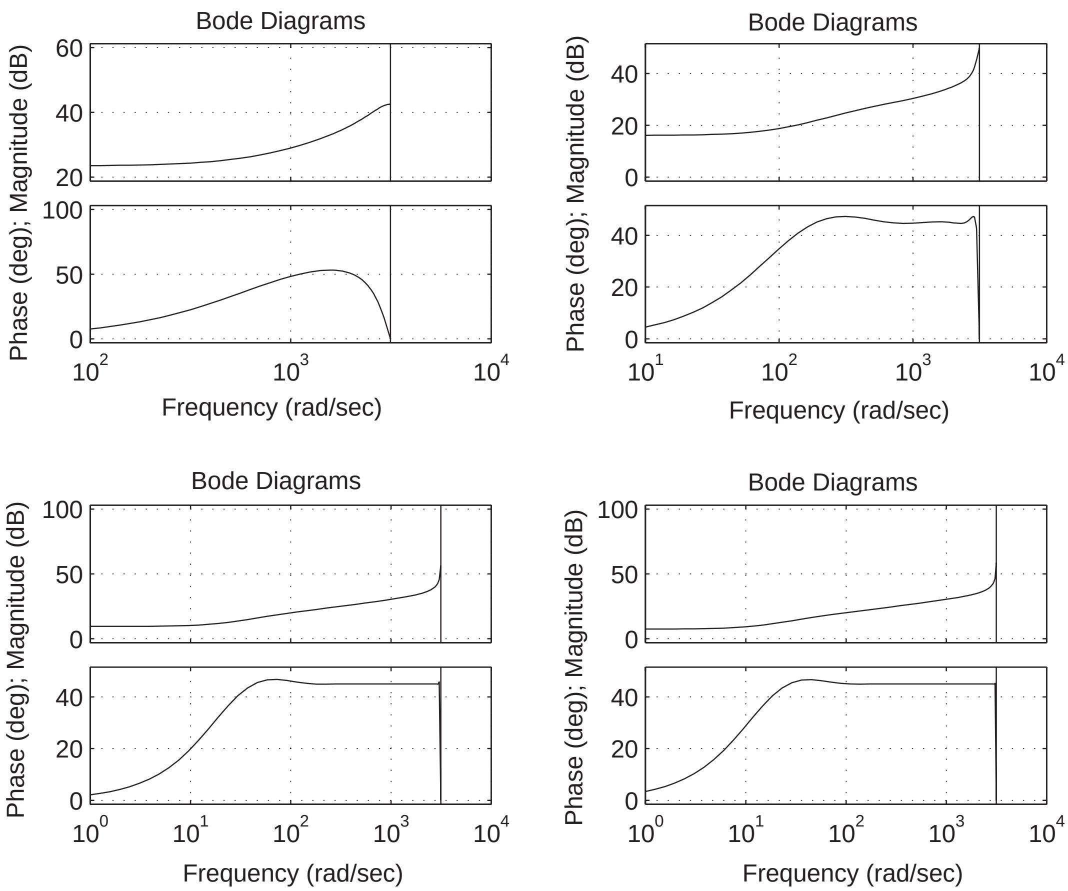

Fig. 2. CFE approximate discretization of $s^{0.5}$ at $T = 0.001$ s. Bode plots (approximation orders 1, 3, 7, 9).

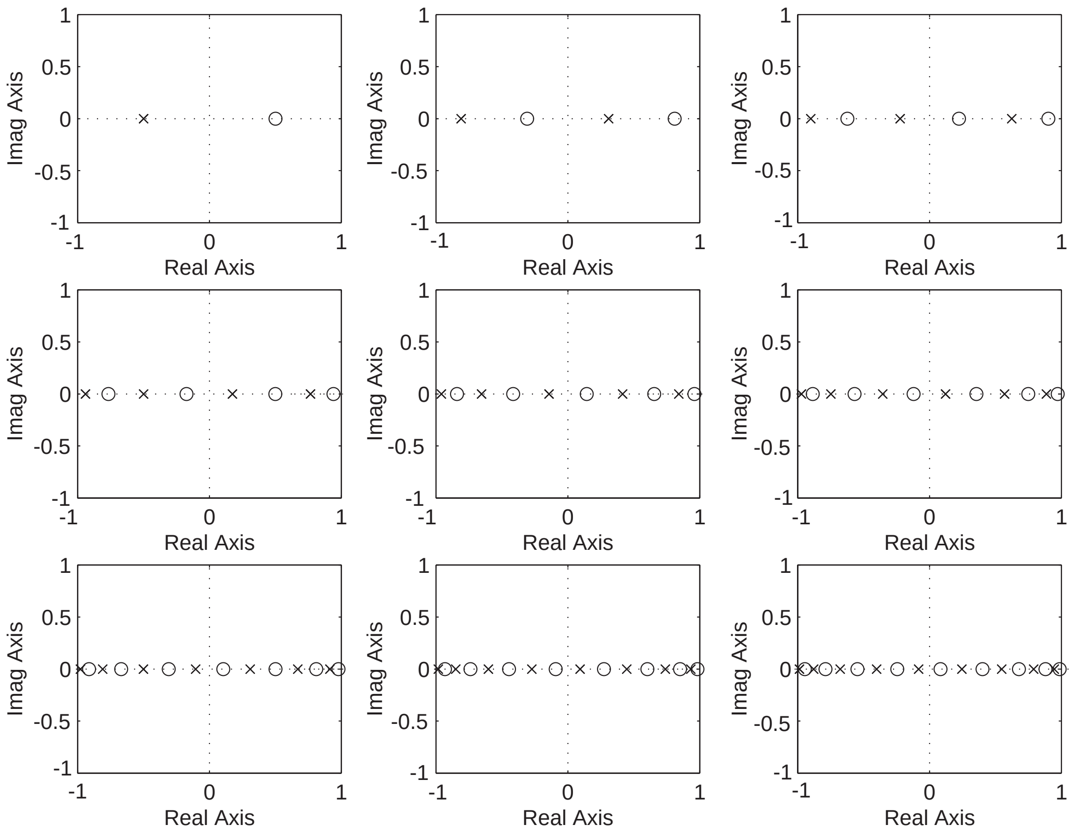

Fig. 3. CFE approximate discretization of $s^{0.5}$ at $T = 0.001$ s. Zero-pole distribution (approximation orders $1, 2, \ldots, 9$).

(ii) the poles and zeros are interlaced along the segment of the real axis corresponding to $z \in (-1, 1)$.

5. An illustrative application example

Consider a system with the following transfer function in the form of a double integrator

$$H(s) = \frac{A}{s^2},$$

where the gain A is uncertain.

As can be seen in [17], this plant is one of the most fundamental systems in control applications, representing single-degree-of-freedom translational and rotational motion, with applications in many practical problems (see [17] and references included): low-friction, free rigid-body motion, single-axis spacecraft rotation and rotary crane motion. The double integrator plant model has also been used in flexible robotics (see [18]).

Suppose a fractional-order controller of the form

$$D(s) = s^r, \quad 0 < r < 1 \tag{13}$$

is to be used. The open-loop transfer function of the controlled system will be of the form

$$F_o(s) = D(s)G(s) = \frac{A}{s^{2-r}}.$$

The above transfer function is in the form of the Bode's ideal transfer function [8] with the following properties:

(a) *Open loop*:
   (1) the amplitude curve has a constant slope of $-(2-r)$;
   (2) the crossover frequency depends only on A;
   (3) the phase curve is a horizontal line at $-(2-r)(\pi/2)$;
   (4) the Nyquist curve is a straight line through the origin with argument $-(2-r)(\pi/2)$
(b) *Closed loop with unity negative feedback*:
   (1) the transfer function has the form

$$F_c(s) = \frac{A}{s^{2-r} + A}; \tag{14}$$

   (2) the gain margin is infinite;
   (3) the phase margin is constant, $\Phi_m = \pi\left(1 - \frac{2-r}{2}\right)$;
   (4) the step response has the expression (see [8,19]):

$$y(t) = At^{2-r}E_{2-r,2-r+1}(-At^{2-r}),$$

   where $E_{2-r,2-r+1}(-At^{2-r})$ is the Mittag–Leffler function in two parameters. Assuming $A \in \mathbb{R}^+$, such a step response exhibits an overshoot independent of parameter A and dependent only on the parameter r, the fractional-order. This is a desired property in some applications such as car suspension control system, etc.

If $A = 100$, $r = 0.5$, the following properties can be achieved:

- phase margin, $\Phi_m = 45^\circ$,
- rise time, $t_r = 0.018$ s,
- overshoot, $M_p = 35\%$,
- peak time, $t_p = 0.029$ s.

In Figs. 4–6, the following results are displayed: Bode plots for $D_1(z)$ and $D_2(z)$ (Fig. 4), the two discrete approximations of the controller $D(s)$ (13) where $D_1(z)$ is via `Tustin+Muir` scheme with $n = 7$ and $D_2(z)$ the `Tustin+CFE` scheme with $p = q = 7$; Bode plots for the controlled system with several values of A (Fig. 5), and the step responses of the controlled system for several values of A (Fig. 6). As can be observed, the `Tustin+CFE` scheme performs a better frequency-domain approximation with a more flat phase response in a wider frequency range. This leads to the

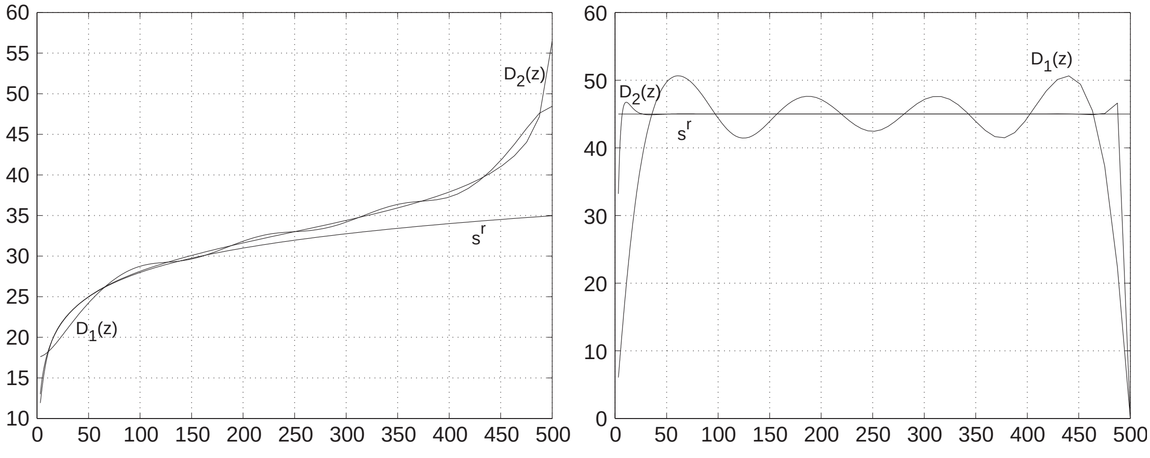

(a) Magnitude Bode plots (dB vs. Hz.) (b) Phase Bode plots(degree vs. Hz.)

Fig. 4. Comparison of the two direct discretization schemes ($D_1(z)$: `Tustin+Muir`; $D_2(z)$: `Tustin+CFE`): (a) Magnitude Bode plots (dB vs. Hz); (b) phase Bode plots (degree vs. Hz).

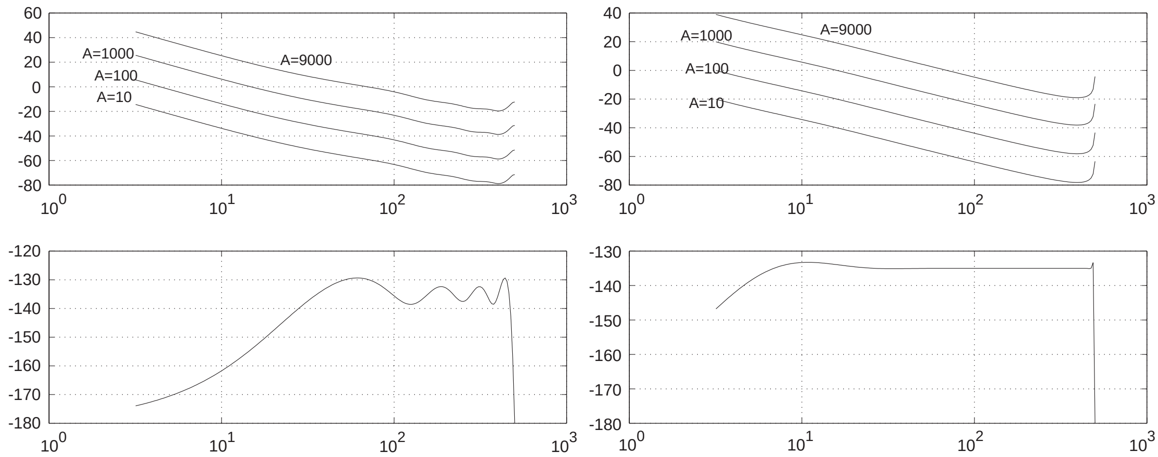

(a) (b)

Fig. 5. Comparison of the two direct discretization schemes at different gains ($D_1(z)$:`Tustin+Muir`; $D_2(z)$:`Tustin+CFE`): (a) Bode plots for `Tustin+Muir` (top: amplitude (dB) vs. frequency (Hz); bottom: phase (deg) vs. frequency (Hz)); (b) Bode plots for `Tustin+CFE` (top: amplitude (dB) vs. frequency (Hz); bottom: phase (deg) vs. frequency (Hz)).

time-domain behavior of the controlled system closer to the theoretical one for a wider range of A values. The most interesting feature of the fractional-order controlled system is the equal-overshoot behavior when A varies. The overshoot is close to 35%, the theoretically predicted value for $A \in (1000, 9000)$ when $D_2(z)$ is used as the controller. When $D_1(z)$ is used, we can see that the 35% overshoot can be maintained only when $A \geqslant 9000$. Clearly, due to a better phase approximation of $D_2(z)$ to $D(s)$, compared to $D_1(z)$, $D_2(z)$ gives better time-domain performance which is also in accordance with the obtained phase margins of the controlled system. We can see that with the introduction of a fractional-order controller, in terms of overshoot and oscillation/damping, the control performance is more robust with

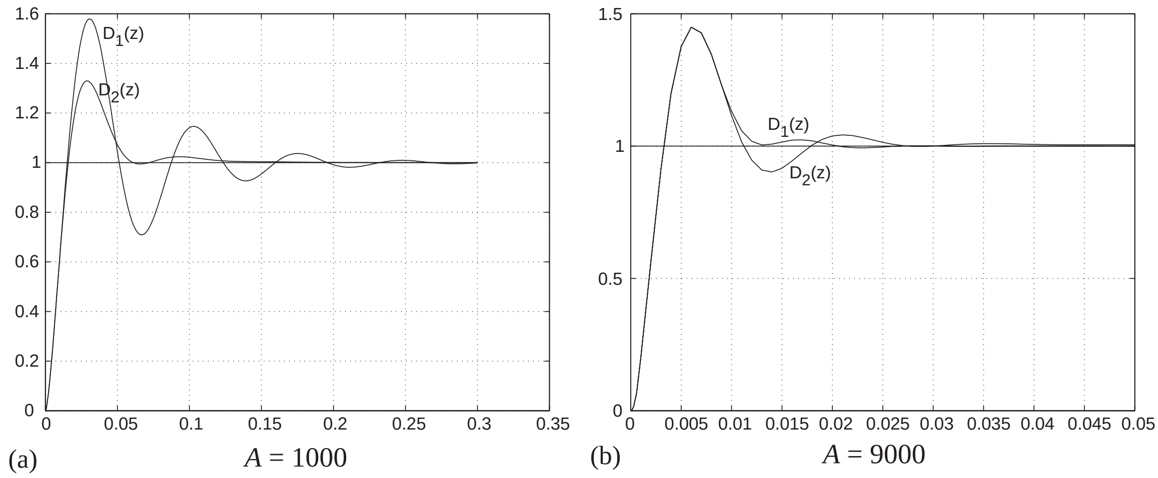

Fig. 6. Step response comparison (output vs. time in second): (a) $A = 1000$; (b) $A = 9000$.

respect to the uncertain plant gain. As we have demonstrated above, the plant gain can be allowed to vary in a very large range. Under the same order of approximation, compared to the `Tustin+Muir` scheme, `Tustin+CFE` scheme gives a better fit to the original continuous FOC. However, `Tustin+Muir` is more attractive in the sense that it has a nice closed-form recursive expansion formulae which may be useful when the order of approximation of FOC would be determined in real time.

6. Concluding remarks

We have presented two direct discretization schemes for implementation of fractional-order controller. The first scheme uses the Muir recursion formula for recursive Tustin operator expansion while the other scheme is by the continued fraction expansion. Practically useful formula and tables are given. Illustrative examples are presented to show the practically usefulness of the two proposed discretization schemes. Comparative remarks between the two methods are also given.

Acknowledgements

We would like to thank the anonymous reviewers for their helpful comments. Blas M. Vinagre is partially supported by the Research Grant 2PR02A024 (Junta de Extremadura and FEDER). YangQuan Chen has been funded in part by the National Academy of Sciences under the Collaboration in Basic Science and Engineering Program/Twinning Program supported by Contract No. INT-0002341 from the National Science Foundation. The contents of this publication do not necessarily reflect the views or policies of the National Academy of Sciences or the

National Science Foundation, nor does mention of trade names, commercial products or organizations imply endorsement by the National Academy of Sciences or the National Science Foundation. The research work of Ivo Petras was supported in part by grant VEGA 1/7098/20 from the Slovak Grant Agency for Science.

References

[1] R. Hilfer, Applications of Fractional Calculus in Physics, World Scientific, Singapore, 2000.
[2] S. Manabe, The non-integer integral and its application to control systems, JIEE (Japan. Inst. Electr. Eng.) J. 80 (860) (1960) 589–597.
[3] M. Axtell, E.M. Bise, Fractional calculus applications in control systems, in: Proceedings of the IEEE 1990 National Aerospace and Electronics Conference, New York, USA, 1990, pp. 563–566.
[4] L. Dorčák, Numerical models for simulation the fractional-order control systems, in: UEF-04-94, The Academy of Science, Institute of Experimental Physics, Kosice, Slovak Republic, 1994, pp. 1–12.
[5] D. Matignon, Stability result on fractional differential equations with applications to control processing, in: IMACS-SMC Proceedings, Lille, France, 1996, pp. 963–968.
[6] A. Oustaloup, La Dérivation non Entière, HERMES, Paris, 1995.
[7] I. Petráš, The fractional-order controllers: methods for their synthesis and applications, J. Electr. Eng. 50 (9–10) (1999) 284–288.
[8] I. Podlubny, Fractional Differential Equations, Academic Press, San Diego, 1999.
[9] B.M. Vinagre, YangQuan Chen. Lecture Note on Fractional Calculus Applications in Automatic Control and Robotics, The 41st IEEE CDC2002 Tutorial Workshop ♯2, 2002, http://mechatronics.ece.usu.edu/foc/ Dec., Las Vegas, Nevada
[10] B. Vinagre, I. Podlubny, A. Hernández, V. Feliu, Some approximations of fractional order operators used in control theory and applications, Fractional Calculus Appl. Anal. 3 (3) (2000) 231–248.
[11] Y.Q. Chen, K.L. Moore, Discretization schemes for fractional order differentiators and integrators, IEEE Trans. Circuits Systems-I Fund. Theory Appl. 49 (3) (2002) 363–367.
[12] K.B. Oldham, J. Spanier, The Fractional Calculus, Academic Press, New York, 1974.
[13] C.H. Lubich, Discretized fractional calculus, SIAM J. Math. Anal. 17 (3) (1986) 704–719.
[14] J.F. Claerbout, Fundamentals of Geophysical Data Processing with Applications to Petroleum Prospecting, Blackwell Scientific Publications, Oxford 1976, http://sepwww.stanford.edu/old-reports/fgdp2/
[15] W.H. Press, W.T. Vetterling, S.A. Teukolsky, B.P. Flannery, Numerical Recipes in C, Cambridge University Press, Cambridge, 1992.
[16] A.I. Khinchin, A.Ya. Khinchin, H. Eagle, Continued Fractions, Dover (Inc Scripta Technica, Translator), New York, 1997.
[17] V.-G. Rao, D.-S. Bernstein, Naive control of the double integrator, IEEE Control System Mag. (2001) 21, 86–97.
[18] V. Feliu, K.-S. Rattan, H.-B. Brown, Adaptive control of a single-link flexible manipulator, IEEE Control System Mag. (1990) 10, 29–33.
[19] L. Debnath, Integral Transforms and Their Applications, CRC Press, Boca Raton, FL, 1995.

Nonlinear Dynamics **29:** 281–296, 2002.

Analogue Realizations of Fractional-Order Controllers

I. PODLUBNY*, *** and I. PETRÁŠ*, ***
Department of Informatics and Process Control, BERG Faculty, Technical University of Košice, 04200 Košice, Slovak Republic

B. M. VINAGRE**
Department of Electronics and Electromechanical Engineering, Industrial Engineering School, University of Extramadura, E-06071 Badajoz, Spain

P. O'LEARY***
Institute of Automation, Montanuniversität Leoben, A-8700 Leoben, Austria

L'. DORČÁK*
Department of Informatics and Process Control, BERG Faculty, Technical University of Košice, 04200 Košice, Slovak Republic

(Received: 16 July 2001; accepted: 7 December 2001)

Abstract. An approach to the design of analogue circuits, implementing fractional-order controllers, is presented. The suggested approach is based on the use of continued fraction expansions; in the case of negative coefficients in a continued fraction expansion, the use of negative impedance converters is proposed. Several possible methods for obtaining suitable rational appromixations and continued fraction expansions are discussed. An example of realization of a fractional-order I^{λ} controller is presented and illustrated by obtained measurements. The suggested approach can be used for the control of very fast processes, where the use of digital controllers is difficult or impossible.

Keywords: Fractional calculus, fractional differentiation, fractional integration, fractional-order controller, realization.

1. Introduction

Although digital controllers are used more and more frequently for controlling many types of complex processes, the role of analogue controllers should not be undervalued. Indeed, digital controllers have some natural limitations, coming from their discrete nature, such as the length of the sampling period and the time of computation, which should be significantly less than the length of the sampling period. This sometimes makes the use of digital controllers practically impossible, especially in case of fast processes, such as vibrations, and the alternative approach to controlling fast processes is represented by analogue controllers.

In this paper we describe an approach to the design of analogue fractional-order controllers.

The paper is organized as follows. First, we recall some basic relationships for describing fractional-order systems and fractional-order controllers. Then we discuss some uses of continued fraction expansions, including their applications in the control theory. Finally, we show how continued fraction expansions can be used for designing analogue circuits, implementing

* Partially supported by grant No. VEGA 1/7098/20 of the Slovak Grant Agency for Science.
** Partially supported by FEDER Research Grant No. IFD97-0755-C02-01.
*** Partially supported by a research grant of the Austrian Institute for Central and Eastern Europe.

fractional-order systems and controllers. We also give an example of implementation of an I^λ controller.

2. Fractional-Order Systems and Controllers

General information about various approaches to fractional-order differentiation and integration can be found in the available monographs on this subject [1–4] and in some other articles in this special issue. Because of this, we do not discuss general definitions here. Instead, we recall only the expressions for describing fractional-order systems and $PI^\lambda D^\mu$ controllers [3, 5], which are subjects of our interest in this paper.

2.1. Fractional Differential Equations and Transfer Functions

A fractional-order control system can be described by a fractional differential equation of the form

$$\begin{aligned} &a_n D^{\alpha_n} y(t) + a_{n-1} D^{\alpha_{n-1}} y(t) + \cdots + a_0 D^{\alpha_0} y(t) \\ &\quad = b_m D^{\beta_m} u(t) + b_{m-1} D^{\beta_{m-1}} u(t) + \cdots + b_0 D^{\beta_0} u(t), \end{aligned} \tag{1}$$

or by a continuous transfer function of the form:

$$G(s) = \frac{b_m s^{\beta_m} + b_{m-1} s^{\beta_{m-1}} + \cdots + b_0 s^{\beta_0}}{a_n s^{\alpha_n} + a_{n-1} s^{\alpha_{n-1}} + \cdots + a_0 s^{\alpha_0}}, \tag{2}$$

where $D^\gamma \equiv {}_0D_t^\gamma$ denotes the Riemann-Liouville or Caputo fractional derivative [3]; a_k $(k = 0, \ldots, n)$, b_k $(k = 0, \ldots, m)$ are constant; and α_k $(k = 0, \ldots, n)$, β_k $(k = 0, \ldots, m)$ are arbitrary real numbers.

Without loss of generality we can assume that $\alpha_n > \alpha_{n-1} > \ldots > \alpha_0$, and $\beta_m > \beta_{m-1} > \ldots > \beta_0$.

2.2. $PI^\lambda D^\mu$ Controllers

The fractional-order $PI^\lambda D^\mu$ controller was proposed in [3, 5, 6] as a generalization of the PID controller with integrator of real order λ and differentiator of real order μ. The transfer function of such type the controller in Laplace domain has form:

$$G_c(s) = \frac{U(s)}{E(s)} = K + T_i s^{-\lambda} + T_d s^{\mu} \quad (\lambda, \mu > 0), \tag{3}$$

where K is the proportional constant, T_i is the integration constant and T_d is the differentiation constant. As we can see (Figure 1), the internal structure of the fractional-order controller consists of the parallel connection the proportional, integration, and derivative part [7]. Transfer function (3) corresponds in time domain with fractional differential equation (4)

$$u(t) = Ke(t) + T_i\, {}_0D_t^{-\lambda} e(t) + T_d\, {}_0D_t^{\mu}. \tag{4}$$

Taking $\lambda = 1$ and $\mu = 1$, we obtain a classical PID controller. If $\lambda = 0$ and/or $T_i = 0$, we obtain a PD^μ controller, etc. All these types of controllers are particular cases of the fractional-order controller, which is more flexible and gives an opportunity to better adjust the dynamical properties of the fractional-order control system.

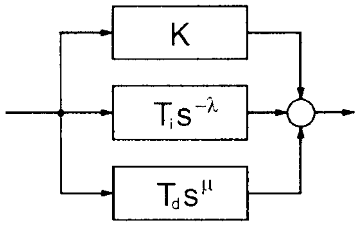

Figure 1. General structure of a $PI^{\lambda}D^{\mu}$ controller.

As we see from Figure 1, a $PI^{\lambda}D^{\mu}$ controller can be easily implemented in analogue form if we know how to build an analogue circuit corresponding to s^{α}, $\alpha \in R$. Below we will demonstrate how this can be done using rational approximations and continued fraction expansions.

It can also be mentioned that the other kind of fractional-order controller, which characterized by the band-limited lead effect, can be found in the available literature [8, 9]:

$$G_c(s) = C\left(\frac{1+\tau s^r}{1+\tau' s^r}\right), \quad r \in R, C \in R, \tau' < \tau. \tag{5}$$

This type of controller can be realized using a recursive distribution of poles and zeros [10].

3. Some Uses of Continued Fractions

In this section we discuss some applications of continued fractions. First we recall their use for approximating functions and investigating stability of linear systems. Then we introduce a new relationship between continued fractions and multiple nested-loop systems.

3.1. CFEs and Approximations of Functions

It is well known that the Continued Fraction Expansions (CFE) is a method for evaluation of functions, that frequently converges much more rapidly than power series expansions, and converges in a much larger domain in the complex plane [11]. The result of such approximation for an irrational function, $G(s)$, can be expressed in the form:

$$\begin{aligned} G(s) &\simeq a_0(s) + \cfrac{b_1(s)}{a_1(s) + \cfrac{b_2(s)}{a_2(s) + \cfrac{b_3(s)}{a_3(s)+\cdots}}} \\ &= a_0(s) + \frac{b_1(s)}{a_1(s)+}\,\frac{b_2(s)}{a_2(s)+}\,\frac{b_3(s)}{a_3(s)+}\,\cdots, \end{aligned} \tag{6}$$

where $a_i s$ and $b_i s$ are rational functions of the variable s, or are constant. The application of the method yields a rational function, $\widehat{G}(s)$, which is an approximation of the irrational function $G(s)$.

On the other hand, for interpolation purposes, rational functions are sometimes superior to polynomials. This is, roughly speaking, due to their ability to model functions with poles. (As it can be seen later, branch points can be considered as accumulations of interlaced poles and zeros). These techniques are based on the approximations of an irrational function, $G(s)$, by a rational function defined by the quotient of two polynomials in the variable s:

$$\begin{aligned} G(s) \;\simeq\; R_{i(i+1)\dots(i+m)} &= \frac{P_\mu(s)}{Q_\nu(s)}, \\ &= \frac{p_0 + p_1 s + \cdots + p_\mu s^\mu}{q_0 + q_1 s + \cdots + q_\nu s^\nu} \qquad (7) \\ m + 1 = \mu + \nu + 1, & \end{aligned}$$

passing through the points $(s_i, G(s_i)), \dots, (s_{i+m}, G(s_{i+m}))$.

3.2. CFE and Stability of Linear Systems

It is also known that continuous fraction expansions can be used for investigating stability of linear systems. For this, the characteristic polynomial $Q(s)$ of the differential equation of the system should be divided in two parts, the 'even' part (containing even powers of s) and the 'odd' part (containing odd powers of s):

$$Q(s) = m(s) + n(s).$$

Then these two parts of the characteristic polynomial are used for creating its *test function* in the form of a fraction, in which the highest power of s is contained in the denominator:

$$R(s) = \frac{m(s)}{n(s)} \quad \left(\text{or} \quad R(s) = \frac{n(s)}{m(s)}\right).$$

The rational function $R(s)$ should be written in the form of a continuous fraction:

$$R(s) = \cfrac{1}{b_1 s + \cfrac{1}{b_2 s + \cfrac{1}{\cfrac{\cdots\cdots\cdots\cdots}{b_{n-1} s + \cfrac{1}{b_n s}}}}}. \qquad (8)$$

If $b_k > 0$, $k = 1, \dots, n$, then the system is stable. If some b_k is negative, then the system is unstable.

Considering the continued fraction (8) as a tool for designing a corresponding LC circuit, we can conclude that stability of a linear system is equivalent to realizability of its test function $R(s)$ with the help of only passive electric components.

3.3. CFE and Nested Multiple-Loop Control Systems

Let us now establish an interesting new relationship between continued fractions and nested multiple-loop control systems.

We first recall the known fact that the transfer function $R(s)$ of the control loop with a negative feedback shown in Figure 2 is given by [7]

$$R(s) = \frac{G(s)}{1 + G(s)H(s)}. \qquad (9)$$

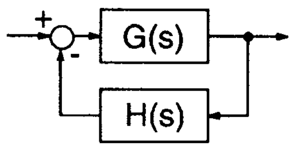

Figure 2. A control loop with a negative feedback.

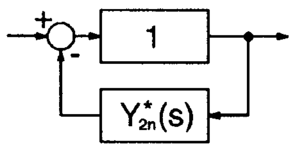

Figure 3. Nested multiple-loop control system – level 1.

From (9) it immediately follows that the transfer function of the circuit shown in Figure 3 is

$$P_{2n}(s) = \frac{1}{1 + 1 \cdot Y^*_{2n}(s)} = \frac{1}{Y_{2n}(s)}, \tag{10}$$

where $Y_{2n}(s) = Y^*_{2n}(s) + 1$.

Using Equations (9) and (10) we obtain the transfer function of the system shown in Figure 4:

$$Q_{2n-1}(s) = Z_{2n-1}(s) + P_{2n}(s) = Z_{2n-1}(s) + \frac{1}{Y_{2n}(s)}. \tag{11}$$

Combining Equations (9) and (10) we find the transfer function of the nested multiple-loop system shown in Figure 5:

$$\begin{aligned} P_{2n-2}(s) &= \frac{Q_{2n-1}(s)}{1 + Q_{2n-1}(s) Y_{2n-2}(s)} = \frac{1}{Y_{2n-2}(s) + \cfrac{1}{Q_{2n-1}(s)}} \\ &= \frac{1}{Y_{2n-2}(s) + \cfrac{1}{Z_{2n-1}(s) + \cfrac{1}{Y_{2n}(s)}}}. \end{aligned} \tag{12}$$

The transfer function of the system shown in Figure 6 is then given by the relationship

$$\begin{aligned} Q_{2n-3}(s) &= Z_{2n-3}(s) + P_{2n-2}(s) \\ &= Z_{2n-3}(s) + \frac{1}{Y_{2n-2}(s) + \cfrac{1}{Z_{2n-1}(s) + \cfrac{1}{Y_{2n}(s)}}}. \end{aligned} \tag{13}$$

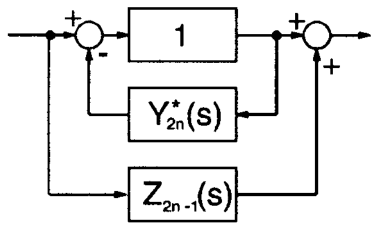

Figure 4. Nested multiple-loop control system – level 2.

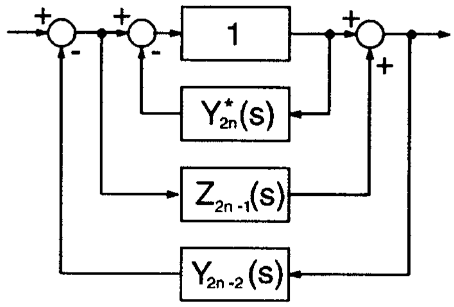

Figure 5. Nested multiple-loop control system – level 3.

Continuing this process, we obtain the transfer function of the nested multiple-loop control system shown in Figure 7 in the form of a continued fraction expansion, which is identical with the Equation (24):

$$Z(s) = Z_1(s) + \cfrac{1}{Y_2(s) + \cfrac{1}{Z_3(s) + \cfrac{1}{Y_4(s) + \cfrac{1}{\begin{array}{c}\cdots\cdots\cdots\cdots\cdots\cdots\\ \cfrac{1}{Y_{2n-2}(s) + \cfrac{1}{Z_{2n-1}(s) + \cfrac{1}{Y_{2n}(s)}}}\end{array}}}}}.$$

Similarly to the above considerations, we can obtain a continued fraction expansion of the transfer function of the other interesting type of a nested multiple-loop control system, depicted in Figure 8:

$$Z(s) = \cfrac{1}{Z_1(s) + \cfrac{1}{Y_2(s) + \cfrac{1}{Z_3(s) + \cfrac{1}{\begin{array}{c}\cdots\cdots\cdots\cdots\cdots\cdots\\ \cfrac{1}{Y_{2n-2}(s) + \cfrac{1}{Z_{2n-1}(s) + \cfrac{1}{Y_{2n}(s)}}}\end{array}}}}}. \tag{14}$$

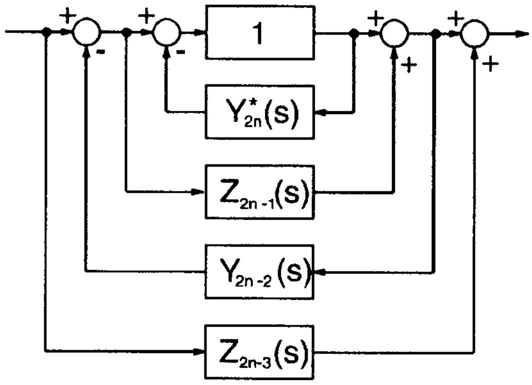

Figure 6. Nested multiple-loop control system – level 4.

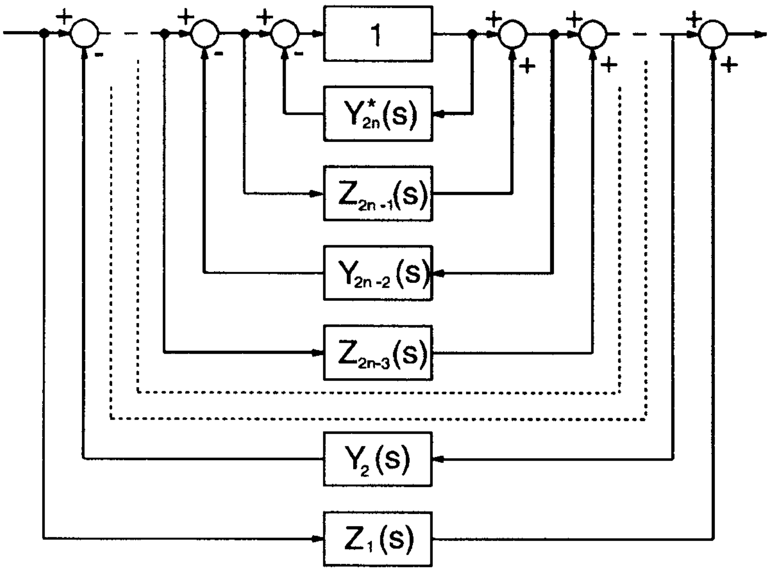

Figure 7. Nested multiple-loop control system of the first type.

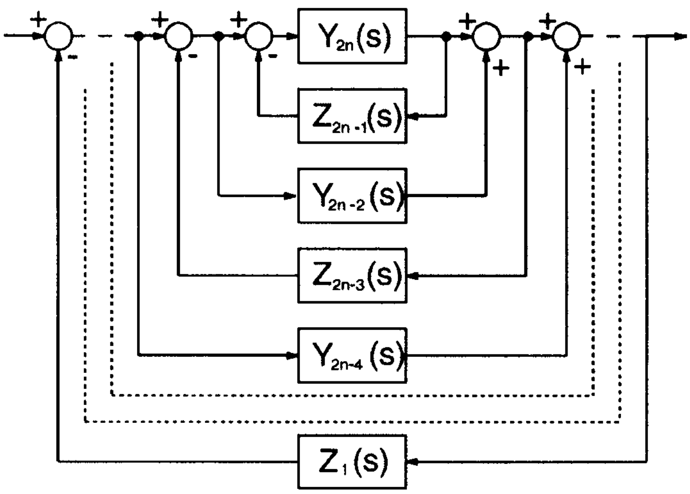

Figure 8. Nested multiple-loop control system of the second type.

Both types of nested multiple-loop systems, presented in this section, can be used for simulations and realizations of arbitrary transcendental transfer functions. For this, the transfer function should be developed in a continued fraction, which after truncation can be represented by a nested multiple-loop system shown in Figures 7 or 8.

4. CFE and Rational Approximations of s^α

In general [12], a rational approximation of the function $G(s) = s^{-\alpha}$, $0 < \alpha < 1$ (the fractional integral operator in the Laplace domain) can be obtained by performing the CFE of the functions:

$$G_h(s) = \frac{1}{(1+sT)^\alpha}, \tag{15}$$

$$G_l(s) = \left(1+\frac{1}{s}\right)^\alpha, \tag{16}$$

where $G_h(s)$ is the approximation for high frequencies ($\omega T \gg 1$), and $G_l(s)$ the approximation for low frequencies ($\omega \ll 1$).

EXAMPLE 1. Performing the CFE of the function (15), with $T = 1$, $\alpha = 0.5$, we obtain

$$H_1(s) = \frac{0.3513s^4 + 1.405s^3 + 0.8433s^2 + 0.1574s + 0.008995}{s^4 + 1.333s^3 + 0.478s^2 + 0.064s + 0.002844}.$$

EXAMPLE 2. Performing the CFE of the function (16), with $T = 1$, $\alpha = 0.5$, we obtain

$$H_2(s) = \frac{s^4 + 4s^3 + 2.4s^2 + 0.448s + 0.0256}{9s^4 + 12s^3 + 4.32s^2 + 0.576s + 0.0256}.$$

5. Other Rational Approximations for s^α

Besides using continued fractions, there are also other methods [13] for obtaining rational approximations of fractional-order systems. However, since a ratio of two polynomials can be expressed in the form of a finite continued fraction, any rational approximation is equivalent to a certain finite continued fraction.

5.1. Carlson's Method

The method proposed by Carlson in [14], derived from a regular Newton process used for iterative approximation of the α-th root, can be considered as belonging to this group. The starting point of the method is the statement of the following relationships:

$$(H(s))^{1/\alpha} - (G(s)) = 0; \qquad H(s) = (G(s))^\alpha. \tag{17}$$

Defining $\alpha = 1/q$, $m = q/2$, in each iteration, starting from the initial value $H_0(s) = 1$, an approximated rational function is obtained in the form:

$$H_i(s) = H_{i-1}(s)\frac{(q-m)\,(H_{i-1}(s))^2 + (q+m)G(s)}{(q+m)\,(H_{i-1}(s))^2 + (q-m)G(s)}. \tag{18}$$

EXAMPLE 3. Starting from $H(s) = (1/s)^{1/2}$, $H_0(s) = 1$, after two iterations, we obtain

$$H_3(s) = \frac{s^4 + 36s^3 + 126s^2 + 84s + 9}{9s^4 + 84s^3 + 126s^2 + 36s + 1}.$$

5.2. Matsuda's Method

The method suggested in [15] is based on the approximation of an irrational function by a rational one, obtained by CFE and fitting the original function in a set of logarithmically spaced points. Assuming that the selected points are s_k, $k = 0, 1, 2, \ldots$, the approximation takes on the form:

$$H(s) = a_0 + \frac{s - s_0}{a_1 +} \frac{s - s_1}{a_2 +} \frac{s - s_2}{a_3 +} \cdots, \tag{19}$$

where

$$a_i = v_i(s_i), \quad v_0(s) = H(s), \quad v_{i+1}(s) = \frac{s - s_i}{v_i(s) - a_i}. \tag{20}$$

EXAMPLE 4. With $G(s) = (1/s)^{1/2}$, $f_{\text{initial}} = 1$, $f_{\text{final}} = 100$, $f_k = \{1, 1.7783, 3.1623, 5.6234, 10, 17.783, 31.623, 56.234, 100\}$, we obtain

$$H_4(s) = \frac{0.08549s^4 + 4.877s^3 + 20.84s^2 + 12.995s + 1}{s^4 + 13s^3 + 20.84s^2 + 4.876s + 0.08551}.$$

5.3. Oustaloup's Method

The method [8–10] is based on the approximation of a function of the form:

$$H(s) = s^\delta, \quad \delta \in R^+ \tag{21}$$

by a rational function

$$\widehat{H}(s) = C \prod_{k=-N}^{N} \frac{1 + s/\omega_k}{1 + s/\omega'_k}, \tag{22}$$

using the following set of synthesis formulas:

$$\begin{aligned} \omega'_0 &= \alpha^{-0.5}\omega_u, \quad \omega_0 = \alpha^{0.5}\omega_u, \quad \frac{\omega'_{k+1}}{\omega'_k} = \frac{\omega_{k+1}}{\omega_k} = \alpha\eta > 1, \\ \frac{\omega'_{k+1}}{\omega_k} &= \eta > 0, \quad \frac{\omega_k}{\omega'_k} = \alpha > 0, \quad N = \frac{\log(\omega_N/\omega_0)}{\log(\alpha\eta)}, \quad \delta = \frac{\log\alpha}{\log(\alpha\eta)}, \end{aligned} \tag{23}$$

with ω_u being the unit gain frequency and the central frequency of a band of frequencies geometrically distributed around it. That is, $\omega_u = \sqrt{\omega_h\omega_b}$, ω_h, ω_b are the high and low transitional frequencies.

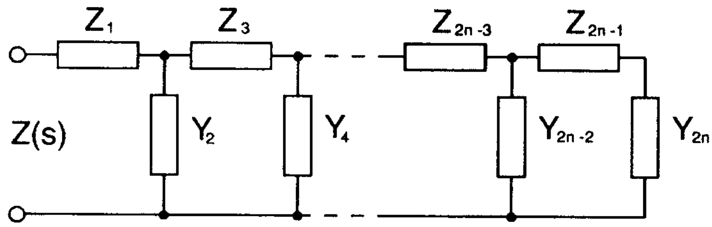

Figure 9. Finite ladder circuit.

EXAMPLE 5. Using the Oustaloup's method with

$$\omega_h = 10^2, \quad \omega_b = 10^{-2},$$

from which we have $\alpha = \eta = 2.5119$, the obtained approximation for $s^{-1/2}$ is

$$H_5(s) = \frac{s^5 + 74.97s^4 + 768.5s^3 + 1218s^2 + 298.5s + 10}{10s^5 + 298.5s^4 + 1218s^3 + 768.5s^2 + 74.97s + 1}.$$

6. Design of Fractances Based on Rational Approximations and CFEs

A circuit exhibiting fractional-order behaviour is called a *fractance* [3].

Design of fractances can be done easily using any of the aforementioned rational approximations or a truncated CFE, which also gives a rational approximation (see, for example, [16]). Truncated CFE does not require any further transformation; a rational approximation based on any other methods must be transformed to the form of a continued fraction. The values of the electric elements, which are necessary for building a fractance, are then determined from the obtained finite continued fraction. If all coefficients of the obtained finite continued fraction are positive, then the fractance can be made of classical passive elements (resistors and capacitors). If some of the coefficients are negative, then the fractance can be made with the help of negative impedance converters (Section 6.2).

6.1. Domino Ladder Circuit

Let us consider the circuit depicted in Figure 9, where $Z_{2k-1}(s)$ and $Y_{2k}(s)$, $k = 1, \ldots, n$, are given impedances of the circuit elements. The resulting impedance $Z(s)$ of the entire circuit can be found easily, if we consider it in the right-to-left direction:

$$Z(s) = Z_1(s) + \cfrac{1}{Y_2(s) + \cfrac{1}{Z_3(s) + \cfrac{1}{Y_4(s) + \cfrac{1}{\cdots\cdots\cdots\cdots\cdots\cdots \atop \cfrac{1}{Y_{2n-2}(s) + \cfrac{1}{Z_{2n-1}(s) + \cfrac{1}{Y_{2n}(s)}}}}}}}. \tag{24}$$

The relationship between the finite domino ladder network, shown in Figure 9, and the continued fraction (24) provides an easy method for designing a circuit with a given impedance

$Z(s)$. For this one has to obtain a continued fraction expansion for $Z(s)$. Then the obtained particular expressions for $Z_{2k-1}(s)$ and $Y_{2k}(s)$, $k = 1, \dots, n$, will give the types of necessary components of the circuit and their nominal values.

EXAMPLE 6. To design a circuit with the impedance

$$Z(s) = \frac{s^4 + 4s^2 + 1}{s^3 + s}, \tag{25}$$

we have to develop $Z(s)$ in continued fraction

$$Z(s) = \frac{s^4 + 4s^2 + 1}{s^3 + s} = s + \cfrac{1}{\frac{1}{3}s + \cfrac{1}{\frac{9}{2}s + \cfrac{1}{\frac{2}{3}s.}}} \tag{26}$$

From this expansion it follows that

$$Z_1(s) = s, \quad Z_3(s) = \frac{9}{2}s, \quad Y_2(s) = \frac{1}{3}s, \quad Y_4(s) = \frac{2}{3}s.$$

Therefore, for the analogue realization in the form of the first Cauer's canonic LC circuit [17] we have to choose the following values of coils and capacitors:

$$L_1 = 1\,[H], \quad L_3 = \frac{9}{2}\,[H], \quad C_2 = \frac{1}{3}\,[F], \quad C_4 = \frac{2}{3}\,[F].$$

EXAMPLE 7. The function $Z(s)$ given by Equation (25) can be written also in the form

$$Z(s) = \frac{s^4 + 4s^2 + 1}{s^3 + s} = \frac{1}{s} + \cfrac{1}{\frac{1}{3s} + \cfrac{1}{\frac{9}{2s} + \cfrac{1}{\frac{2}{3s}.}}} \tag{27}$$

From this expansion it follows that

$$Z_1(s) = \frac{1}{s}, \quad Z_3(s) = \frac{9}{2s}, \quad Y_2(s) = \frac{1}{3s}, \quad Y_4(s) = \frac{2}{3s}.$$

Therefore, for the analogue realization in the form of the second Cauer's canonic LC circuit [17] we have to choose the following values of coils and capacitors:

$$C_1 = 1\,[F], \quad C_3 = \frac{2}{9}\,[F], \quad L_2 = 3\,[H], \quad L_4 = \frac{3}{2}\,[H].$$

EXAMPLE 8. To design a circuit with the impedance

$$Z(s) = \frac{s^4 + 3s^2 + 8}{2s^3 + 4s}, \tag{28}$$

one has to obtain a continuous fraction representation of the function $Z(s)$,

$$Z(s) = \frac{s^4 + 3s^2 + 8}{2s^3 + 4s} = \frac{1}{2}s + \cfrac{1}{2s + \cfrac{1}{-\frac{1}{12}s + \cfrac{1}{-\frac{3}{2}s}}}. \tag{29}$$

From this expansion it follows that

$$Z_1(s) = \frac{1}{2}s, \quad Z_3(s) = -\frac{1}{12}s, \quad Y_2(s) = 2s, \quad Y_4(s) = -\frac{3}{2}s.$$

Therefore, for the analogue realization in the form of the first Cauer's canonic LC circuit [17] we have to choose the following values of coils and capacitors:

$$L_1 = \frac{1}{2}\,[H], \quad L_3 = -\frac{1}{12}\,[H], \quad C_2 = 2\,[F], \quad C_4 = -\frac{3}{2}\,[F].$$

Here we see negative inductances and capacitance. Such elements cannot be realized using passive electric components. However, they can be realized with the help of active components, namely operating amplifiers.

6.2. Negative-Impedance Converters

The previous example shows that the use of CFE for analogue realization of arbitrary transfer functions may lead to the appearance of negative impedances. This observation is not unknown. For example, in the paper [12], Dutta Roy recalls Khovanskii's continued fraction expansion for $x^{1/2}$ found in [18] and makes a remark that

> ... if x is replaced by the complex frequency variable s, then the realization would require a negative resistance. Thus, the [Khovanskii's] CFEs do not seem to be useful for realization of fractional inductor or capacitor.

Then he describes a method for circumventing this difficulty, which gives a continued fraction expansion with positive coefficients.

However, the possibility of realization of negative impedances in electric circuits has been pointed out by Bode [19, chapter IX]. Later, in 1970s, operational amplifiers appeared, which significantly simplified creation of circuits exhibiting negative resistances, negative capacitances, and negative inductances. Such circuits are called *negative-impedance converters* [20].

The simplest scheme of a negative-impedance converter (or current inverter) is shown in Figure 10. The circuit consists of an operational amplifier, two resistors of equal resistance R, and a component with the impedance Z. The entire circuit, considered as a single element, has negative impedance $-Z$. This means that $I_{\text{in}} = V_{\text{in}}/(-Z)$).

For example, taking a resistor of resistance R_Z instead of the element Z, we obtain a circuit, which behaves like a negative resistance $-R_Z$. The negative resistance means that if such an element of negative resistance, for instance, -10 kΩ is connected in series with a classical 20 kΩ resistor, then the resistance of the resulting connection is 10 kΩ.

Let us now recall Example 8. Using negative-impedance converters, it is possible to design a circuit with the required impedance $Z(s)$, which will contain a negative capacitance C_4 and a negative inductance L_3.

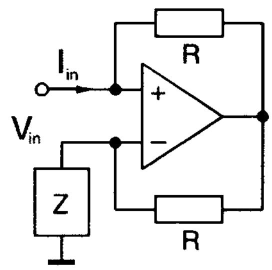

Figure 10. Negative-impedance converter.

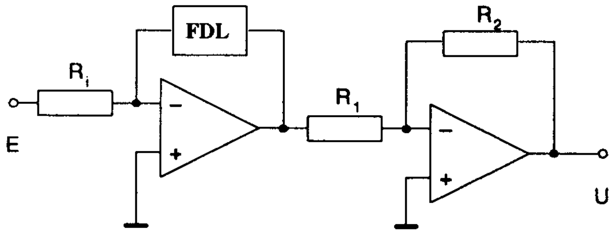

Figure 11. Analogue fractional-order I^λ controller.

7. Example: Fractional-Order I^λ Controller

For experimental measurement we built a fractional-order I^λ controller which is a particular case of the $PI^\lambda D^\mu$ controller, (if $K = 0$ and $T_d = 0$). The controller was realized in the form of the finite domino ladder ($n = 12$), connected to feedback in operational amplifier (Figure 11). It should be noted that the described methods work for arbitrary orders, but the circuit elements with computed values are not usually available. Because of this, in our experiment we proposed and realized the integrator with order $\lambda = 0.5$. It should be mentioned that this simple case of the controller order can be realized also using the methods described in [21–24], which do not involve explicit rational approximations.

In the case, if we will use identical resistors (R-series) and identical capacitors (C-shunt) in the FDL, then the behaviour of the circuit will be as a half-order integrator/differentiator. We used the resistor values $R = 1k\Omega$ ($R_j = R,\ j = 1, \ldots, n$) and the capacitor values $C = 1\mu F$ ($C_j = C,\ j = 1, \ldots, n$). For better measurement results we used two operational amplifiers TL081CN in inverting connection.

A block diagram of the analogue fractional-order I^λ controller realization is shown in Figure 11.

The resistors R_1 and R_2 are $R_1 = R_2 = 22$ kΩ. The integration constant T_i can be computed from relationship $T_i = 1/\sqrt{R/(R_i^2 * C)}$, and for $R_i = 22$ kΩ we have $T_i = 1.4374$. The transfer function of the realized analogue fractional-order I^λ controller is

$$G_c(s) = 1.4374\ \mathrm{s}^{-0.5}. \tag{30}$$

Adjustment of the integration constant T_i of the fractional-order I^λ controller depicted in Figure 11 was done by resistor R_i. If we change the resistor R_i, the integration constant changes the value in the required interval.

In Figures 12 and 13 the measured characteristics of realized analogue fractional-order I^λ controller are presented. In Figure 12 Bode plots a shown, and in Figure 13 is the time response

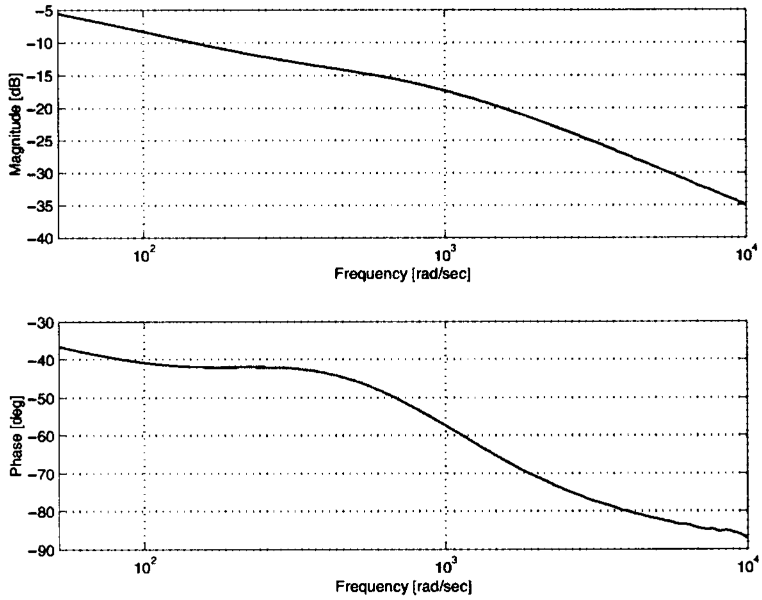

Figure 12. Bode plots of the $I^{1/2}$ controller (measurements).

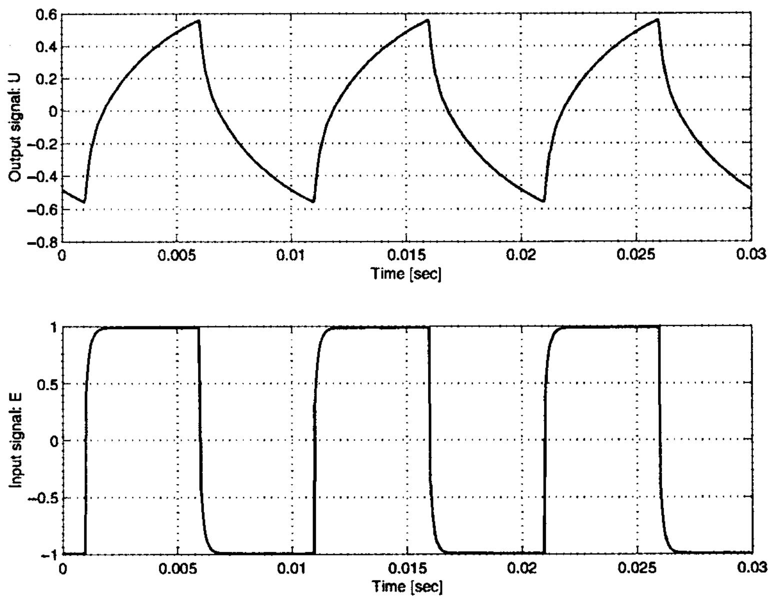

Figure 13. Time response of the $I^{1/2}$ controller to unit step input (measurements).

to the square input signal (unit step). We used frequency 100 Hz and amplitude ±10 V. It can be seen from Figure 12 that the realized analogue of fractional-order I^{λ} controller provides a good approximation in the frequency range $[10^2\ \mathrm{rad/sec}, 5 \cdot 10^2\ \mathrm{rad/sec}]$.

Measurements were done using IWATSU Digital Storagescope DS-8617 100 MHz, Hewlett Packard 35670A dynamic signal analyzer, Hewlett Packard 33120A 15 MHz function/ arbitrary waveform generator, power supply Thurlby-Thandar PL320QMD.

8. Conclusion

In this paper we have demonstrated that the suggested use of continued fraction expansions is a good general method for obtaining analogue devices (fractances) described by fractional differential equations or by fractional-order transfer functions. Moreover, this approach can be used for realization of other types of systems with transcendental transfer functions, which can be developed in continued fractions. Furthermore, it has been shown that any rational approximation of the transfer function can be used for designing the corresponding analogue circuit, even if some of the coefficients of the resulting continued fraction are negative.

We have also introduced two types of nested multiple-loop systems, which can be easily used for modelling, simulation, and realization of fractional-order systems and controllers, and more generally for modelling, simulation and realization of systems, for which a rational approximation of the transfer function can be obtained.

The exposition has been illustrated with several examples, including analogue realization of an I^{λ} controller, for which experimental results were presented.

References

1. Miller, K. S. and Ross, B., *An Introduction to the Fractional Calculus and Fractional Differential Equations*, Wiley, New York, 1993.
2. Oldham, K. B. and Spanier, J., *The Fractional Calculus*, Academic Press, New York, 1974.
3. Podlubny, I., *Fractional Differential Equations*, Academic Press, San Diego, CA, 1999.
4. Samko, S. G., Kilbas, A. A., and Maritchev, O. I., *Integrals and Derivatives of the Fractional Order and Some of Their Applications*, Nauka i Tekhnika, Minsk, 1987 [in Russian].
5. Podlubny, I., ‘Fractional-order systems and $PI^{\lambda}D^{\mu}$-controllers’, *IEEE Transactions on Automatic Control* **44**, 1999, 208–214.
6. Podlubny, I., ‘Fractional-order systems and fractional-order controllers’, UEF-03-94, Slovak Academy of Sciences, Kosice, 1994.
7. Dorf, R. C. and Bishop, R. H., *Modern Control Systems*, Addison-Wesley, New York, 1990.
8. Oustaloup, A., *Systèmes Asservis Linéaires d’Ordre Fractionnaire: Théorie et Pratique*, Editions Masson, Paris, 1983.
9. Oustaloup, A., *La Dérivation non Entière*, Hermès, Paris, 1995.
10. Oustaloup, A., Levron, F., Mathieu, B., and Nanot, F. M., ‘Frequency-band complex noninteger differentiator: Characterization and synthesis’, *IEEE Transactions on Circuit and Systems – I: Fundamental Theory and Application* **47**, 2000, 25–39.
11. Press, W. H., Teukolsky, S. A., Vetterling, W. T., and Flannery, B. P., *Numerical Recipes in C. The Art of Scientific Computing*, 2nd edition, Cambridge University Press, Cambridge, 1992.
12. Dutta Roy, S. C., ‘On the realization of a constant-argument immitance of fractional operator’, *IEEE Transactions on Circuit Theory* **14**, 1967, 264–374.
13. Vinagre, B. M., Podlubny, I., Hernandez, A., and Feliu, V., ‘On realization of fractional-order controllers’, in *Proceedings of the Conference Internationale Francophone d’Automatique*, Lille, Jule 5–8, P. Borne, J.-P. Richard, and Ph. Vanheeghe (eds.), 2000, pp. 945–950.
14. Carlson, G. E. and Halijak, C. A., ‘Approximation of fractional capacitors $(1/s)^{1/n}$ by a regular Newton process’, *IEEE Transactions on Circuit Theory* **11**, 1964, 210–213.
15. Matsuda, K. and Fujii, H., ‘H_{∞}–optimized wave-absorbing control: analytical and experimental results’, *Journal of Guidance, Control, and Dynamics* **16**, 1993, 1146–1153.
16. Heymans, N. and Bauwens, J.-C., ‘Fractal rheological models and fractional differential equations for viscoelastic behavior’, *Rheologica Acta* **33**, 1994, 210–219.
17. Kvasil, J. and Čajka, J., *An Introduction to Synthesis of Linear Circuits*, SNTL/ALFA, Prague, 1981 [in Czech].
18. Khovanskii, A. N., *The Application of Continued Fractions and Their Generalizations to Problems in Approximation Theory*, Noordhoff, Groningen, 1963.

19. Bode, H. W., *Network Analysis and Feedback Amplifier Design*, Tung Hwa Book Company, Shanghai, China, 1949.
20. Dostal, J., *Operational Amplifiers*, Butterworth-Heinemann, Boston, MA, 1993.
21. Nakagava, M. and Sorimachi, K., 'Basic characteristics of a fractance device', *IEICE Transactions Fundamentals* **E75-A**, 1992, 1814–1818.
22. Oldham, K. B. and Zoski, C. G., 'Analogue instrumentation for processing polarographic data', *Journal of Electroanalytical Chemistry* **157**, 1983, 27–51.
23. Petráš, I. and Dorčák, L'., 'Some possibilities for realization of fractional order controller', *Envirautom* **4**, 1999, 83–90 [in Slovak].
24. Wang, J. C., 'Realizations of generalized Warburg impedance with RC ladder networks and transmission lines', *Journal of Electrochemical Society* **134**, 1987, 1915–1920.